

# *Settle3D*

3D settlement for foundations

**Stress Analysis Verification Manual**

© 2007-2012 Rocscience Inc.

# Table of Contents

## **Settle3D Stress Verification Problems**

---

|    |   |    |
|----|---|----|
| 1  | Vertical Stresses underneath Rectangular Footings due to Uniform Loading.....                         | 1  |
| 2  | Vertical Stresses beneath Circular Footings due to Uniform Loading .....                              | 5  |
| 3  | Vertical Stresses under Square Footings due to Triangular Loading .....                               | 7  |
| 4  | Vertical Stresses below a Foundation due to Embankment Loading .....                                  | 11 |
| 5  | Vertical Stresses between Multiple Footings.....  | 15 |
| 6  | Vertical Stresses below an Infinite Strip Subjected to Uniform Loading.....                           | 20 |
| 7  | Vertical Stresses underneath an Irregular Shape Footing due to Uniform Loading ....                   | 22 |
| 8  | Analysis of Mean Stress.....  | 24 |
| 9  | Immediate Settlement .....  | 28 |
| 10 | Uniform Vertical Loading on Circular Surface Area of Two-Layer System .....                           | 32 |
| 11 | Uniform Vertical Loading on Circular Surface Area of Three-Layer System .....                         | 35 |
| 12 | Vertical Strip Loading on Surface of Material Underlain by Rigid Infinite Layer ...                   | 44 |
| 13 | Uniform Vertical Loading on Circular Surface Area of Material Underlain by Rigid Infinite Layer ..... | 46 |
| 14 | Immediate Settlement beneath a Rigid Circular Footing.....  | 49 |
| 15 | Rotation of a Rigid Circular Footing .....  | 51 |
| 16 | Immediate Settlement beneath a Rigid Rectangular Footing .....  | 53 |
| 17 | Rotation of a Rigid Rectangular Footing.....  | 57 |
| 18 | Immediate Settlement beneath a Rigid Circular Footing on a Finite Layer .....                         | 60 |
| 19 | Rotation of a Rigid Circular Footing on a Finite Layer.....   | 64 |
| 20 | Vertical Stress beneath Uniform Circular load based on Westergaard's Theory .....                     | 67 |
| 21 | Vertical Stress beneath Uniform Square load based on Westergaard's Theory .....                       | 71 |

|   |    |
|---|----|
| 22 Vertical Stress due to Uniform Loading on an Irregular Shaped Footing using Westergaard's Theory ..... | 75 |
| 23 Horizontal Stresses due to Uniform Loading on a Square Footing using Boussinesq Theory .....           | 79 |

# 1 Vertical Stresses underneath Rectangular Footings due to Uniform Loading

## 1.1 Problem description

This problem verifies the vertical stresses beneath rectangular footing of a length of  $L$  and a width of  $B$ . The model geometry and the locations of points of interests are shown in Figure 1.1. The footing is subjected to a uniform loading ( $q$ ) of 1 kPa. Three footings were considered in this verification with the different  $L/B$  ratio of:

- Case 1:  $L/B = 1$  where,  $B = 1$  m
- Case 2:  $L/B = 2$
- Case 3:  $L/B = 4$

The vertical stress results are compared to analytical solution, the integration of Boussinesq equation over the rectangle, for each case.

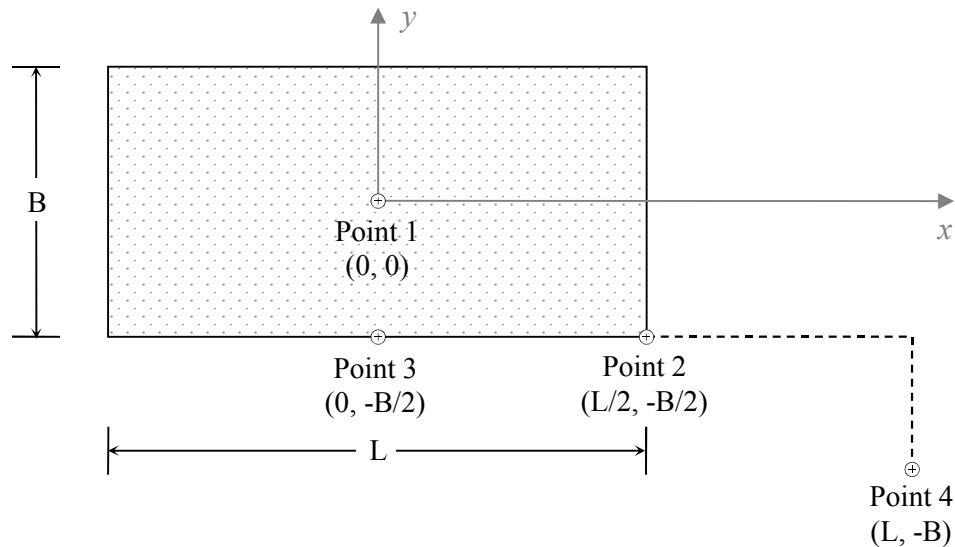


*Figure 1.1 – Model Geometry & Points of Interest Locations*

## 1.2 Closed Form Solution

Rectangle is a common geometry for footings. Vertical stress profile for this type of footings can be obtained analytically by integrating the Boussinesq equation over the rectangular domain. The integration version which is most widely used is that of Newmark:

$$\sigma_z = q \frac{1}{4\pi} \left[ \frac{2MN \sqrt{V}}{V + V_1} \frac{V+1}{V} + \tan^{-1} \left( \frac{2MN \sqrt{V}}{V - V_1} \right) \right]$$

where

$$M = \frac{B}{z}$$

$$N = \frac{L}{z}$$

$$V = M^2 + N^2 + 1$$

$$V_1 = (MN)^2$$

and when  $V_1 > V$  the  $\tan^{-1}$  term will become negative and  $\pi$  needs to be added (Bowles, 1996).

### 1.3 Results and Discussion

Figures 1.2, 1.3, 1.4, and 1.5 show vertical stress profiles at Point 1, Point 2, Point 3, and Point 4, respectively, given by *Settle3D* compared to the analytical solutions.

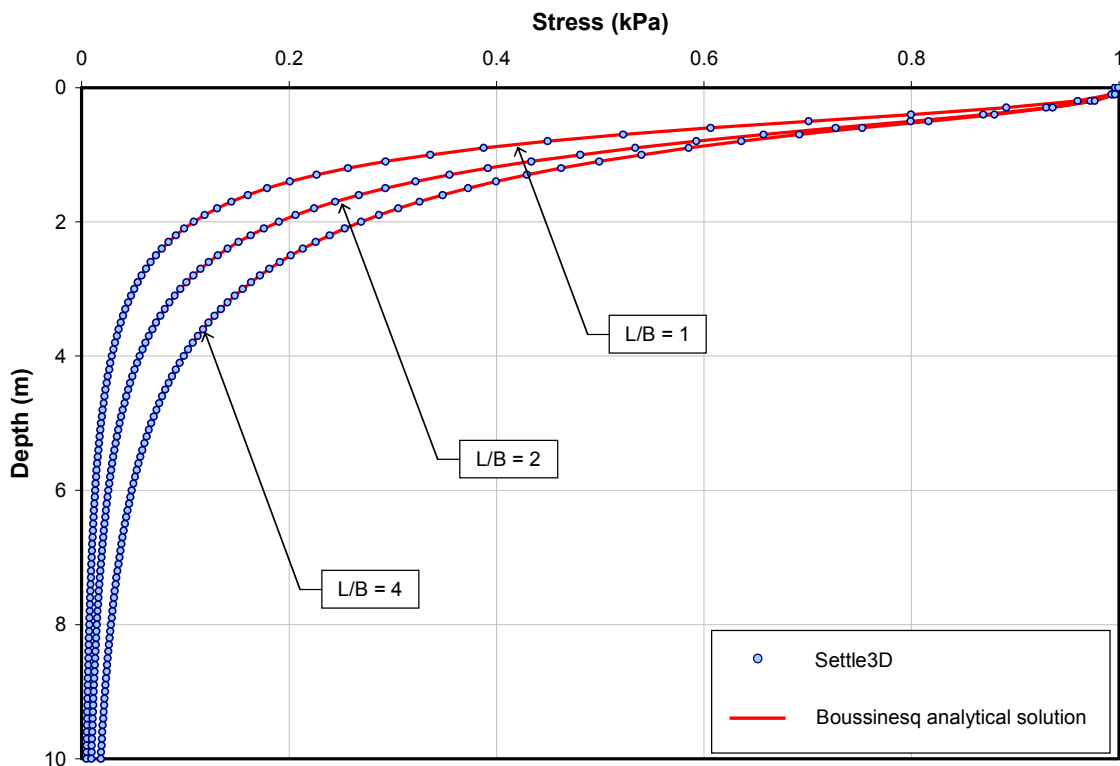


*Fig. 1.2 Vertical Stress Profile at Point 1*

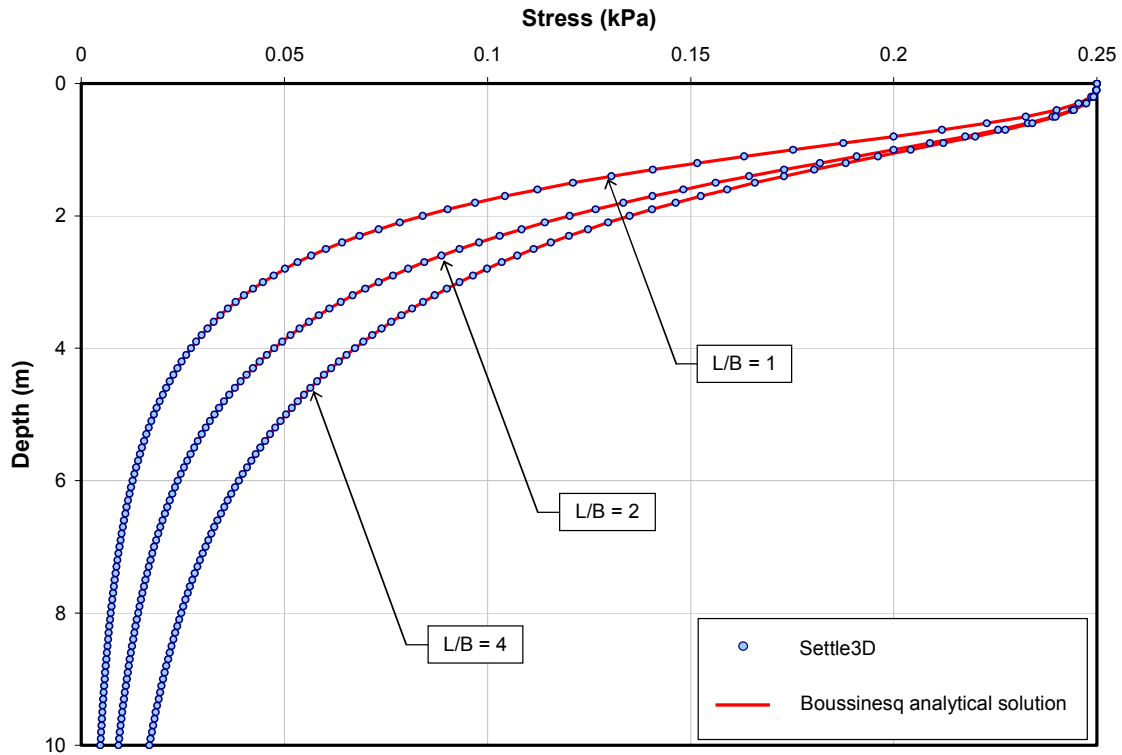


*Fig. 1.3 Vertical Stress Profile at Point 2*

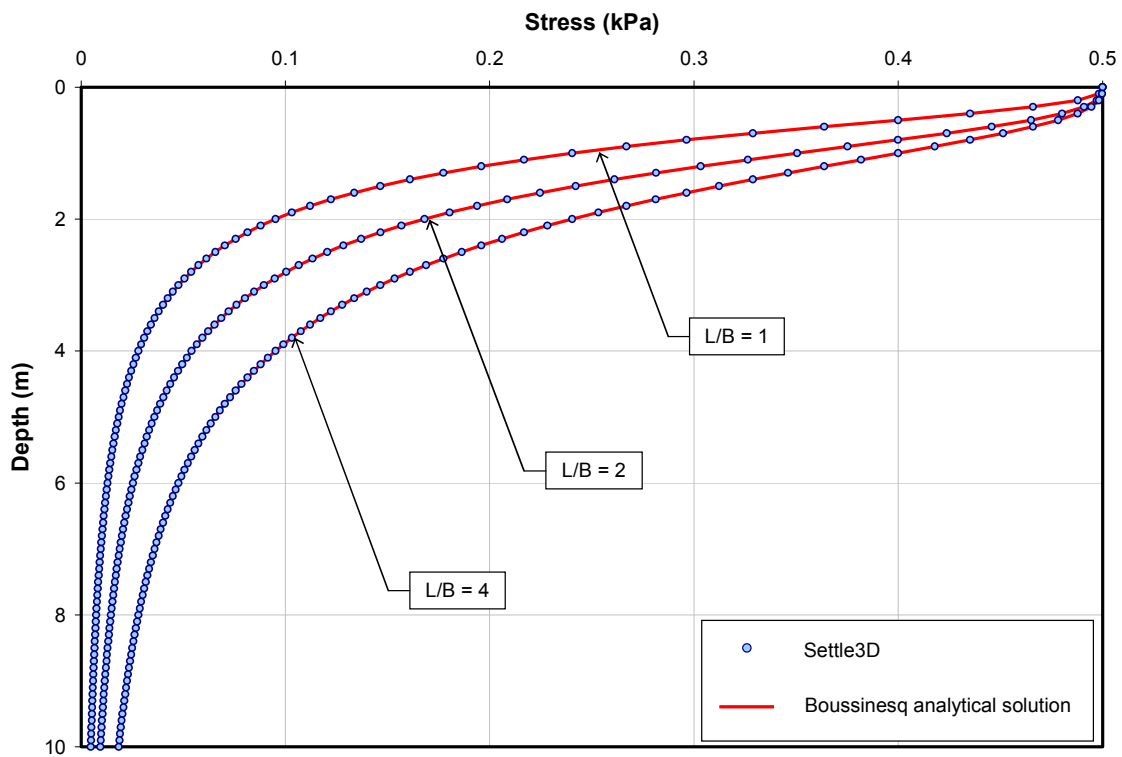


*Fig. 1.4 Vertical Stress Profile at Point 3*

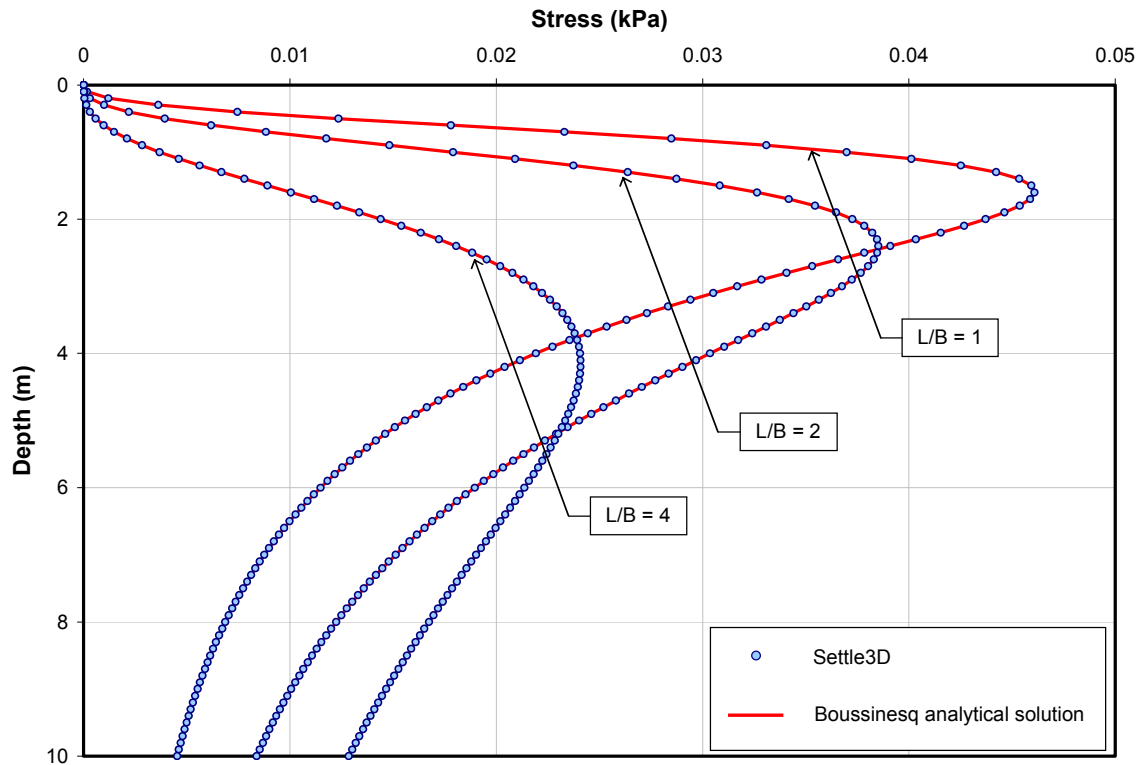


**Fig. 1.5 Vertical Stress Profile atPoint 4**

## 1.4 References

1. H. G. Poulos and E. H. Davis (1974), *Elastic Solutions for Soil and Rock Mechanics*, New York: John Wiley & Sons.
2. J. E. Bowles (1996), *Foundation Analysis and Design*, 5<sup>th</sup> Ed., New York: McGraw-Hill.

## 2 Vertical Stresses beneath Circular Footings due to Uniform Loading

### 2.1 Problem description

This problem verifies the vertical stresses beneath the center of circular footing of a radius  $a$  m. The model geometry is shown in Figure 2.1. The footing is subjected to a uniform loading ( $q$ ) of 1 kPa. Three footings were considered in this verification with the different radius ( $a$ ) of:

- Case 1:  $a = 1$  m
- Case 2:  $a = 2$  m
- Case 3:  $a = 4$  m

The vertical stress result is compared to Boussinesq analytical solution.

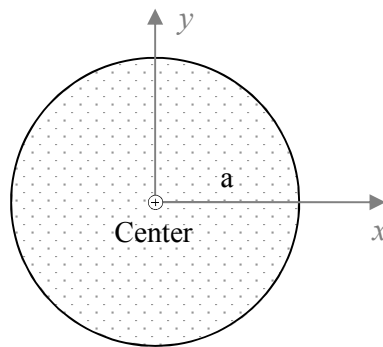


*Figure 2.1 – Model Geometry*

### 2.2 Closed Form Solution

Vertical stress below the center of a circular footing can be obtained analytically by integrating the Boussinesq equation over the circular domain. The solution is given by [1]:

$$\sigma_z = q \left[ 1 - \left( \frac{1}{1 + (a/z)^2} \right)^{3/2} \right]$$

## 2.3 Results and Discussion

Figure 2.2 shows vertical stress profiles underneath the center of the circle given by *Settle3D* compared to the analytical solutions.

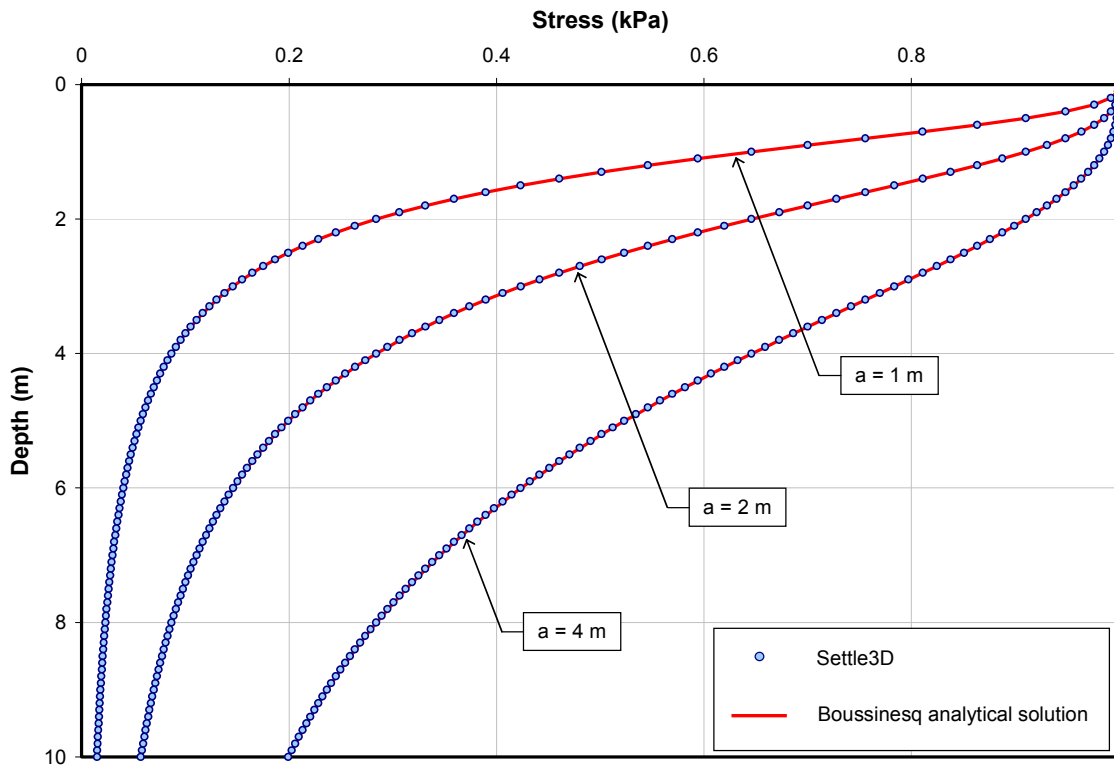


*Fig. 2.2 Vertical Stress underneath the Center*

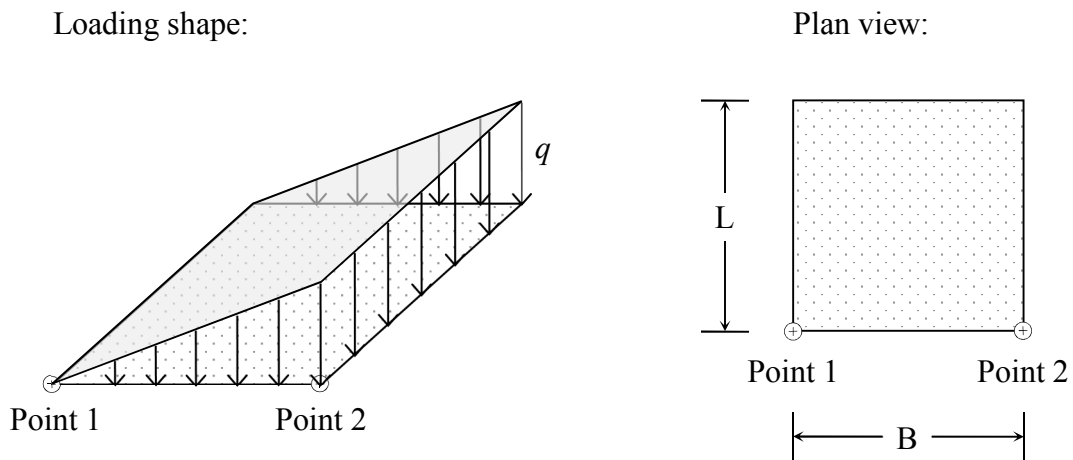
## 2.4 References

1. H. G. Poulos and E. H. Davis (1974), *Elastic Solutions for Soil and Rock Mechanics*, New York: John Wiley & Sons.
2. J. E. Bowles (1996), *Foundation Analysis and Design*, 5<sup>th</sup> Ed., New York: McGraw-Hill.

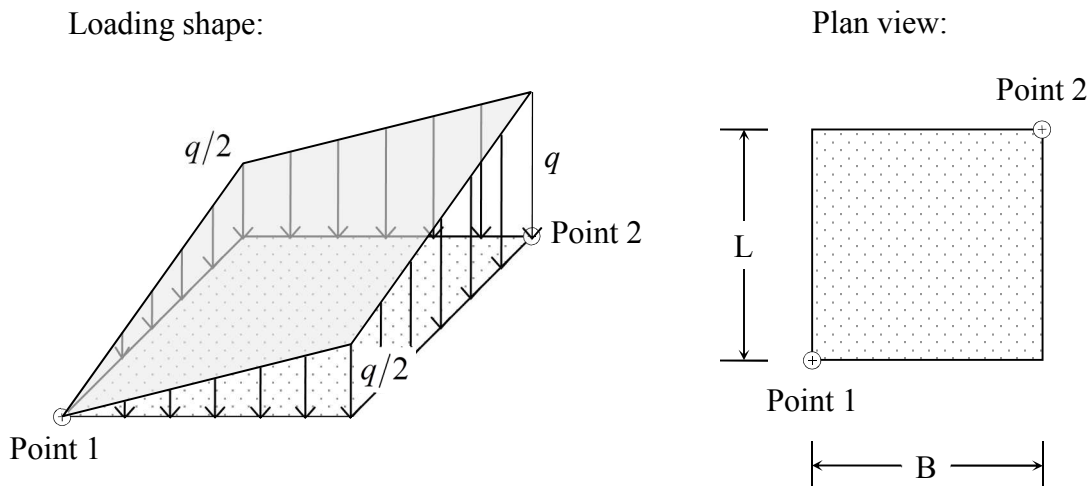
# 3 Vertical Stresses under Square Footings due to Triangular Loading

## 3.1 Problem description

This problem verifies the vertical stresses below the corners of rectangular footing with a dimension of  $L \times B$  subjected to triangular loading. Two loading shapes are considered: one-way linear load intensity and two-way linear load intensity. The model geometry and the points of interest are shown in Figure 3.1. The models have a dimension of  $1\text{ m} \times 1\text{ m}$  and a load value ( $q$ ) of  $1\text{ kPa}$ . The vertical stress results are compared to analytical solutions.



**Case 1 (one-way linear load intensity)**



**Case 2 (two-way linear load intensity)**

*Figure 3.1 – Model Geometry*

### 3.2 Closed Form Solution

Vitone and Valsangkar (1986) formulated equations to calculate vertical stress underneath points 1 and 2 of the two cases. The equations are:

#### Case 1 (one-way linear load intensity):

At point 1,

$$\sigma_z = \frac{qL}{2\pi B} \left( \frac{z}{R_L} - \frac{z^3}{R_B^2 R_D} \right)$$

At point 2,

$$\sigma_z = \frac{qL}{2\pi B} \left\{ \frac{z R_D}{R_L^2} - \frac{z}{R_L} + \frac{B}{L} \sin^{-1} \left( \frac{BL}{(B^2 L^2 + R_D^2 z^2)^{1/2}} \right) \right\}$$

#### Case 2 (two-way linear load intensity):

At point 1,

$$\sigma_z = \frac{q}{4\pi} \left\{ \frac{L}{B} \left( \frac{z}{R_L} - \frac{z^3}{R_D R_B^2} \right) + \frac{B}{L} \left( \frac{z}{R_B} - \frac{z^3}{R_D R_L^2} \right) \right\}$$

At point 2,

$$\sigma_z = \frac{q}{4\pi} \left\{ \frac{L}{B} \left( \frac{z R_D}{R_L^2} - \frac{z}{R_L} \right) + \frac{B}{L} \left( \frac{z R_D}{R_B^2} - \frac{z}{R_B} \right) + 2 \sin^{-1} \left( \frac{BL}{(B^2 L^2 + R_D^2 z^2)^{1/2}} \right) \right\}$$

where  $R_B^2 = B^2 + z^2$

$$R_L^2 = L^2 + z^2$$

$$R_D^2 = B^2 + L^2 + z^2$$

### 3.3 Results and Discussion

Figures 3.2 and 3.3 show vertical stress profiles of points 1 and 2 for Case 1 and Case 2 respectively given by **Settle3D** compared to the analytical solutions.

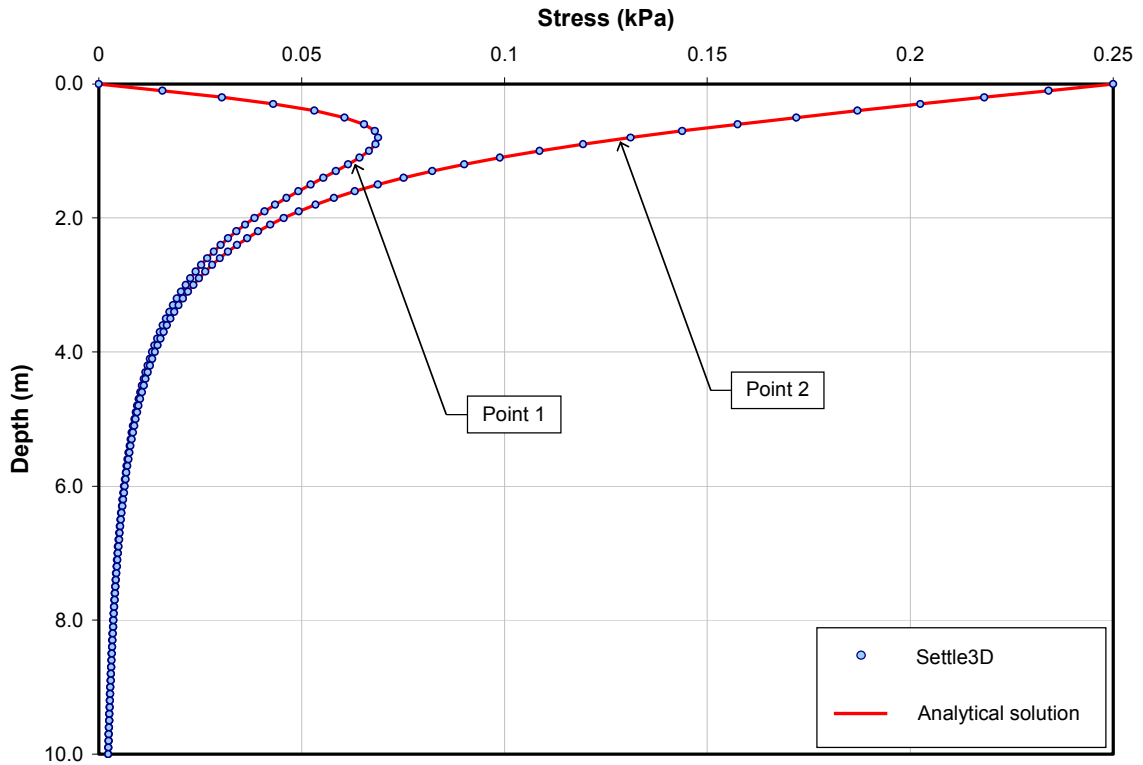


*Fig. 3.2 Vertical Stress Profiles of Case 1*

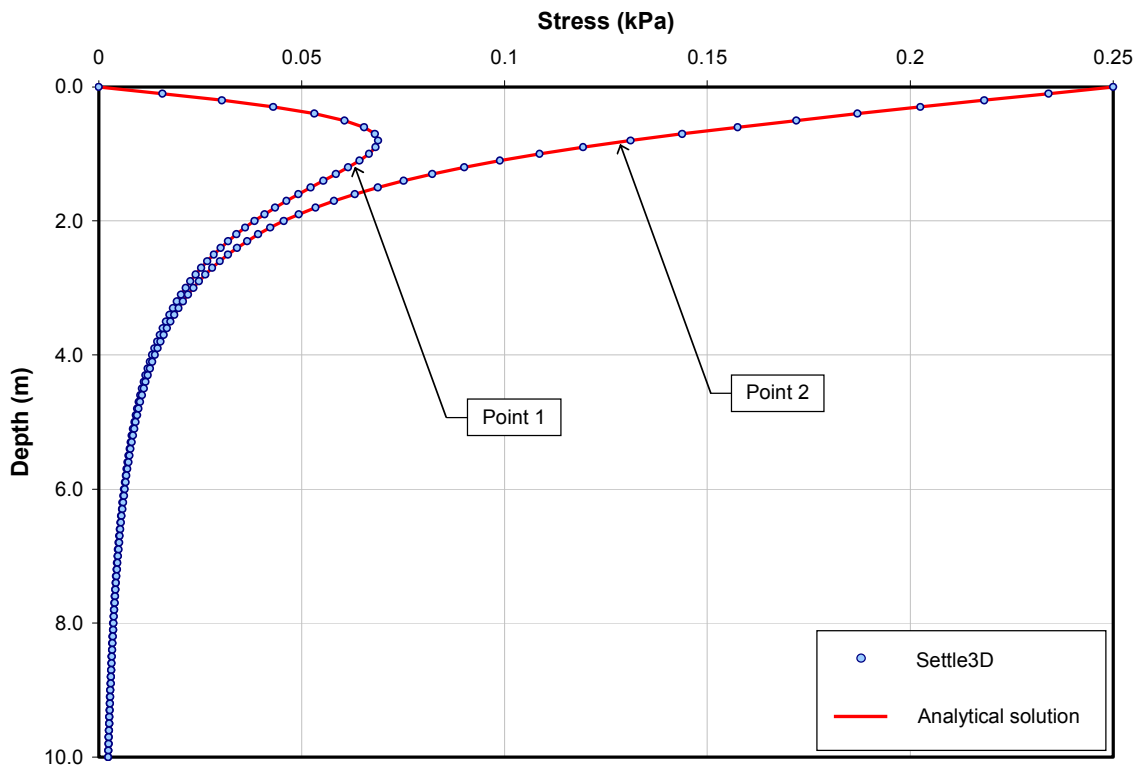


*Fig. 3.3 Vertical Stress Profiles of Case 2*

### 3.4 References

1. D. M. Vitone and A. J. Valsangkar (1986), "Stresses from Loads over Rectangular Areas", JGED, ASCE, vol. 112, no. 10, Oct, pp. 961-964.
2. J. E. Bowles (1996), *Foundation Analysis and Design*, 5<sup>th</sup> Ed., New York: McGraw-Hill.

## 4 Vertical Stresses below a Foundation due to Embankment Loading

### 4.1 Problem description

This problem verifies the vertical stresses under a foundation subjected to embankment loading. The model geometry with its properties and the points of interest are shown in Figure 4.1. The vertical stress results are compared to analytical solution.

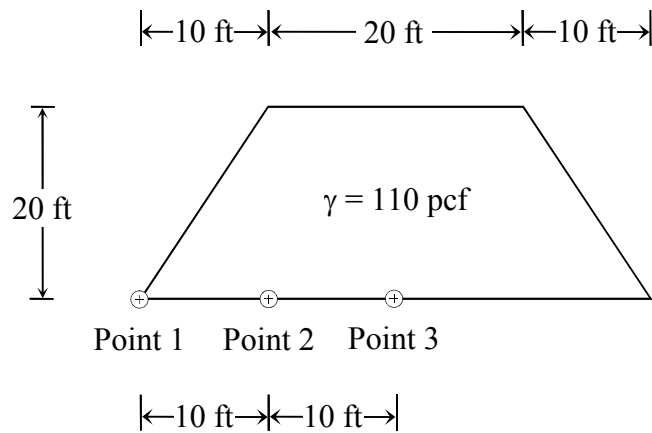


*Figure 4.1 – Model Geometry*

### 4.2 Closed Form Solution

For the general case shown below:

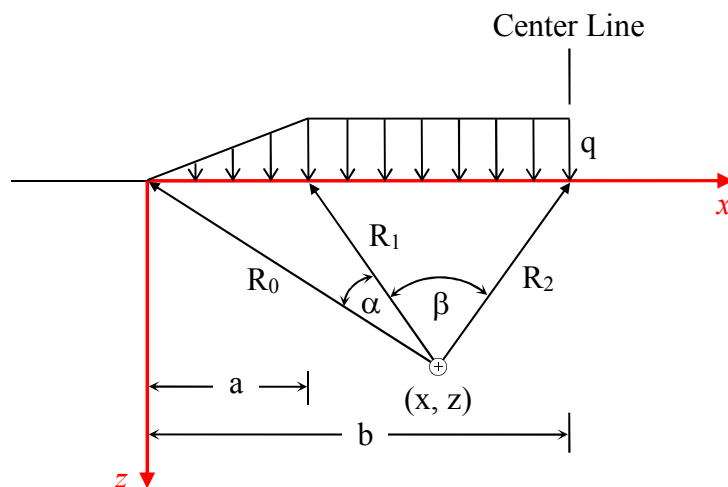


*Figure 4.2 – General Case of Vertical Embankment Loading*

Vertical stress at point (x, z) is given by:

$$\sigma_z = \frac{q}{\pi} \left[ \beta + \frac{x\alpha}{a} - \frac{z}{R_2^2}(x-b) \right]$$

Vertical stress under Point 1 can be computed by using the following superposition:

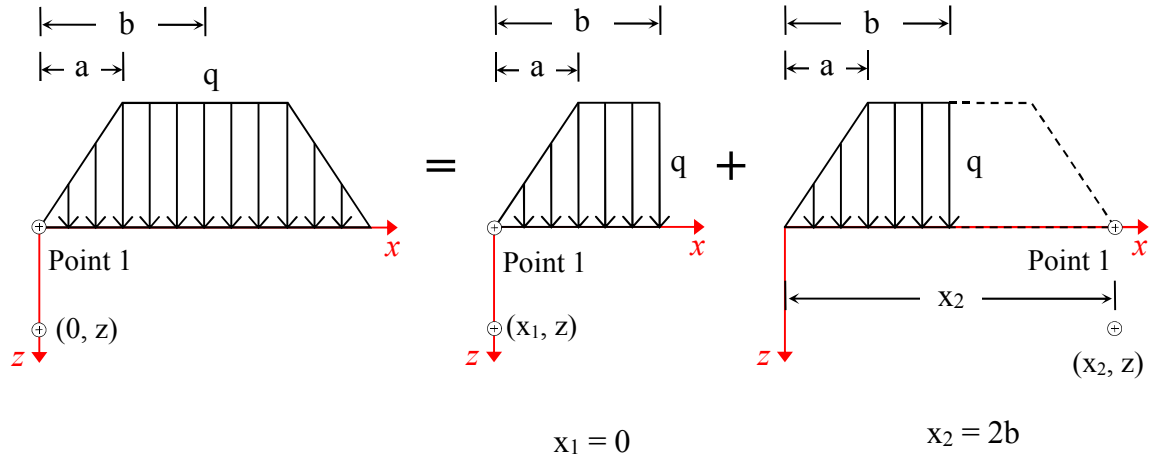


**Figure 4.3 – Superposition Scheme for Vertical Stress Underneath Point 1**

The superposition to compute vertical stress below Point 2 is given by:

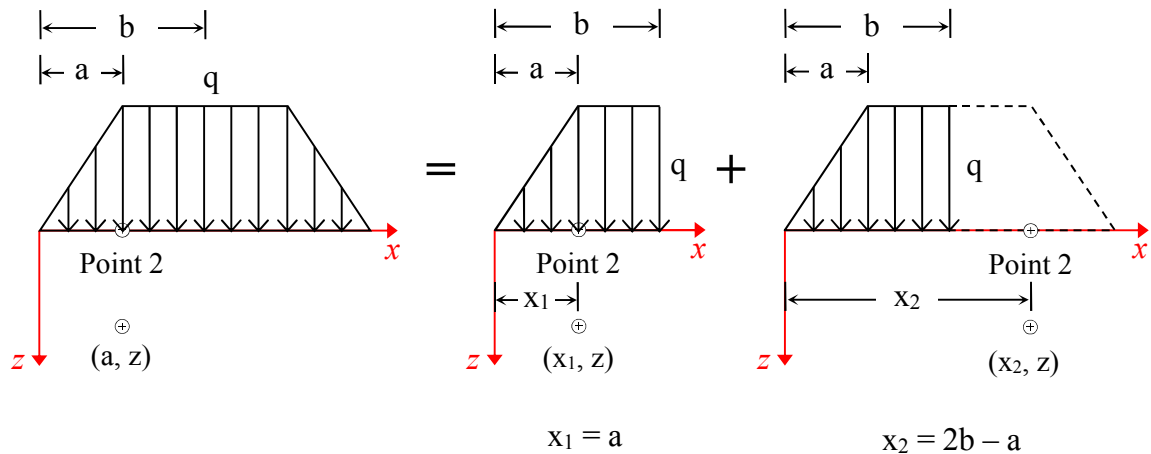


**Figure 4.4 – Superposition Scheme for Vertical Stress Underneath Point 2**

Lastly, vertical stress beneath Point 3 can be computed as the following:

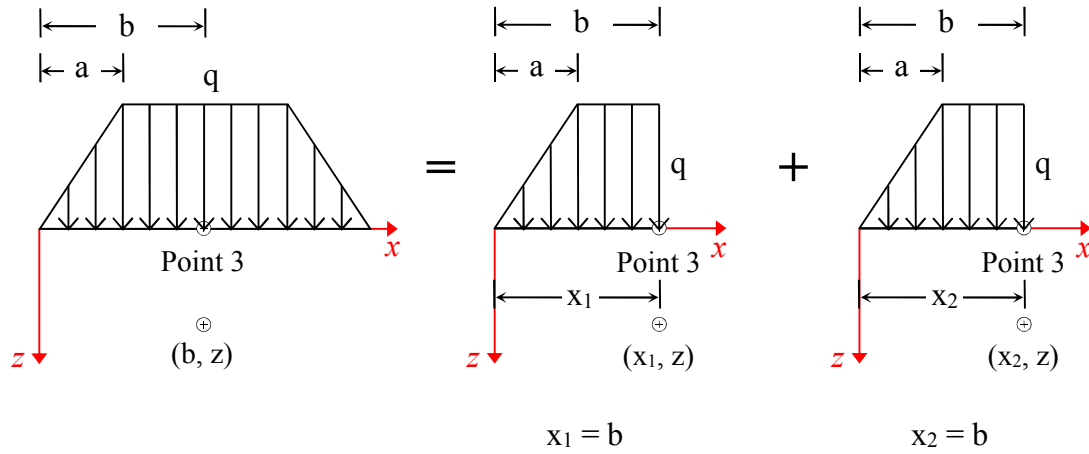
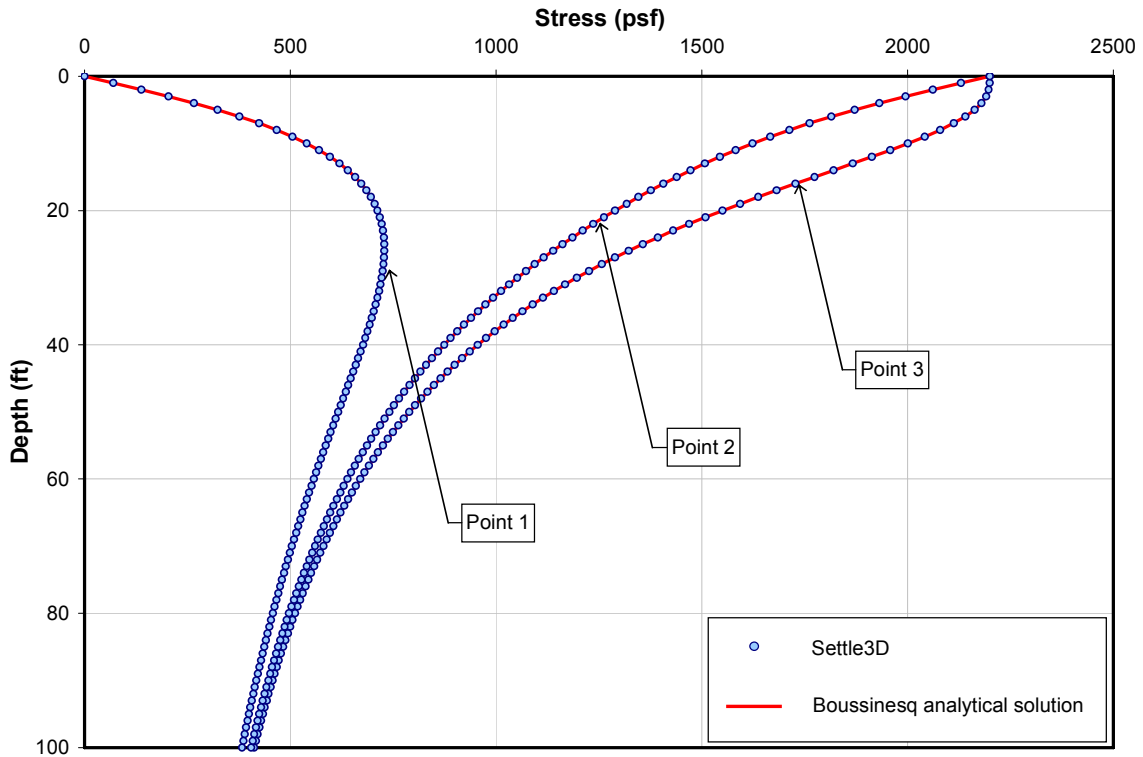


Figure 4.5 – Superposition Scheme for Vertical Stress Underneath Point 3

### 4.3 Results and Discussion

Figure 4.6 shows vertical stress profiles underneath the three points given by *Settle3D* compared to the analytical solutions.



*Fig. 4.6 Vertical Stress Profiles*

**4.4 References**

1. H. G. Poulos and E. H. Davis (1974), *Elastic Solutions for Soil and Rock Mechanics*, New York: John Wiley & Sons.

## 5 Vertical Stresses between Multiple Footings

### 5.1 Problem description

This problem verifies the vertical stresses under the surface between two footings. The footings are subjected to a uniform loading ( $q$ ) of 1 kPa and their dimension is 1 m x 1 m. The model geometry and the points of interest are shown in Figure 5.1. Four footing schemes with different values of  $h$  and  $d$  (see Figure 5.1) were considered. They are as follows:

- Case 1:  $h = 1$  m &  $d = 0.5$  m,
- Case 2:  $h = 1$  m &  $d = 1$  m,
- Case 3:  $h = 0$  &  $d = 0.5$  m,
- Case 4:  $h = 0$  &  $d = 1$  m.

The vertical stress results are compared to analytical solution.

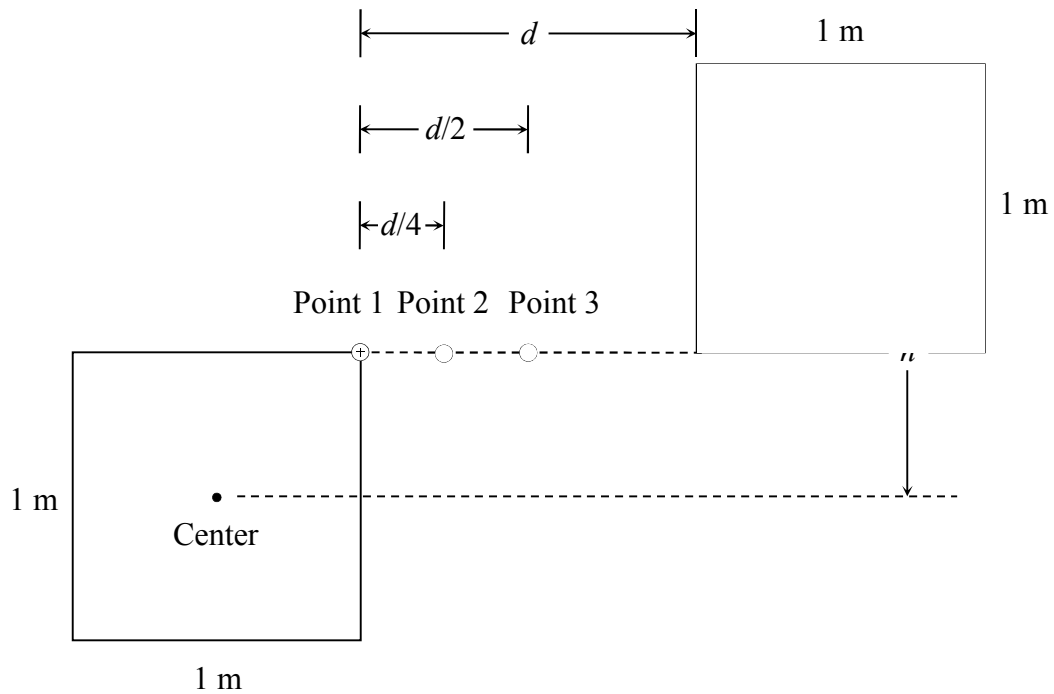


*Figure 5.1 – Model Geometry*

## 5.2 Closed Form Solution

Vertical stresses at any depth ( $z$ ) below Point 1, Point 2 and Point 3 are calculated using Newmark's integration:

$$\sigma_z = q \frac{1}{4\pi} \left[ \frac{2MN \sqrt{V}}{V + V_1} \frac{V+1}{V} + \tan^{-1} \left( \frac{2MN \sqrt{V}}{V - V_1} \right) \right]$$

where  $M = \frac{B}{z}$

$$N = \frac{L}{z}$$

$$V = M^2 + N^2 + 1$$

$$V_1 = (MN)^2$$

and when  $V_1 > V$  the  $\tan^{-1}$  term will become negative and  $\pi$  needs to be added (Bowles, 1996).

### 5.3 Results and Discussion

Figures 5.2 – 5.5 show vertical stress profiles under the surface of point locations. Four cases of various distances between the loads are compared to analytical solutions

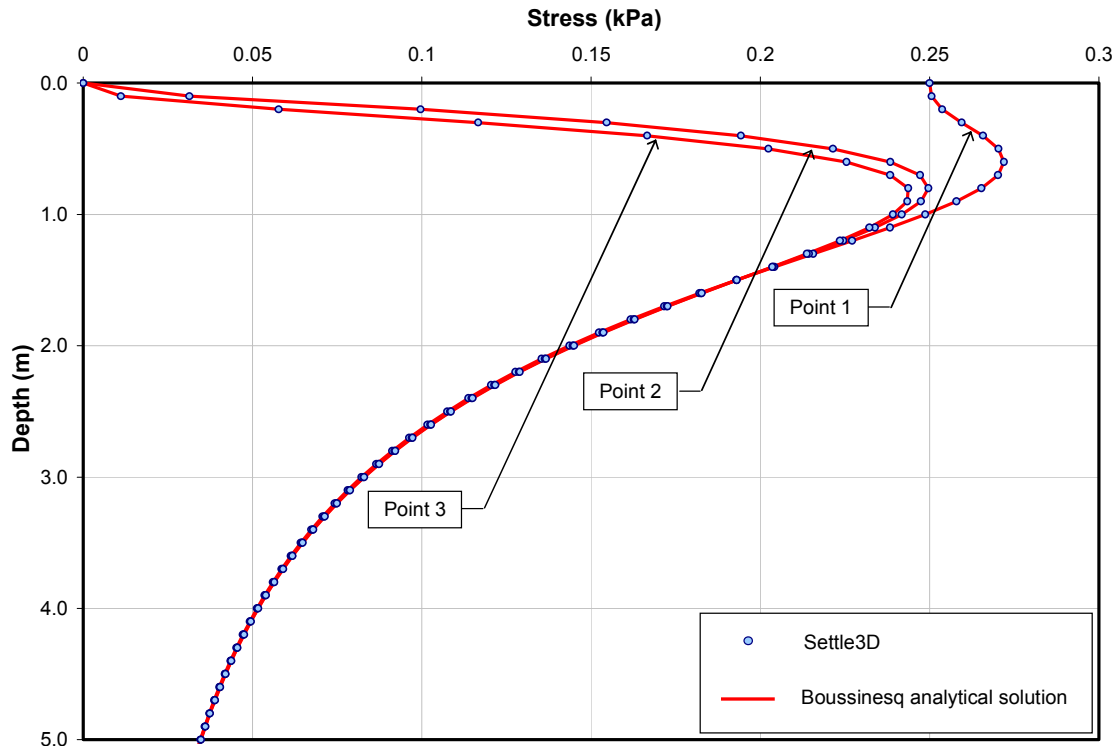


*Fig. 5.2 Vertical Stress Profile for Case 1*

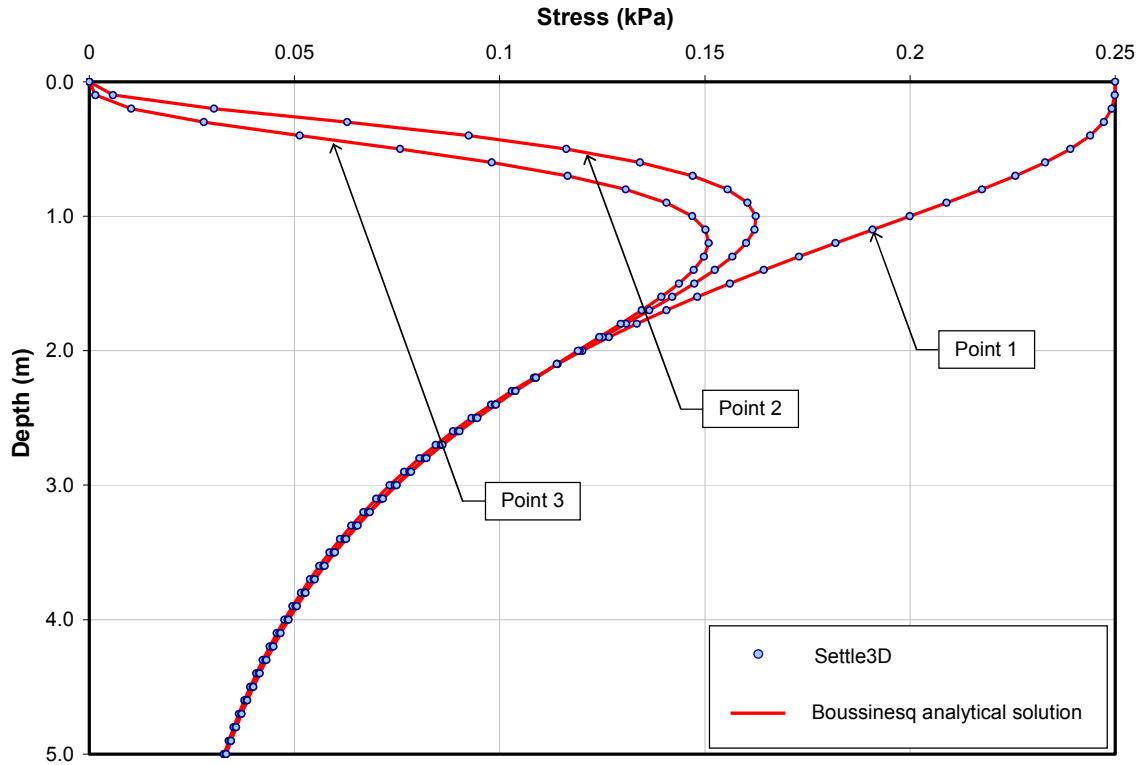


*Fig. 5.3 Vertical Stress Profile for Case 2*

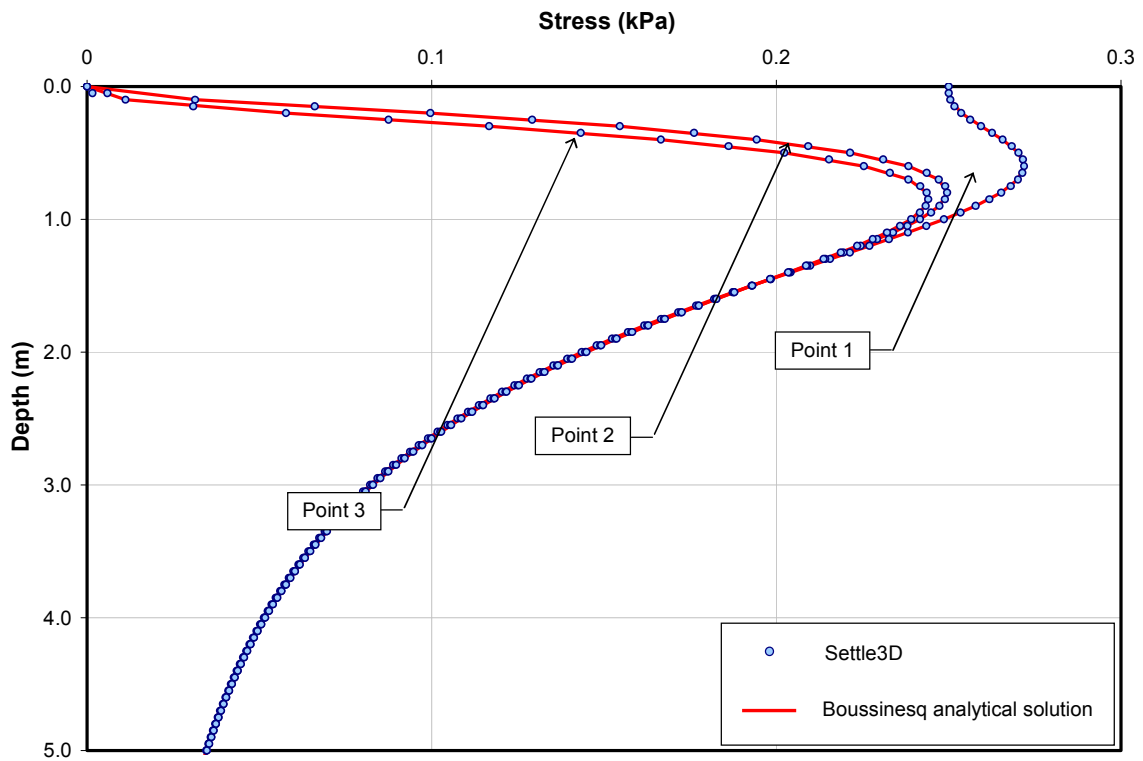


*Fig. 5.4 Vertical Stress Profile for Case 3*

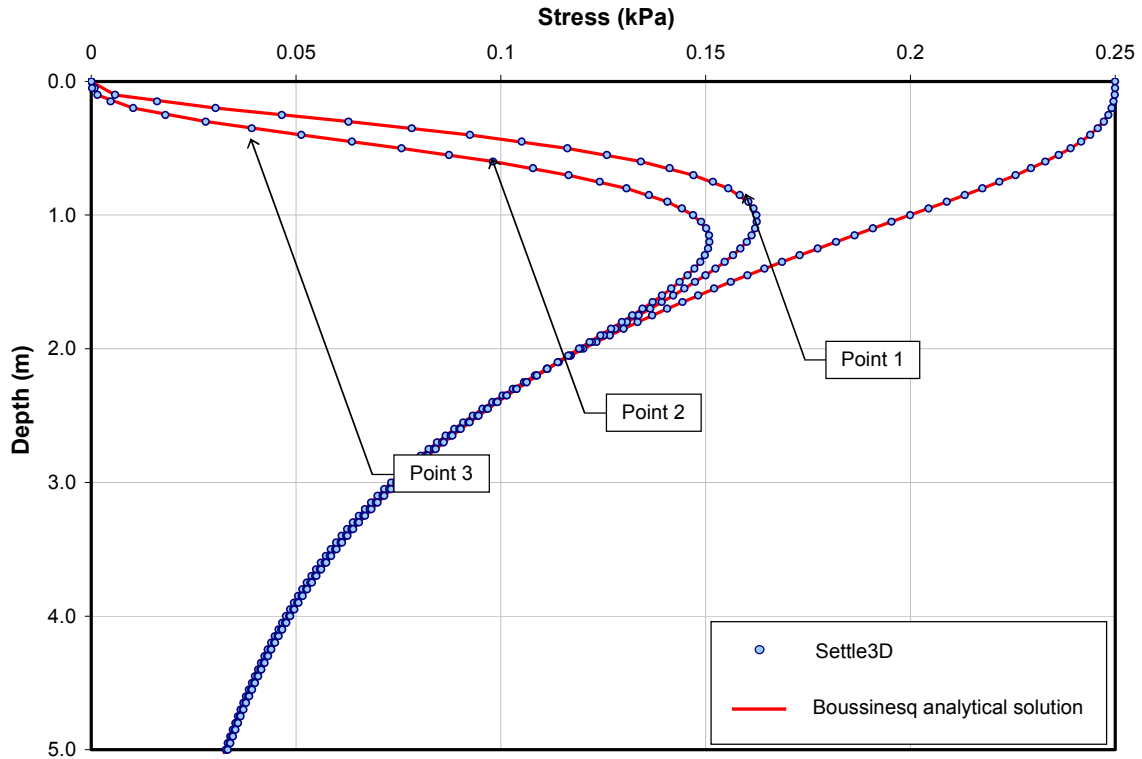


*Fig. 5.5 Vertical Stress Profile for Case 4*

## 5.4 References

1. H. G. Poulos and E. H. Davis (1974), *Elastic Solutions for Soil and Rock Mechanics*, New York: John Wiley & Sons.
2. J. E. Bowles (1996), *Foundation Analysis and Design*, 5<sup>th</sup> Ed., New York: McGraw-Hill.

## 6 Vertical Stresses below an Infinite Strip Subjected to Uniform Loading

### 6.1 Problem description

This problem verifies the vertical stresses beneath an infinite strip footing subjected to uniform loading. The model geometry with the location of points of interest is shown in Figure 6.1. The vertical stress results are compared to analytical solution.

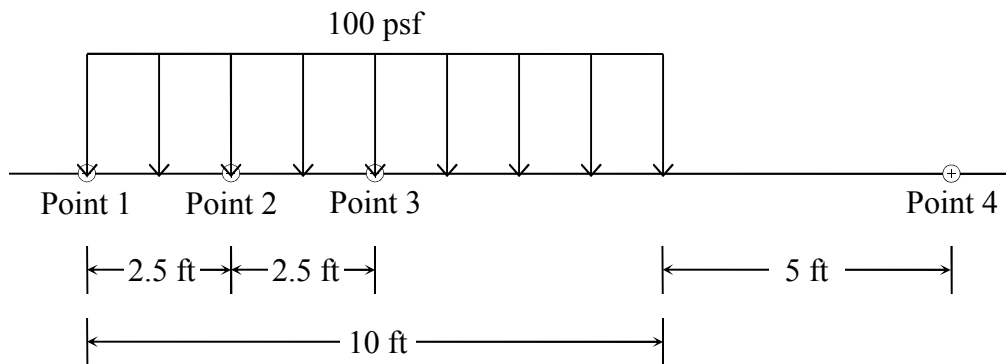


*Figure 6.1 – Model Geometry*

### 6.2 Closed Form Solution

For the general case shown below:

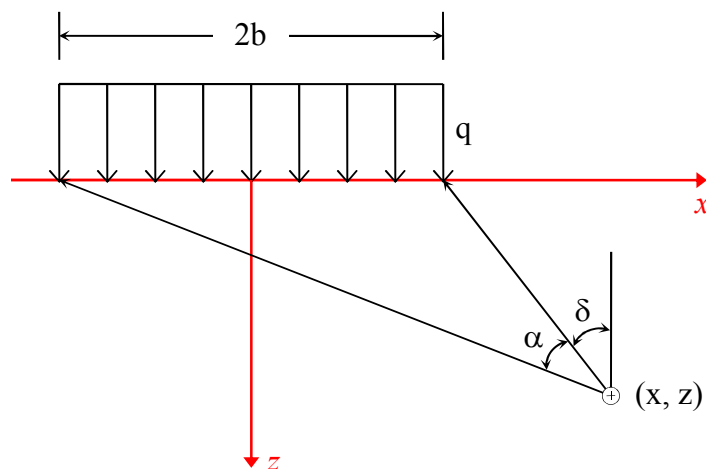


*Figure 6.2 – General Case of Uniform Loading on an Infinite Strip*

Vertical stress at any point (x, z) is given by:

$$\sigma_z = \frac{q}{\pi} [\alpha + \sin \alpha \cos(\alpha + 2\delta)]$$

### 6.3 Results and Discussion

Figure 6.3 shows vertical stress profiles underneath the four points given by *Settle3D* compared to the analytical solutions.

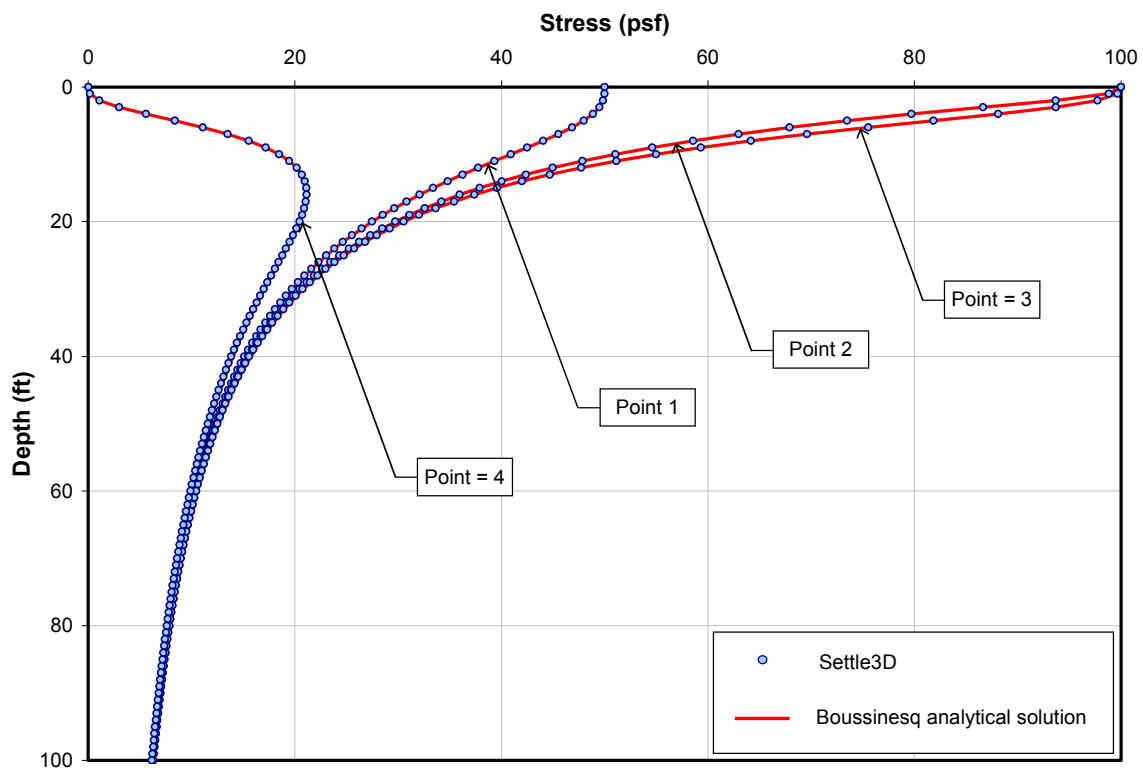


*Fig. 6.3 Vertical Stress Profiles*

### 6.4 References

1. H. G. Poulos and E. H. Davis (1974), *Elastic Solutions for Soil and Rock Mechanics*, New York: John Wiley & Sons.

## 7 Vertical Stresses underneath an Irregular Shape Footing due to Uniform Loading

### 7.1 Problem description

This problem verifies the vertical stresses below one of the corners of an irregular shape footing. The footing is subjected to a uniform loading ( $q$ ) of 1 kPa. The model geometry is shown in Figure 7.1. The vertical stress results are compared to analytical solution.

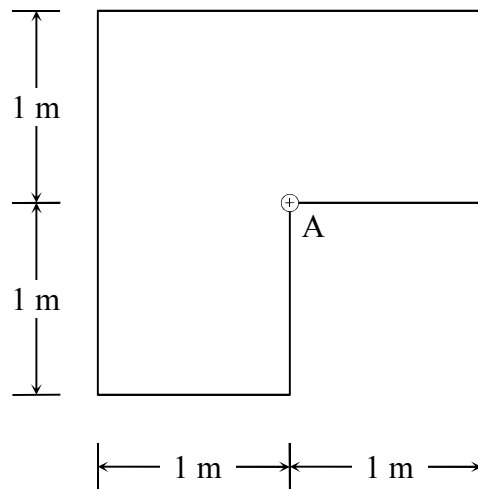


*Figure 7.1 – Model Geometry*

### 7.2 Closed Form Solution

Vertical stress at any depth ( $z$ ) below Point A is obtained by using Newmark's integration:

$$\sigma_z = q \frac{1}{4\pi} \left[ \frac{2MN \sqrt{V} V+1}{V+V_1} \frac{V+1}{V} + \tan^{-1} \left( \frac{2MN \sqrt{V}}{V-V_1} \right) \right]$$

where

$$M = \frac{B}{z}$$

$$N = \frac{L}{z}$$

$$V = M^2 + N^2 + 1$$

$$V_1 = (MN)^2$$

and when  $V_1 > V$  the  $\tan^{-1}$  term will become negative and  $\pi$  needs to be added (Bowles, 1996).

### 7.3 Results and Discussion

Figure 7.2 shows vertical stress profile at Point A given by *Settle3D* compared to the analytical solutions.

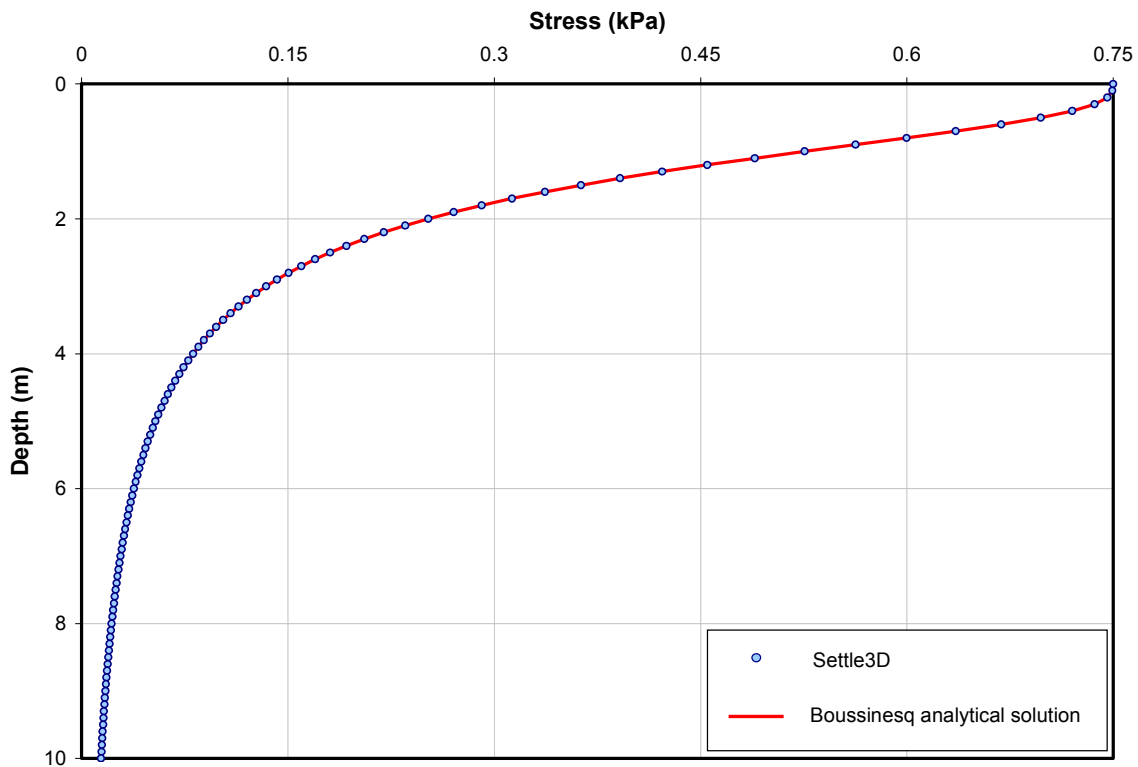


*Fig. 7.2 Vertical Stress Profiles at Point A*

### 7.4 References

1. H. G. Poulos and E. H. Davis (1974), *Elastic Solutions for Soil and Rock Mechanics*, New York: John Wiley & Sons.
2. J. E. Bowles (1996), *Foundation Analysis and Design*, 5<sup>th</sup> Ed., New York: McGraw-Hill.

## 8 Analysis of Mean Stress

### 8.1 Problem description

This problem verifies the mean stresses distribution beneath two types of uniform loading: circular and infinite strip. The loading used in this verification example ( $q$ ) is 100 kPa.

The mean stress results at the center of each load are compared to analytical solutions.

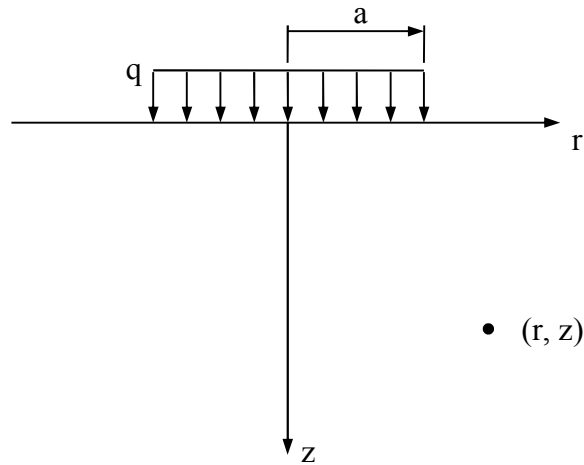


*Figure 8.1 – Model Geometry for Circular Loading*

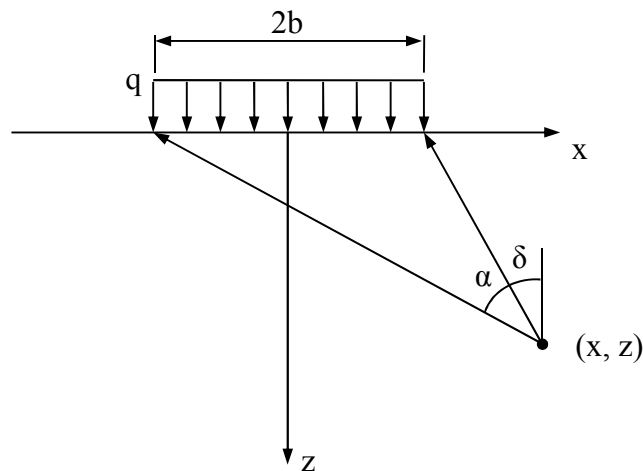


*Figure 8.2 – Model Geometry for Strip Loading*

## 8.2 Closed Form Solution

### Circular Loading

On the vertical axis (i.e.  $r=0$ ):

$$\sigma_z = q \left\{ 1 - \left[ \frac{1}{1 + (a/z)^2} \right]^{\frac{3}{2}} \right\}$$

$$\sigma_r = \sigma_\theta = \frac{q}{2} \left\{ (1 + 2\nu) - \frac{2(1 + \nu)z}{(a^2 + z^2)^{1/2}} + \frac{z^3}{(a^2 + z^2)^{3/2}} \right\}$$

$$\text{and } \sigma_m = \frac{\sigma_z + \sigma_r + \sigma_\theta}{3}$$

### Infinite Strip

$$\sigma_z = \frac{q}{\pi} \{ \alpha + \sin \alpha \cos(\alpha + 2\delta) \}$$

$$\sigma_x = \frac{q}{\pi} \{ \alpha - \sin \alpha \cos(\alpha + 2\delta) \}$$

$$\sigma_y = \frac{2q}{\pi} \nu \alpha$$

$$\text{and } \sigma_m = \frac{\sigma_z + \sigma_x + \sigma_y}{3}$$

### 8.3 Results and Discussion

Figures 8.3 and 8.4 show mean stress profiles at for the circular load and infinite strip load respectively, given by *Settle3D* compared to the analytical solutions.

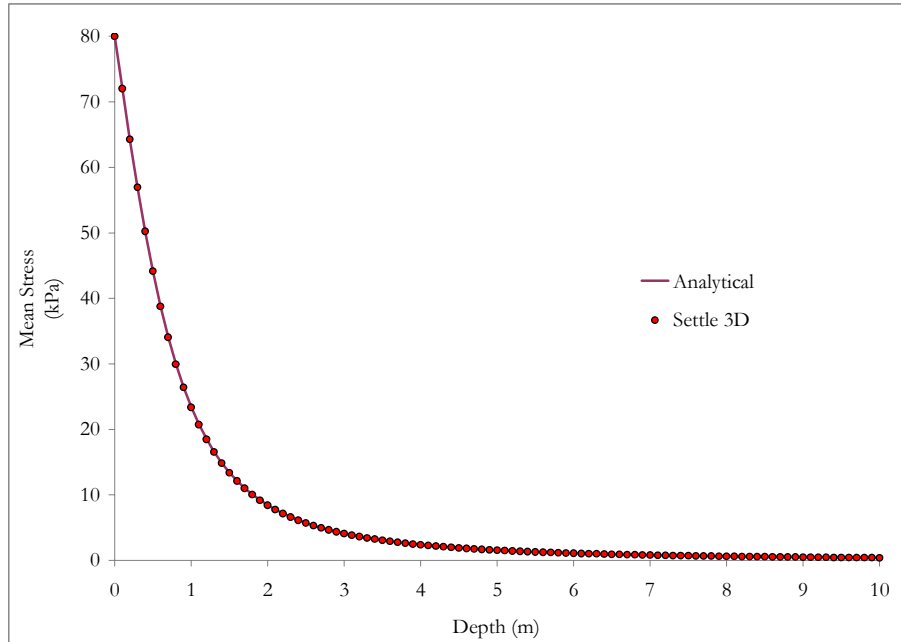


*Fig. 8.3 Mean Stress Profile for Circular Load*

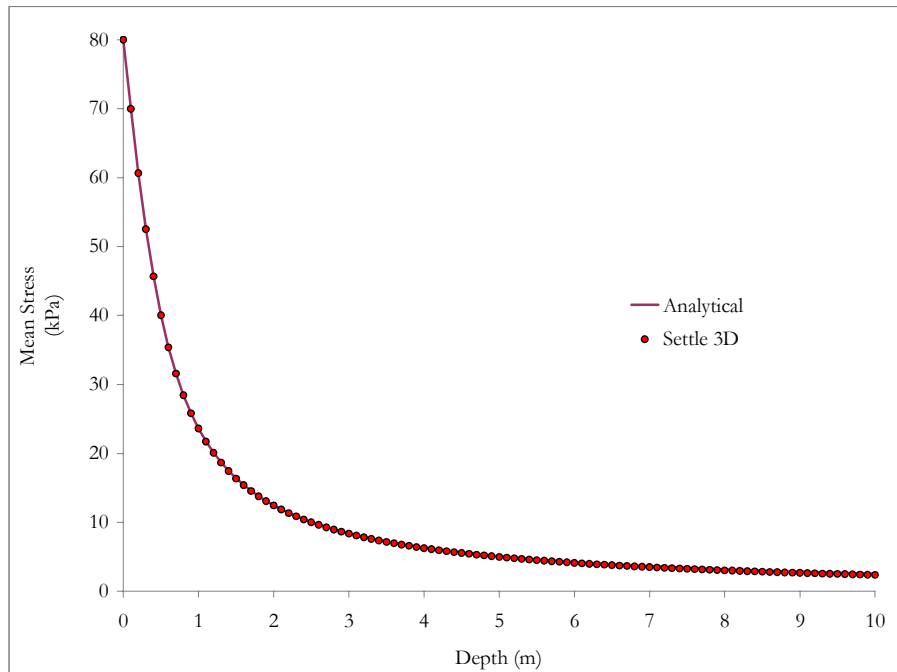


*Fig. 8.3 Mean Stress Profile for Infinite Strip Load*

## 8.4 References

1. H. G. Poulos and E. H. Davis (1974), *Elastic Solutions for Soil and Rock Mechanics*, New York: John Wiley & Sons.

# 9 Immediate Settlement

## 9.1 Problem description

This problem verifies the mean immediate settlement beneath two types of uniform loading: circular (2.5 m radius) and rectangular (5x10 m). The loading used in this verification example ( $q$ ) is 100 kPa. The modulus of elasticity ( $E$ ) is varied between 1800 kPa and 70000 kPa.

The immediate settlement at the center of each load is compared to a method proposed by Mayne and Poulos.

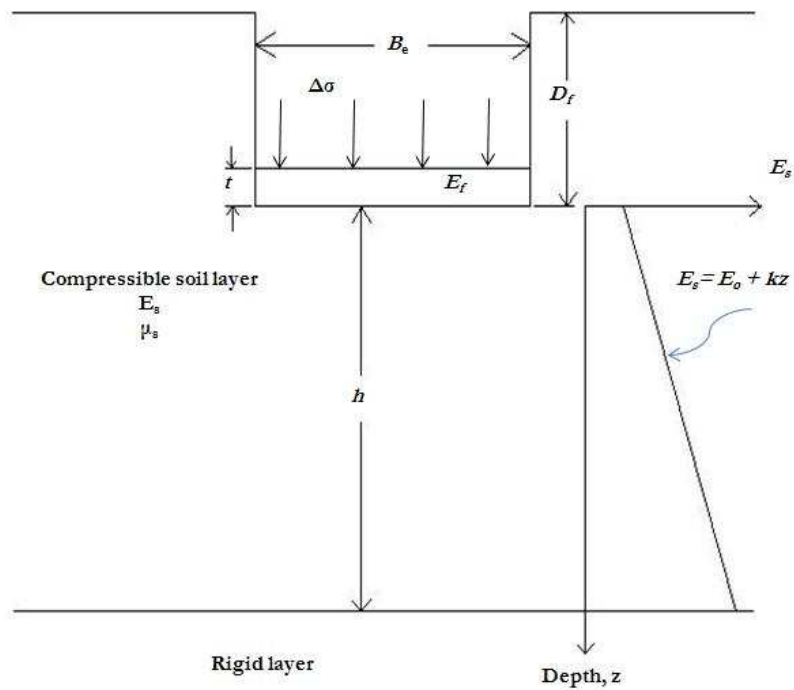


Figure 9.1 – Model Geometry

## 9.2 Closed Form Solution

Mayne and Poulos (1999) proposed a method for calculating the immediate settlement at the centre of foundations that accounts for the rigidity of the foundation, the depth of embedment of the foundation, the change in strength of soil with depth and the location of a rigid layer. The settlement is calculated using the following equation:

$$S_e = \frac{\Delta\sigma B_e I_G I_F I_E}{E_o (1 - \mu_s^2)}$$

where  $I_G$  is an influence factor for the variation of  $E_s$  with depth,  $I_F$  is a foundation rigidity correction factor,  $I_E$  is a foundation embedment correction factor.  $I_G$  varies according to Figure 9.2, and  $I_F$  and  $I_E$  are calculated using the following equations (see Figure 9.1 for parameter definitions):

$$I_F = \frac{\pi}{4} + \frac{1}{4.6 + 10 \left( \frac{E_f}{E_o + \frac{B_e}{2} k} \right) \left( \frac{2t}{B_e} \right)^2} \quad I_E = 1 - \frac{1}{3.5 \exp(1.22\mu_s - 0.4) \left( \frac{B_e}{D_f} + 1.6 \right)}$$

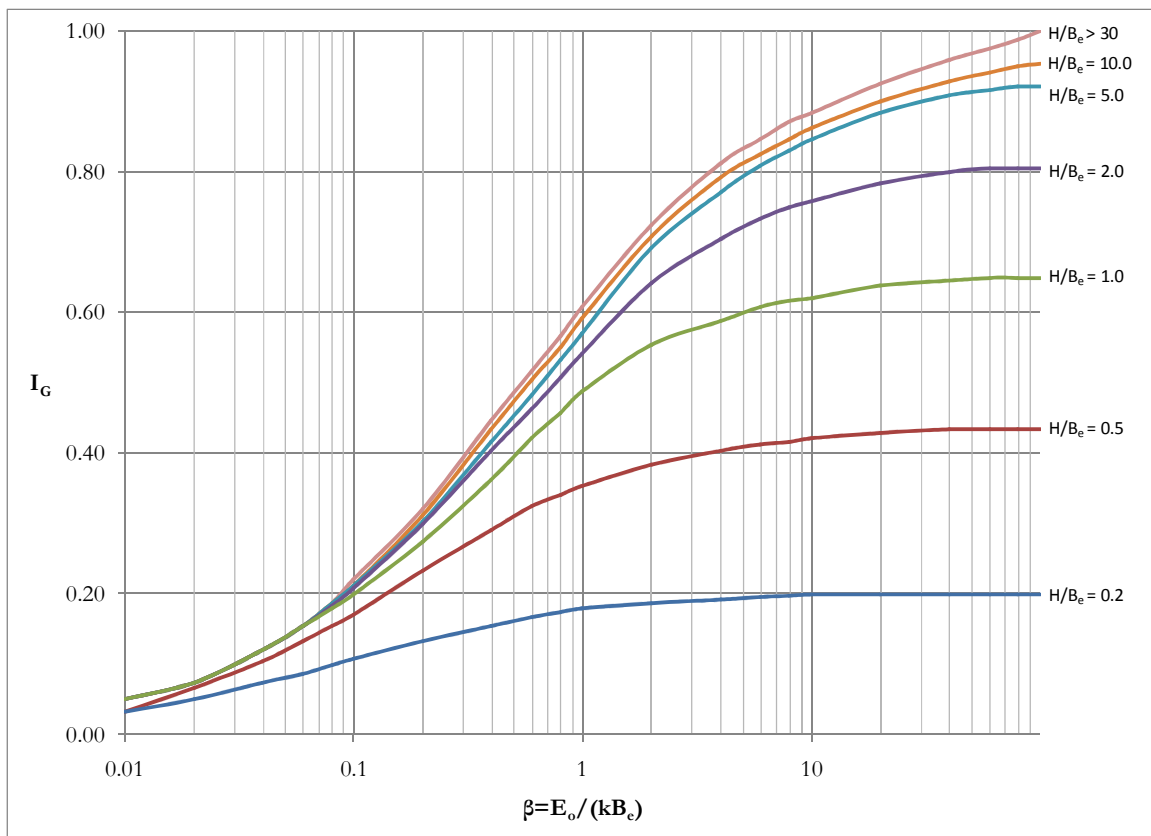
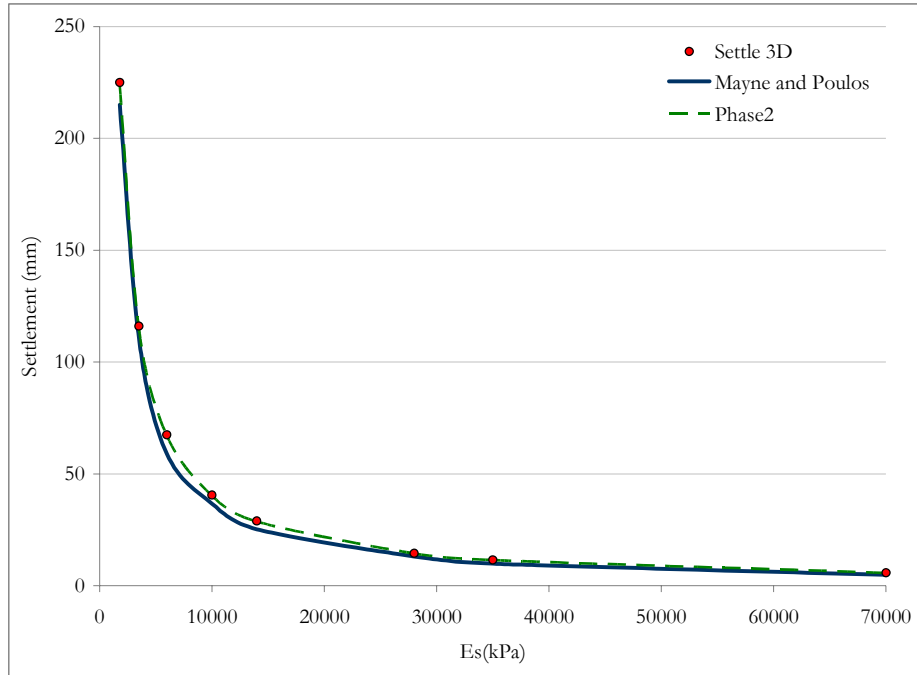


Figure 9.2 – Variation of  $I_G$  with  $\beta$

### 9.3 Results and Discussion

Figures 9.3 and 9.4 show immediate settlement values for the circular and rectangular load, given by *Settle3D* compared to the method proposed by Mayne and Poulos.



**Fig. 9.3 Immediate Settlement for Circular Load**

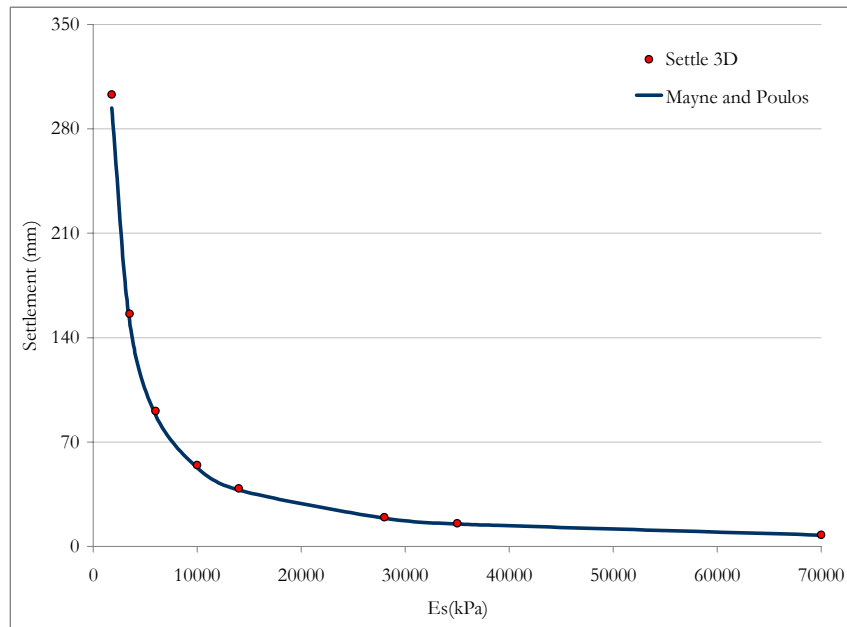


**Fig. 9.4 Immediate Settlement for Rectangular Load**

## 9.4 References

1. Das, Braja M., *Principle of Geotechnical Engineering*, Fifth Edition, Brooks/Cole, 2002.

# 10 Uniform Vertical Loading on Circular Surface Area of Two-Layer System

## 10.1 Problem description

This example verifies the vertical stress at a location along the perfectly bonded interface under uniform vertical loading at the surface. The first (upper) layer has a height of  $h_1$  (m) while the second layer is assumed to be of infinite height  $h_2$  (m). The two-layered system of materials is subjected to a uniform vertical loading ( $p$ ) of 1 kPa acting over a circular area of radius  $a$  (m). The model geometry is shown on Figure 10.1. On the figure, the radial direction (horizontal axis) is labeled  $r$  while the vertical axis (that passes through the centre of the circular loading area) is labeled  $z$ . The elastic constants – Young’s moduli  $E_1$  and  $E_2$  and Poisson’s ratios  $\nu_1$  and  $\nu_2$  – of the materials are also indicated.

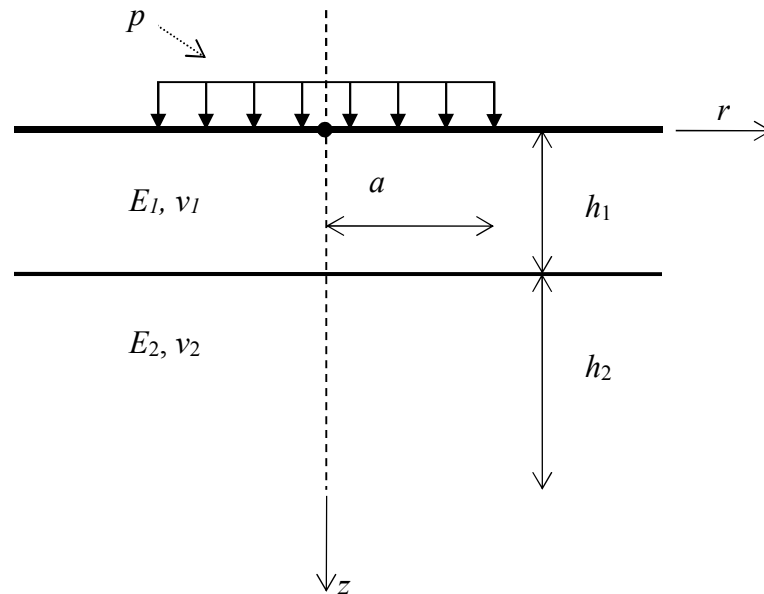


Figure 10.1 – Model Geometry

## 10.2 Results and Discussion

### 10.2.1 Part 1

Part 1 of the verification, the results of which are shown on Figure 10.2, plots the elastic moduli ratio  $E_1/E_2$  against normalized vertical interface stress (on the  $z$  axis) for four different  $r/a$  ratios. The five different cases considered are as follows:

- Case 1:  $E_1/E_2 = 0.1$
- Case 2:  $E_1/E_2 = 1$
- Case 3:  $E_1/E_2 = 10$
- Case 4:  $E_1/E_2 = 100$

- Case 5:  $E_1/E_2 = 1000$

This part of the verification assumes an  $h_1/a$  ratio equal to 1, i.e. height of layer 1 equal to the radius of the circular loading area. For each of the above cases, normalized vertical interface stresses were calculated at values of the elastic moduli ratio  $E_1/E_2 = 0.1, 1.0, 10, 100, 1000$ .

The results of the multiple-layer algorithm in *Settle<sup>3D</sup>* are compared to those of the Fox (1948) two-layered analytical solution and values from the finite element program *Phase<sup>2</sup>*.

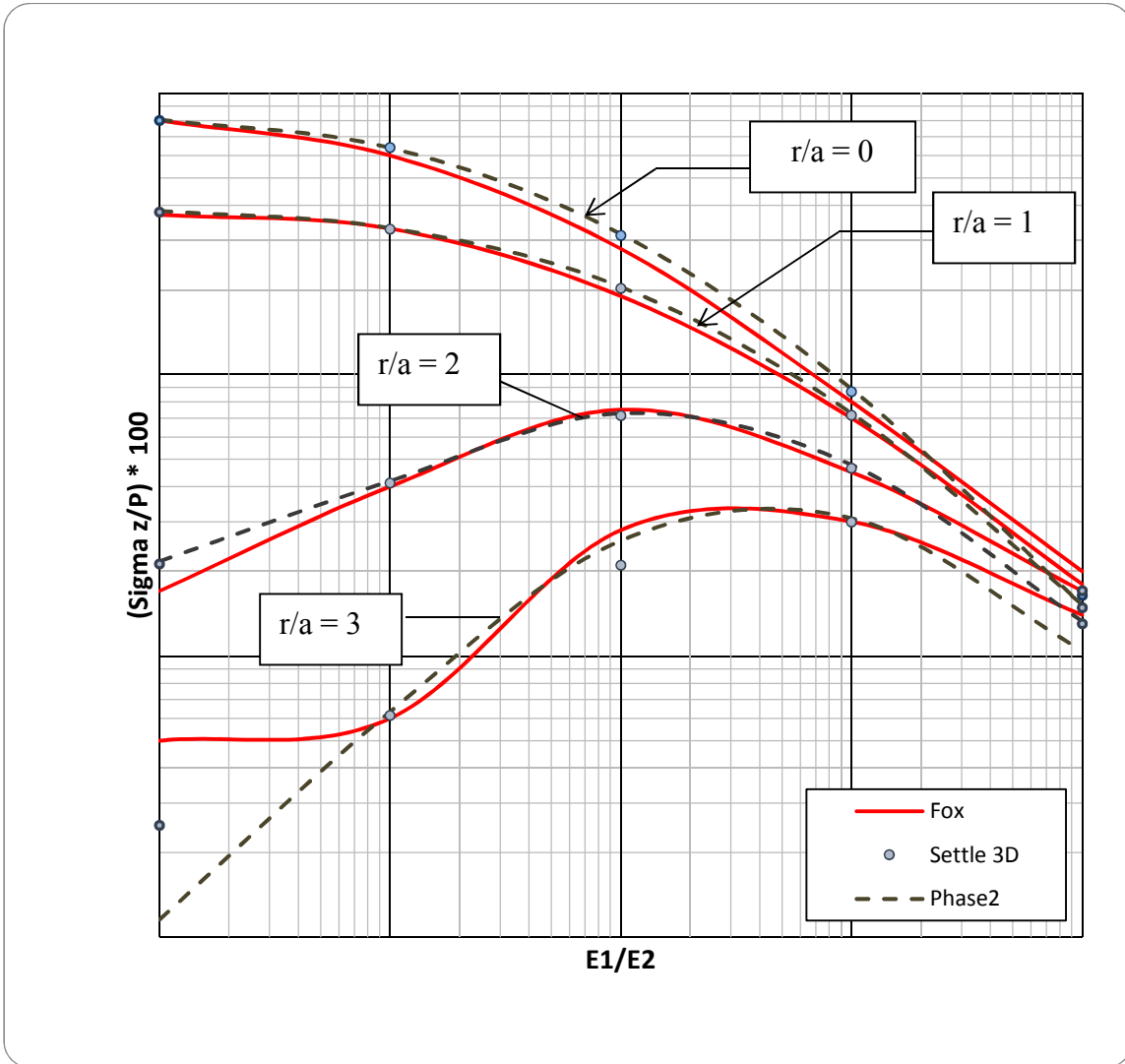


**Figure 10.2 – Normalized vertical stress on the axis at the interface (for the ratio  $h_1/a = 1$ )**

### 10.2.2 Part 2

Part 2 of the verification, the results of which are shown on Figure 10.3, plots the elastic moduli ratio  $E_1/E_2$  against normalized vertical interface stress (on the  $z$  axis) for three different cases of the ratio  $h_1/a$ .

The ratios are as follows:

- Case 6:  $h_1/a = 0.5$
- Case 7:  $h_1/a = 1.0$
- Case 8:  $h_1/a = 2.0$

For each of the above cases, normalized vertical interface stresses are calculated at values of the elastic moduli ratio  $E_1/E_2 = 0.1, 1.0, 10, 100, 1000$ . The results of *Settle*<sup>3D</sup> are compared to those of Fox (1948) and values obtained from the finite element program *Phase*<sup>2</sup>.

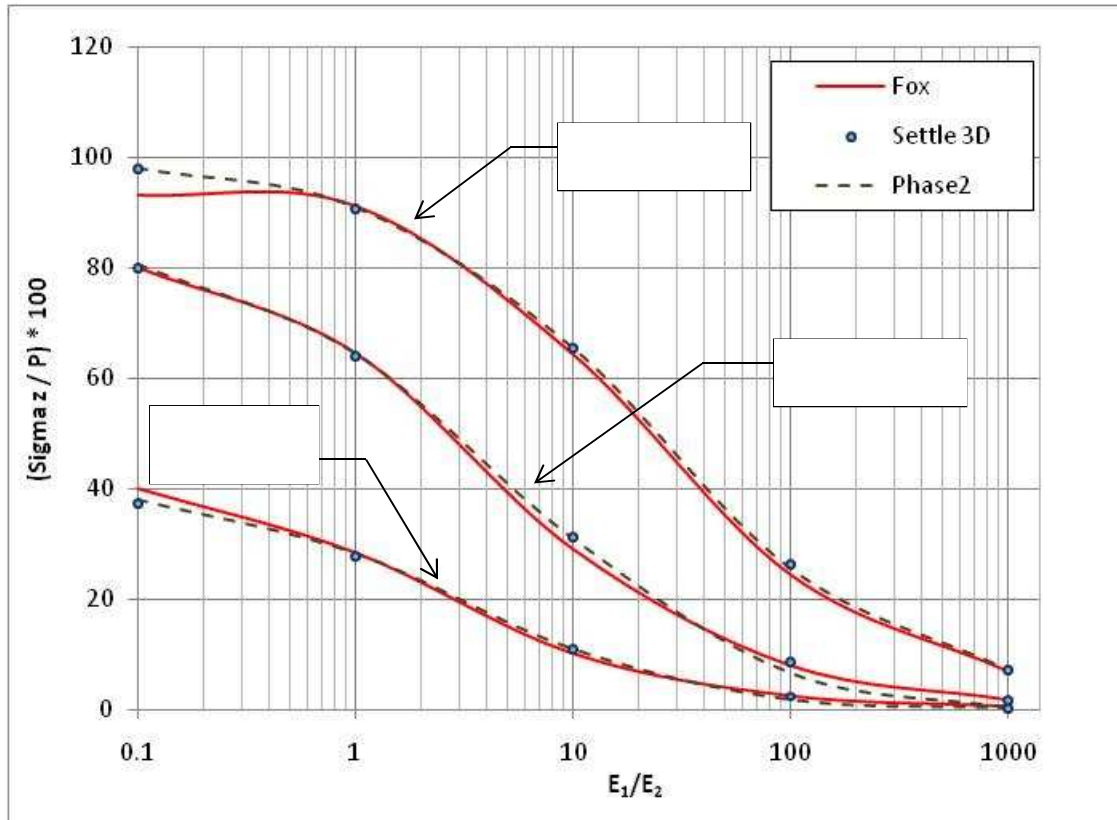


Figure 10.3 – Normalized vertical stress on the axis at the interface for different  $h_1/a$  ratios

### 10.3 References

1. H. G. Poulos and E. H. Davis (1974), *Elastic Solutions for Soil and Rock Mechanics*, New York: John Wiley & Sons.
2. Fox, L. (1948), *Computations of traffic stresses in a simple road structure*, Proceedings 2<sup>nd</sup> International Conference on Soil Mechanics and Foundation Engineering, Vol.2 pp. 236-246.

# 11 Uniform Vertical Loading on Circular Surface Area of Three-Layer System

## 11.1 Problem description

This example verifies the vertical stresses at the two perfectly bonded interfaces of a three layer system under uniform vertical loading at the surface. The first (uppermost) layer has a height of  $h_1$  (m), the second layer a height of  $h_2$  (m), while the third is assumed to be of infinite height. The three-layered system of materials is subjected to a uniform vertical loading ( $p$ ) of 1 kPa acting over a circular area of radius  $a$  (m) equal to 1 (m).

The model geometry is shown on Figure 11.1. On the figure, the radial direction (horizontal axis) is labeled  $r$  while the vertical axis (that passes through the centre of the circular loading area) is labeled  $z$ . The elastic constants – Young’s moduli  $E_1, E_2$  and  $E_3$  and Poisson’s ratios  $\nu_1, \nu_2$  and  $\nu_3$  – of the materials are also indicated. The vertical stresses at the interfaces are evaluated at the  $z$  vertical axis (i.e. at  $r=0$ ).

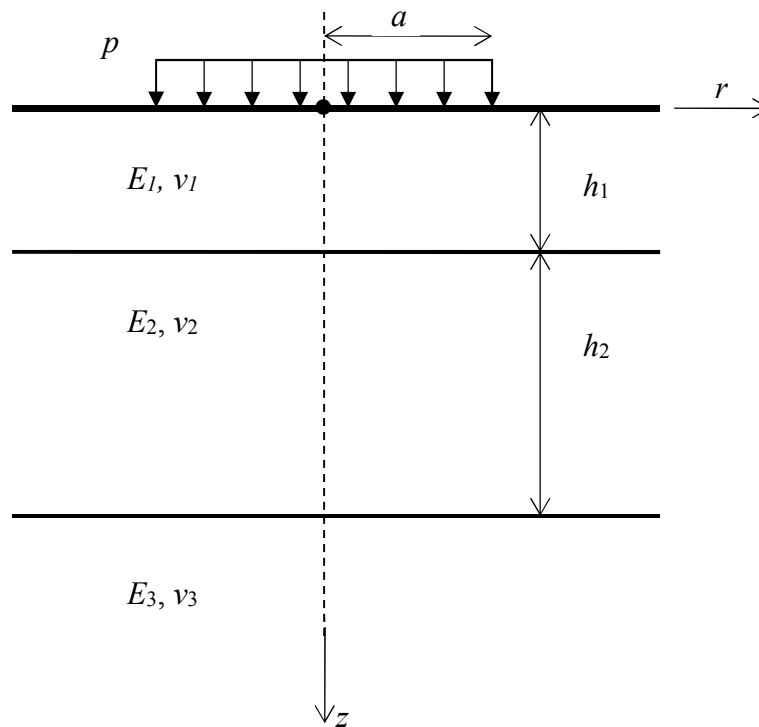


Figure 11.1 – Model Geometry

## 11.2 Results and Discussion

### 11.2.1 Part 1

For Part 1 of the verification the following notations are employed:

$$a_1 = a/h_1$$

$$H = h/h_2$$

$$K_1 = E_1/E_2$$

$$K_2 = E_2/E_3$$

The Poisson's ratios of all three materials are assumed to be 0.5 (i.e.  $\nu_1 = \nu_2 = \nu_3 = 0.5$ ). A ratio  $a_1 = 0.1$  is also assumed. The following cases of the ratio  $H$  are considered:

- Case 1:  $H = 0.125$
- Case 2:  $H = 0.25$
- Case 3:  $H = 0.5$
- Case 4:  $H = 1.0$
- Case 5:  $H = 2.0$
- Case 6:  $H = 4.0$

Lastly, vertical stresses for the two interfaces were evaluated (on the  $z$  axis) at the following  $K_1$  and  $K_2$  ratios:  $K_1 = 0.2, 2, 20, 200$ , and  $K_2 = 0.2, 2, 20, 200$ .

The vertical stress results calculated by the *Settle*<sup>3D</sup> multiple-layer method are compared to those given in the tabulated solutions of Jones (1962), which are also provided in Poulos and Davis (1974). Figures 11.2 to 11.13 show the plots for the first and second interfaces for the different cases of  $H$ .

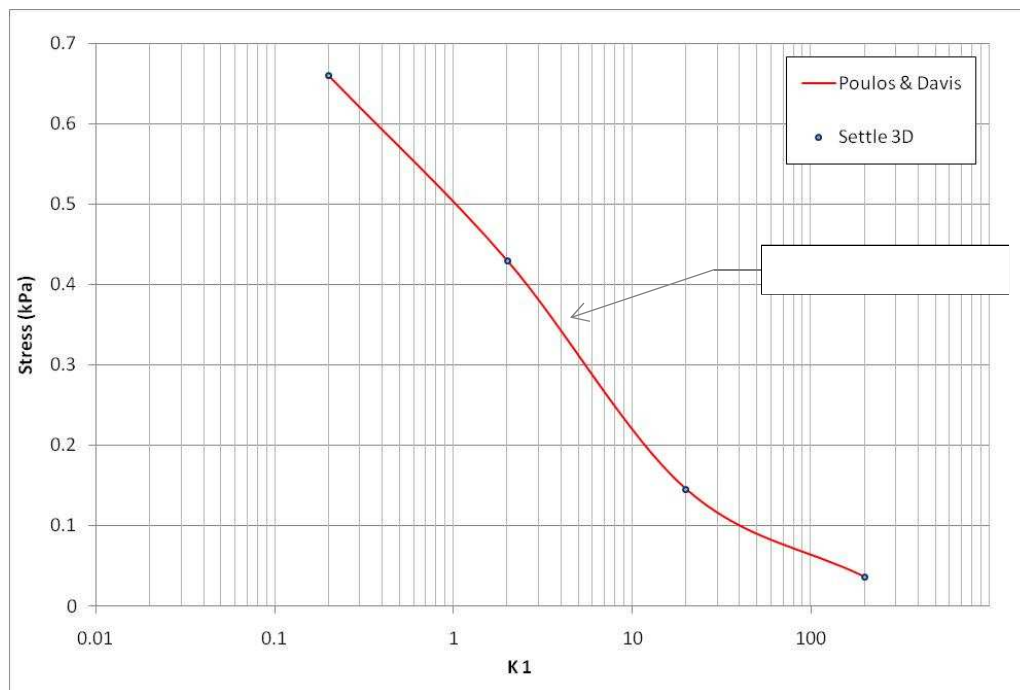


**Figure 11.2 – Vertical stress underneath loading centre at first interface (for  $H=0.125$ )**

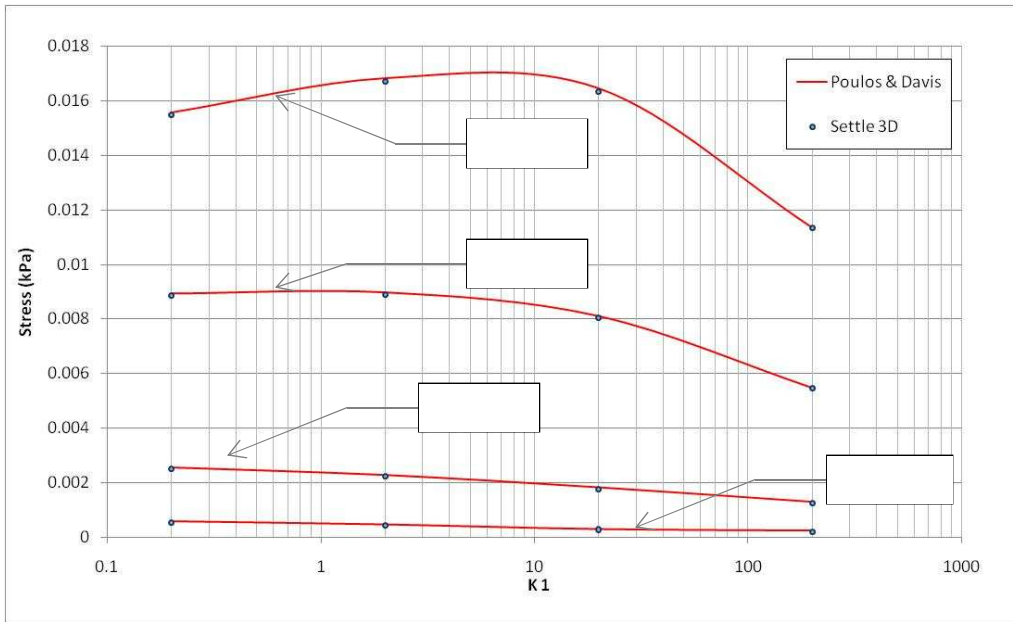


Figure 11.3 – Vertical stress underneath loading centre at second interface (for  $H=0.125$ )

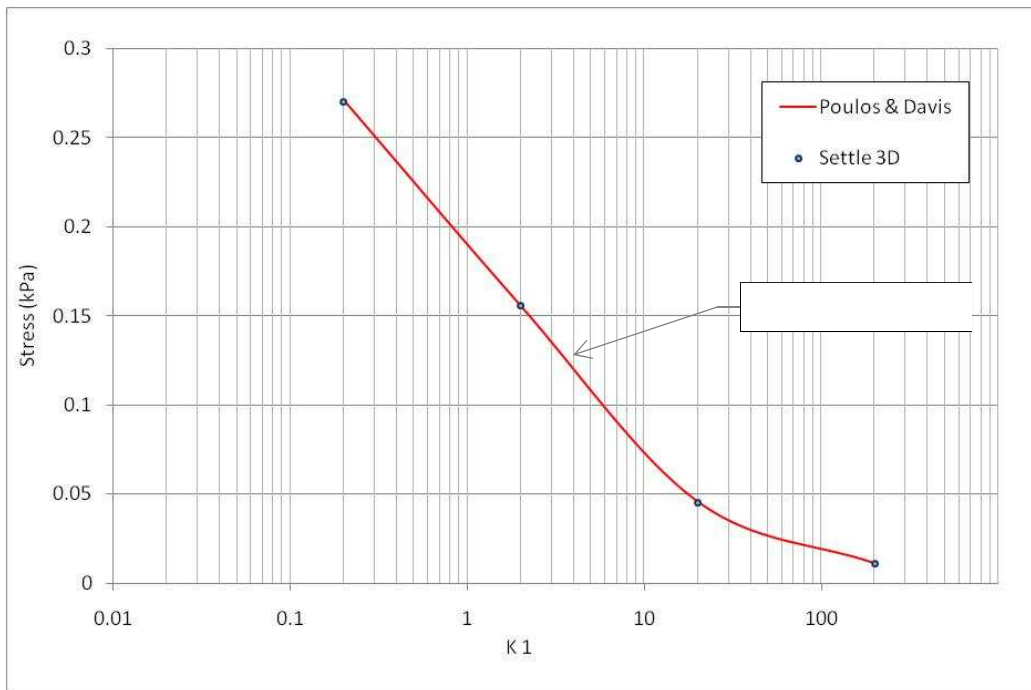


Figure 11.4 – Vertical stress underneath loading centre at first interface (for  $H=0.25$ )

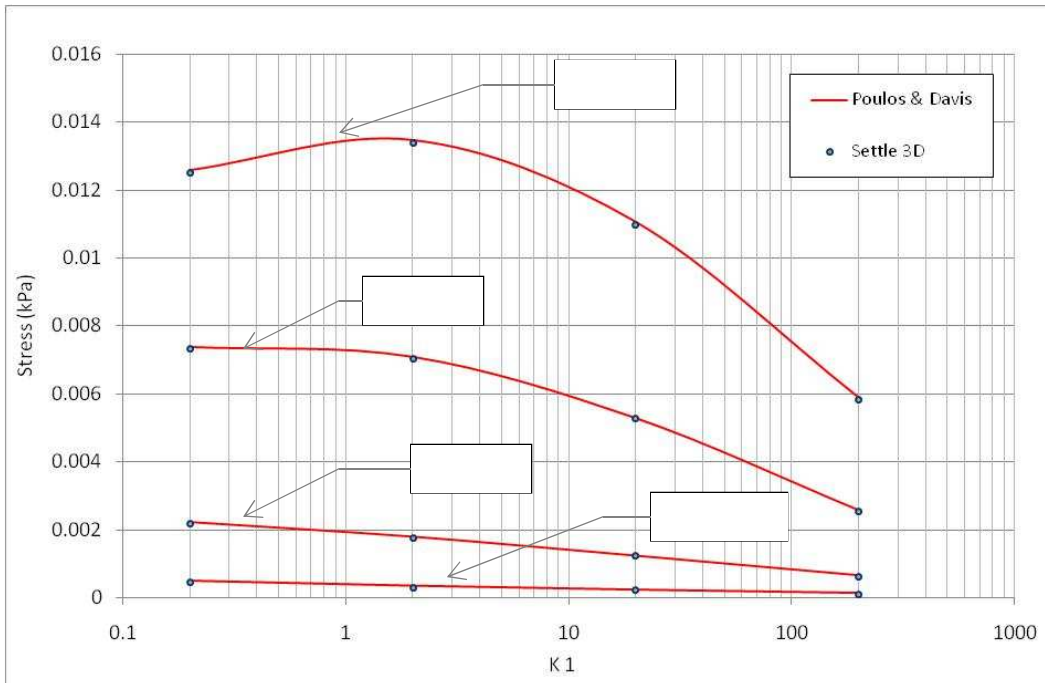


Figure 11.5 – Vertical stress underneath loading centre at second interface (for  $H=0.25$ )

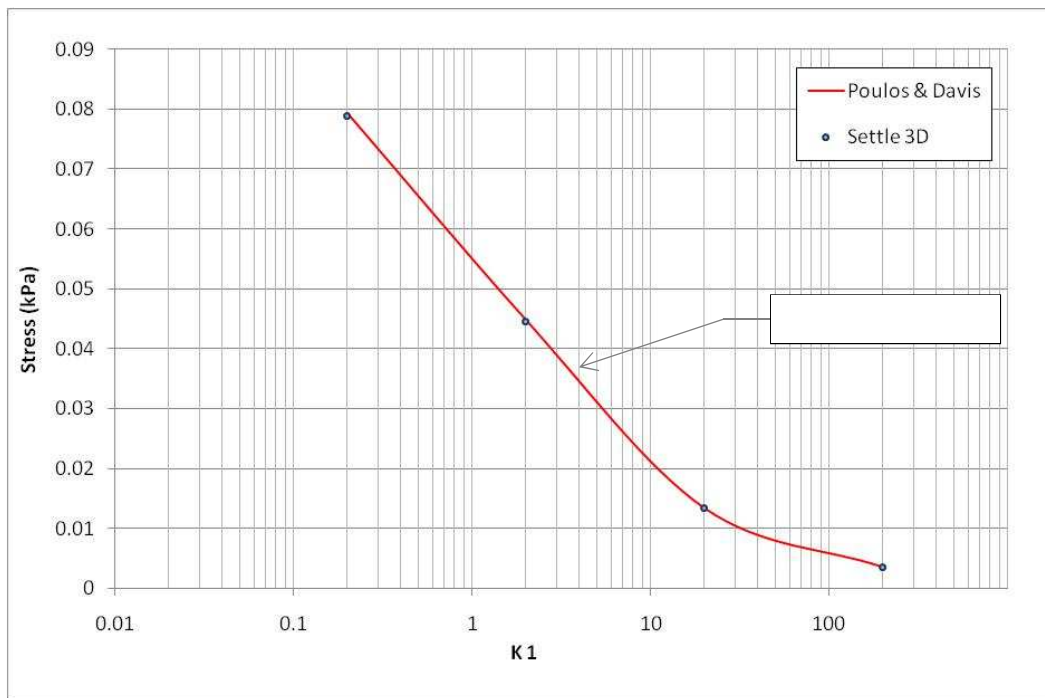
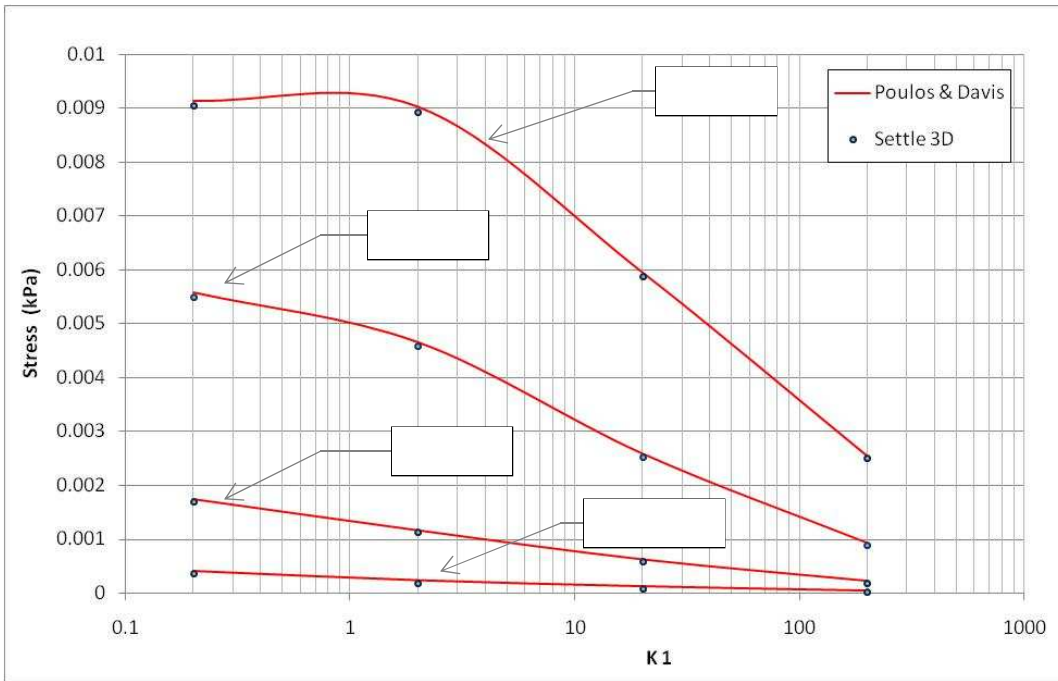
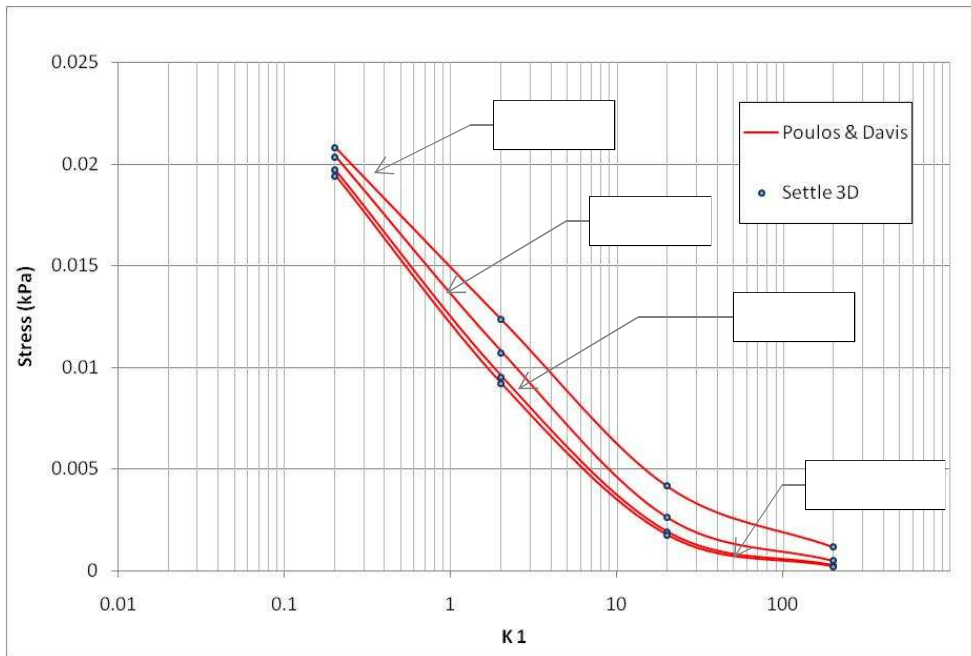


Figure 11.6 – Vertical stress underneath loading centre at first interface (for  $H=0.5$ )



**Figure 11.7 – Vertical stress underneath loading centre at second interface (for  $H=0.5$ )**



**Figure 11.8 – Vertical stress underneath loading centre at first interface (for  $H=1.0$ )**

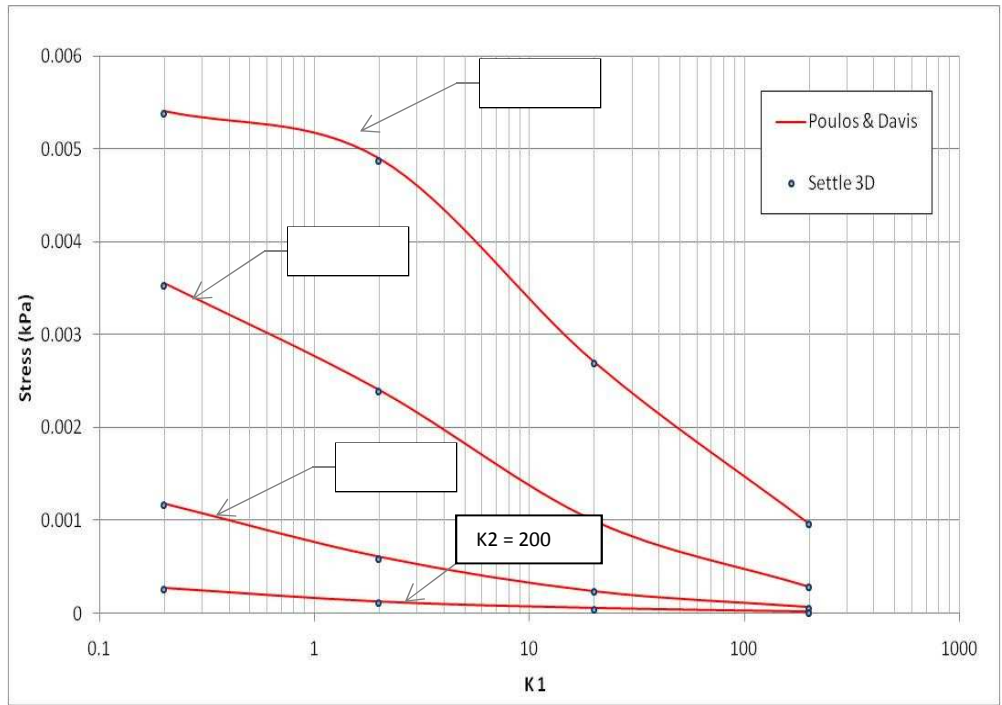


**Figure 11.9 – Vertical stress underneath loading centre at second interface (for  $H=1.0$ )**

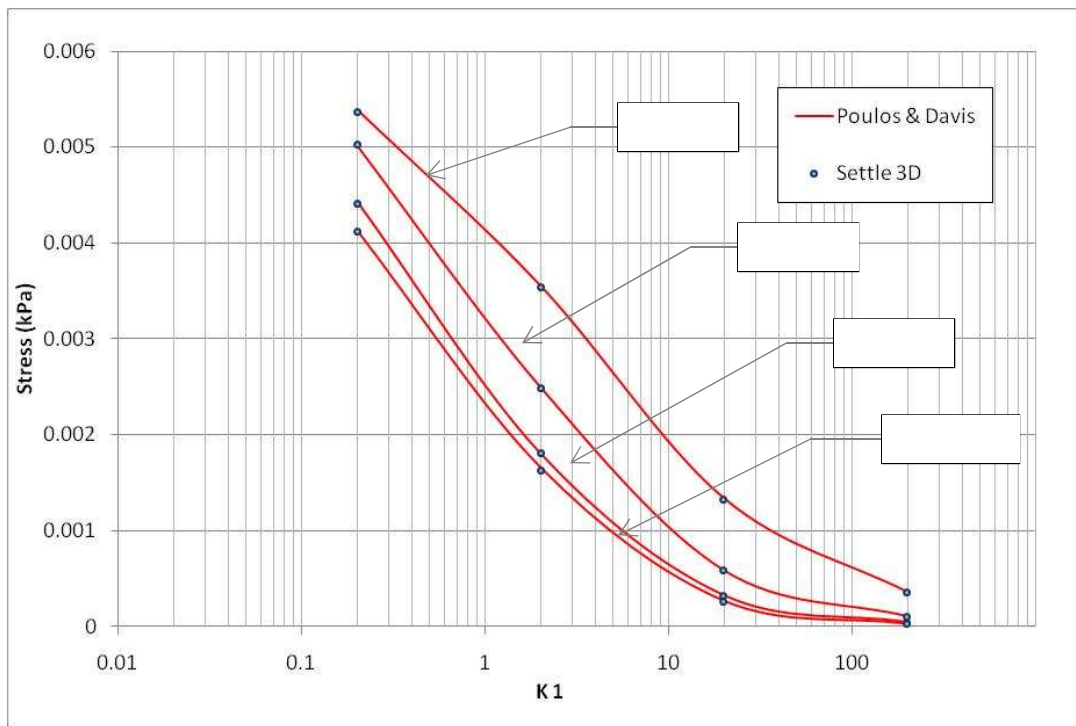


**Figure 11.10 – Vertical stress underneath loading centre at first interface (for  $H=2.0$ )**

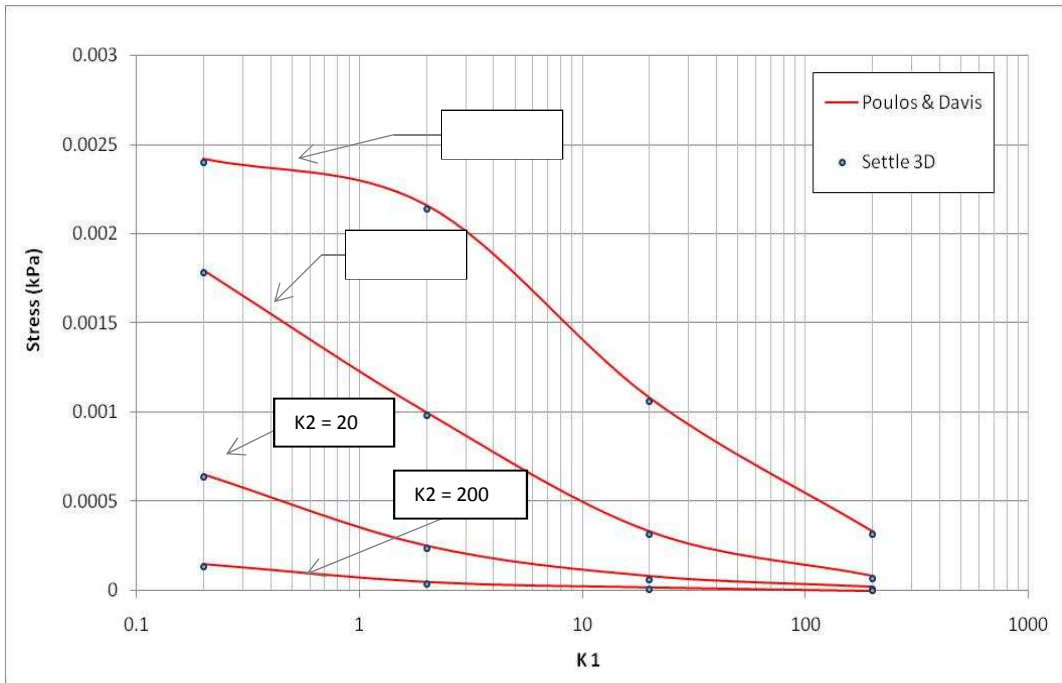


**Figure 11.11 – Vertical stress underneath loading centre at second interface (for  $H=2.0$ )**

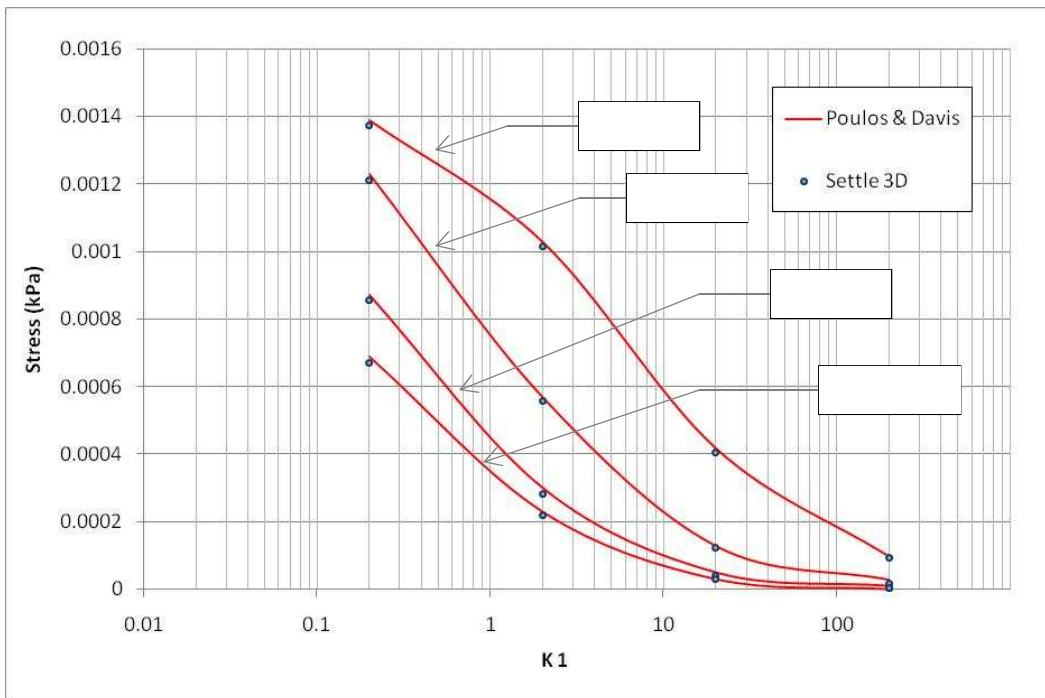


**Figure 11.12 – Vertical stress underneath loading centre at first interface (for  $H=4.0$ )**

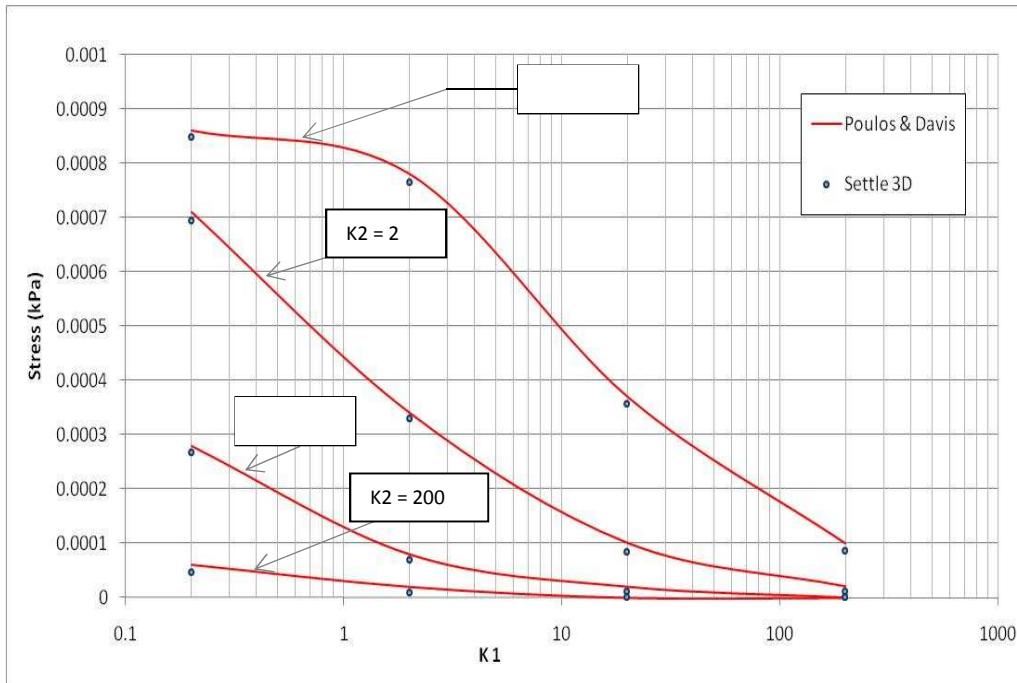


**Figure 11.13 – Vertical stress underneath loading centre at second interface (for  $H=4.0$ )**

### 11.2.2 Part 2

Part 2 of the verification considers the case in which  $H = 1.0$ . It assumes  $a_1 = 1.0$  and evaluates vertical stresses for the two interfaces at the following  $K_1$  and  $K_2$  values:  $K_1 = 5, 10, 50, 100$  and  $K_2 = 5, 10, 50, 100$ . Vertical stresses calculated by *Settle*<sup>3D</sup> at the interfaces are compared to values given by the analytical solution of Acum and Fox (1951).

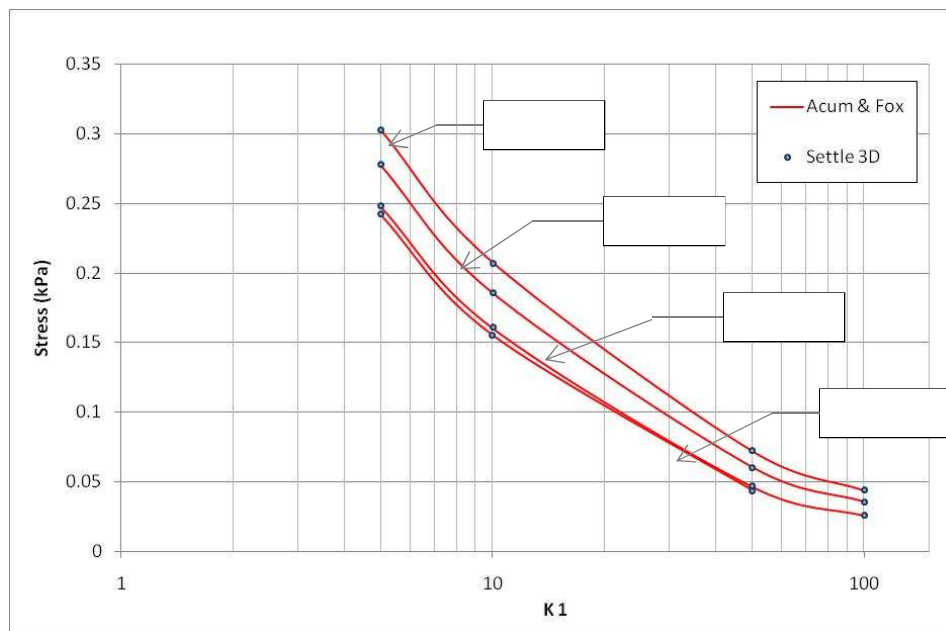


**Figure 11.14 – Vertical stress underneath loading centre at first interface ( $H=1.0$ )**

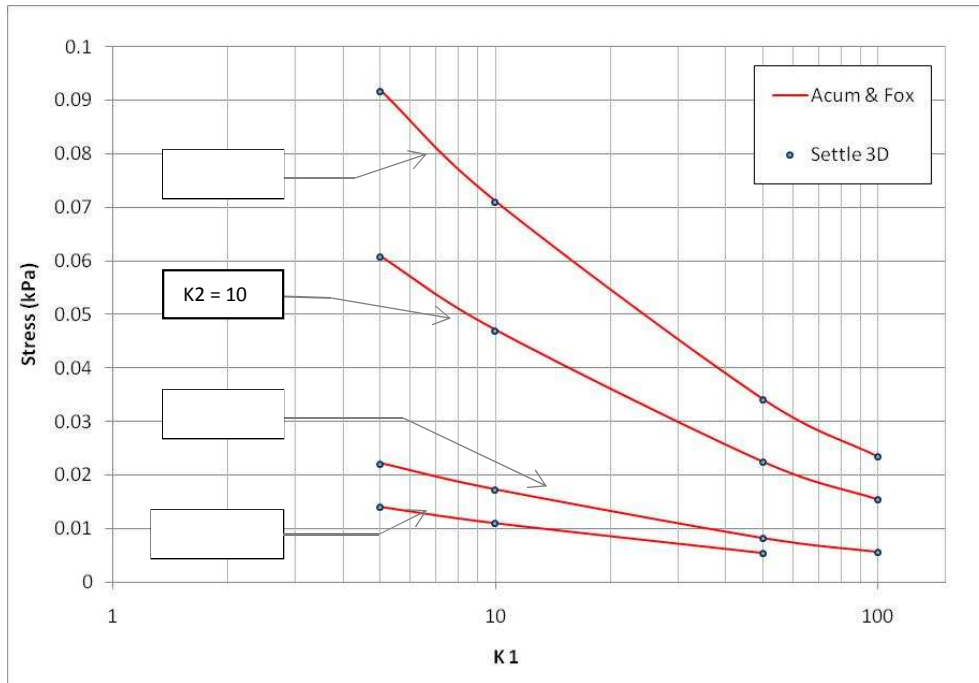


**Figure 11.15 – Vertical stress underneath loading centre at second interface ( $H=1.0$ )**

### 11.3 References

1. H. G. Poulos and E. H. Davis (1974), *Elastic Solutions for Soil and Rock Mechanics*, New York: John Wiley & Sons.
2. Jones, A. (1962). *Tables of stresses in three-layer elastic systems*. High. Res. Board, Bull. 342, pp. 128-155.
3. W.E.A. Acum and L. Fox (1951). *Computation of load stresses in a three-layer elastic system*. *Geotechnique*, No. 2, pp. 293-300.

## 12 Vertical Strip Loading on Surface of Material Underlain by Rigid Infinite Layer

### 12.1 Problem description

This example verifies the vertical stresses beneath a strip loading with width  $a$  (m) acting on the surface of a two-layer system. The upper layer of height  $h_1$  (m) is underlain by a rigid material of infinite height. The interface between the two materials is assumed to be perfectly bonded (rough). The strip loading ( $p$ ) is uniform with a magnitude of 1 kPa. The model geometry is shown on Figure 12.1. On the figure, the horizontal direction is labeled  $x$  while the vertical axis (that passes through the centre of the strip loading) is labeled  $z$ . The elastic constants – Young's modulus  $E_1$  and Poisson's ratio  $\nu_1$  – of the upper material layer are also indicated.

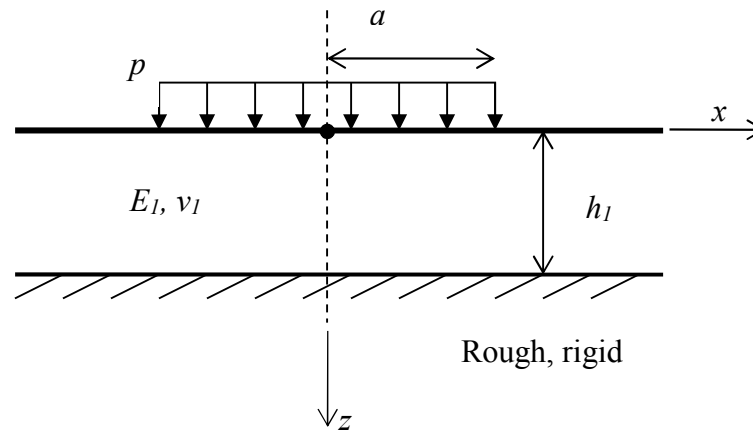


Figure 12.1 – Model Geometry

### 12.2 Results and Discussion

Vertical stresses are calculated along a vertical axis passing through the edge of the strip loading, i.e. along the axis  $x = a$ . In the example the ratio  $h_1/a$  is assumed equal to 4.0.

The following two Poisson's ratio cases are studied:

- Case 1:  $\nu = 0.2$
- Case 2:  $\nu = 0.5$

The vertical stresses computed by the multiple-layer algorithm in *Settle*<sup>3D</sup> are compared to those of Poulos (1967) and the Boussinesq method in *Settle*<sup>3D</sup>.

Figure 12.2 shows the normalized vertical stresses on the axis beneath the edge of the strip loading for the two cases of Poisson's ratio.

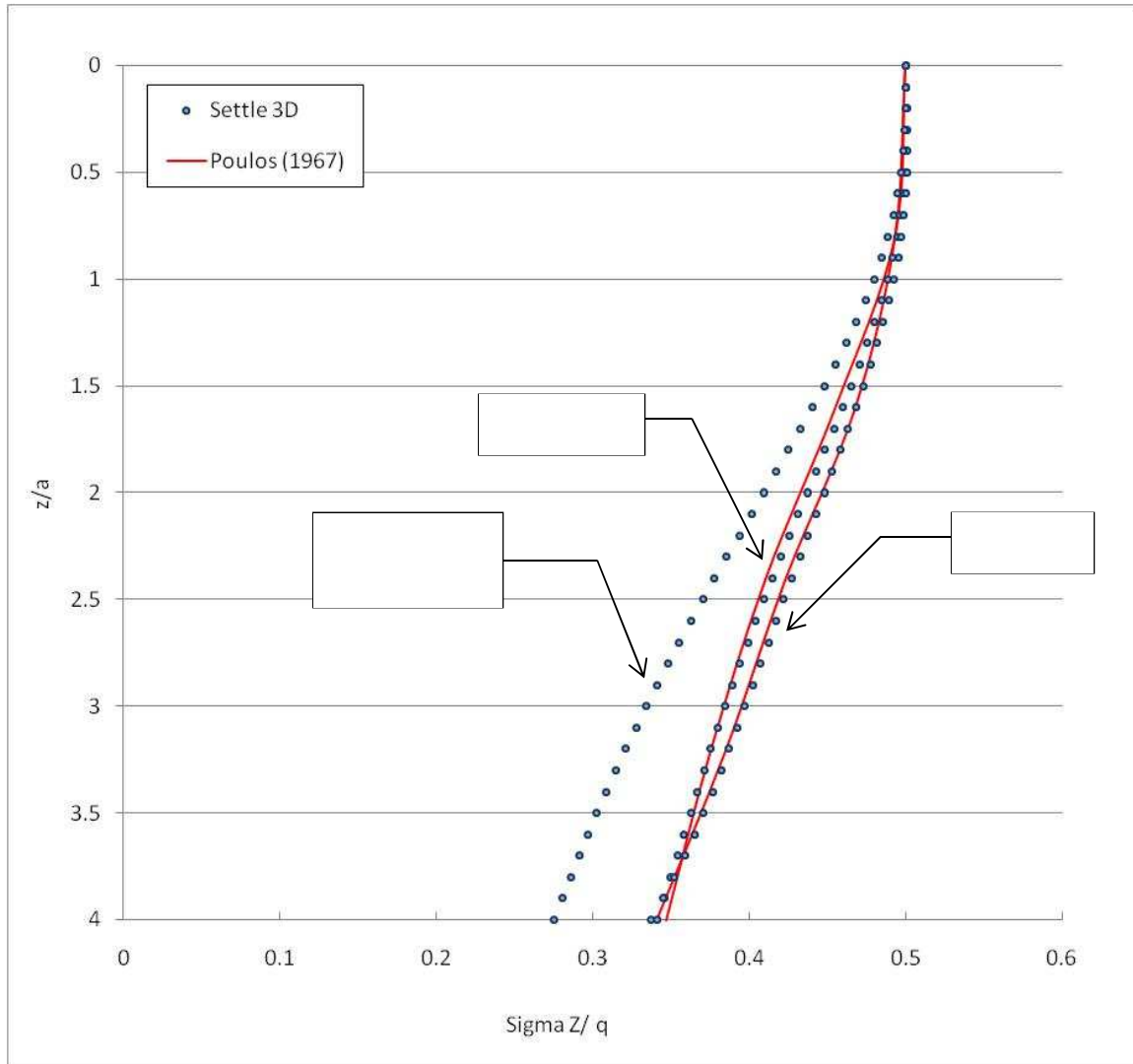


**Fig. 12.2 Normalized vertical interface stress along axis beneath edge of strip loading**

### 12.3 References

1. H. G. Poulos (1967), Stresses and displacements in an elastic layer underlain by a rough rigid base, *Geotechnique*, 17, pp. 378-410.
2. J. C. Small, J.R. Booker (1984), *Finite layer analysis of layered elastic materials using a flexibility approach Part I – Strip loadings*, *International Journal for Numerical Methods in Engineering*, Vol.20 pp. 1025-1037.

# 13 Uniform Vertical Loading on Circular Surface Area of Material Underlain by Rigid Infinite Layer

## 13.1 Problem description

This example verifies the vertical stresses in a two-layer system under a uniform vertical loading applied over a circular surface area. The upper layer of height  $h_1$  (m) is underlain by a rigid material of infinite height. The interface between the two materials is assumed to be perfectly bonded (rough). The uniform vertical loading ( $p$ ) of 1 kPa magnitude is applied over a circular area of radius  $a$  (m). The model geometry is shown on Figure 13.1. On the figure, the radial (horizontal) direction is labeled  $r$  while the vertical axis (that passes through the centre of the loading area) is labeled  $z$ . The elastic constants – Young’s modulus  $E_1$  and Poisson’s ratio  $\nu_1$  – of the upper material layer are also indicated.

The following four cases of the height of the upper layer are considered:  $h_1 = 1.0, 2.0, 4.0, 6.0$  m. In each of the cases  $\nu_1 = 0.3$  and  $a = 1.0$  m

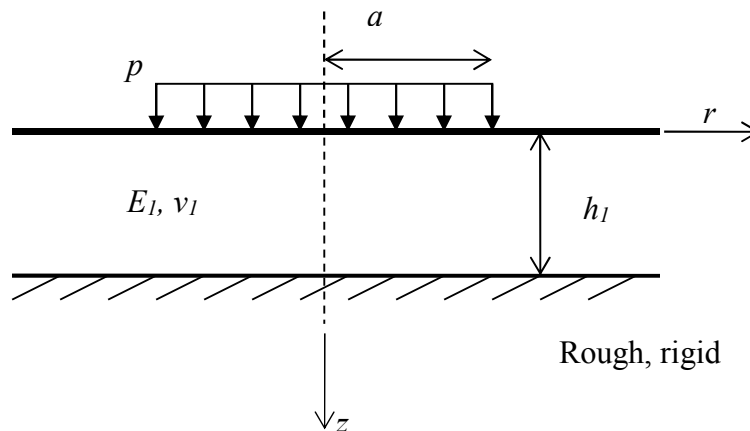
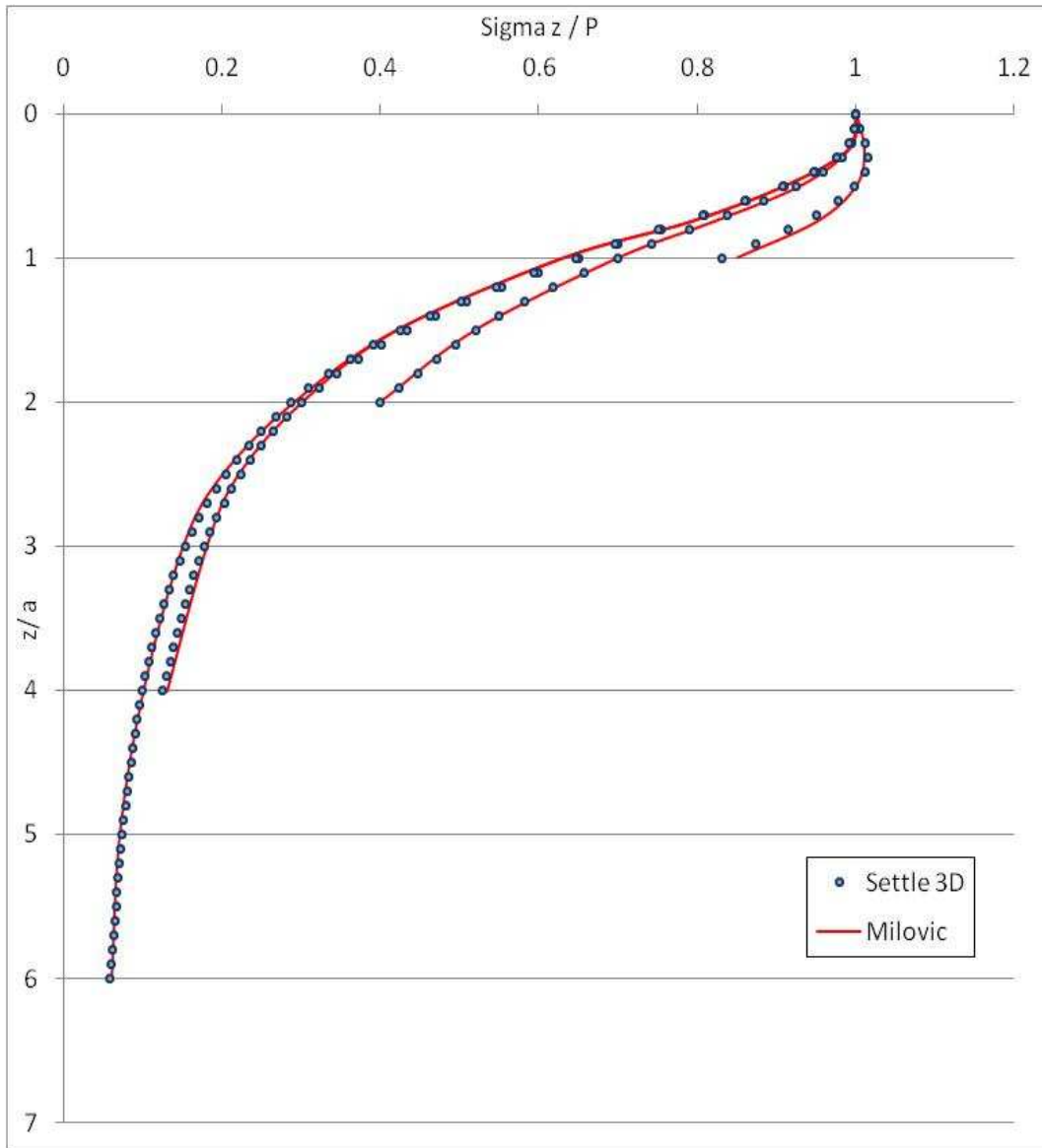


Figure 13.1 – Model Geometry

## 13.2 Results and Discussion

The vertical stresses computed by *Settle*<sup>3D</sup> in the upper layer along the  $z$  axis, and a second vertical axis ( $r = a$ ) that passes through the edge of the loading area, are compared to those of Milovic given in Poulos and Davis (1974). Figures 13.2 and 13.3 show the normalized vertical stresses through the central and edge axes, respectively.



**Figure 13.2 – Normalized vertical stresses along axis passing through centre of circular loading area**

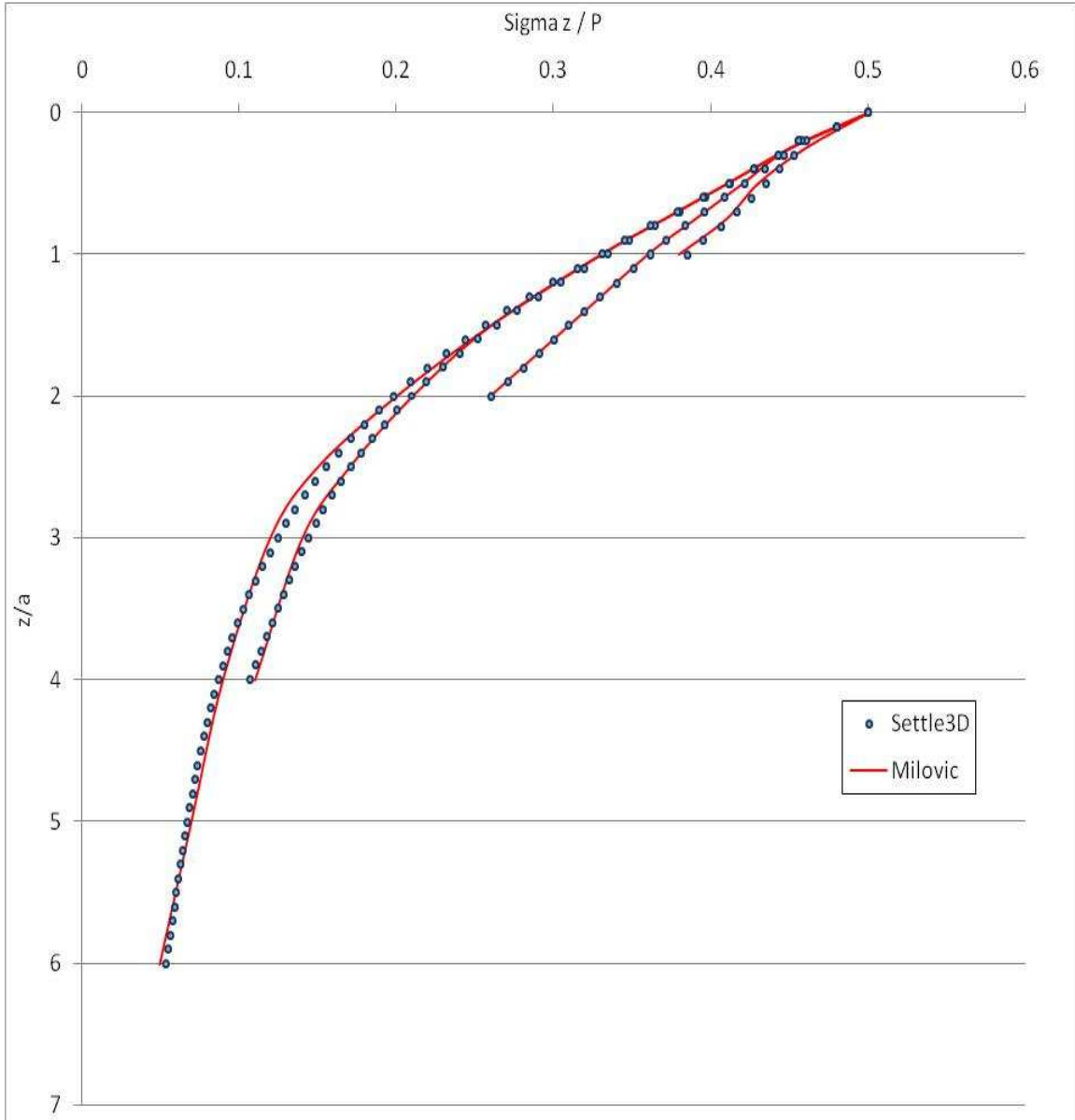


**Figure 13.3 – Normalized vertical stresses along axis passing through edge of circular loading area**

### 13.3 References

1. H. G. Poulos and E. H. Davis (1974), *Elastic Solutions for Soil and Rock Mechanics*, New York: John Wiley & Sons.

# 14 Immediate Settlement beneath a Rigid Circular Footing

## 14.1 Problem Description

This problem verifies the immediate settlement beneath a rigid circular footing. The notation with regards to the co-ordinate system is shown in Figure 14.1. In the figure, the origin of the coordinate system is taken as the point of application of the total load  $P$ . The distance from the origin is then given by  $r$ .

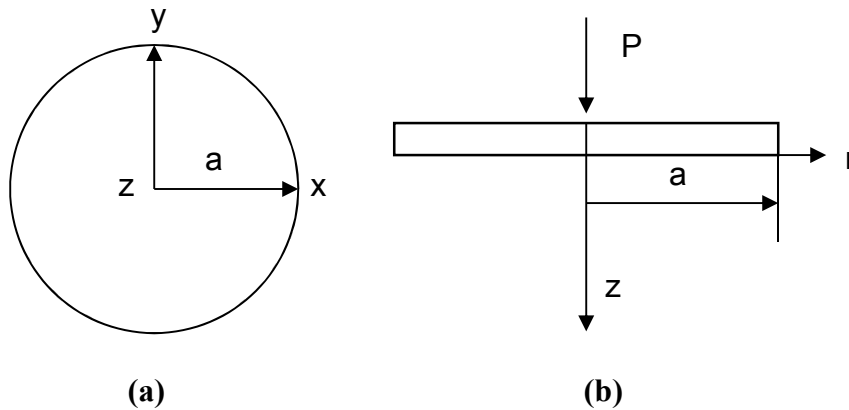


*Figure 14.1 – The notation with regard to the co-ordinate system.*

The circular footing is subjected to a total load of 10 kN. The vertical displacement of a circle due to symmetric loading was analyzed. Seven cases of varying radii were considered. The cases include radii  $a$  of values 1, 1.25, 1.75, 3, 5, 7 and 10 m. In all cases, the soil modulus  $E$  was equal to 100 kPa and Poisson's ratio  $\nu$  was equal to 0.2.

## 14.2 Closed Form Solutions

The vertical surface displacement of the circle shown in Figure 14.1 is given by:

$$\delta_z = \frac{\pi}{2} (1 - \nu^2) \frac{P_{av} a}{E} \quad [1]$$

where:  $P_{av} = \frac{P}{\pi a^2}$  which is the average pressure across the surface.

### 14.3 Results and Discussion

The resulting displacements obtained from *Settle3D* are compared to the analytical solution given by equation [1]. The Boussinesq method was selected for the stress calculation of *Settle3D*. Figure 14.2 shows the vertical displacement of the origin as a function of the radius.

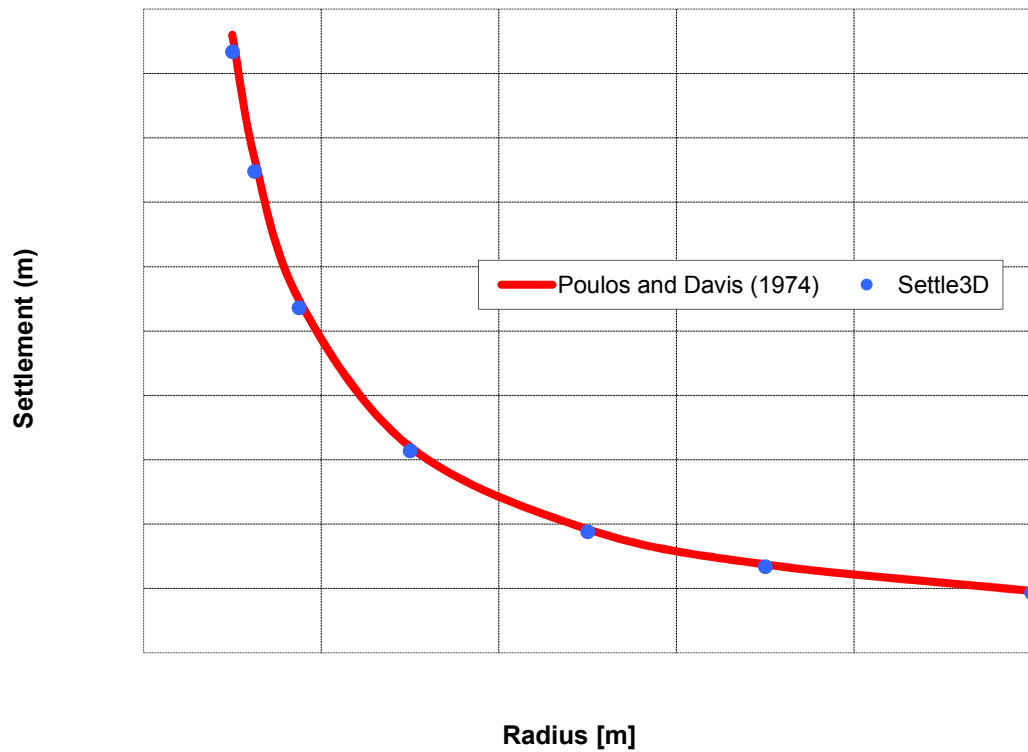


*Figure 14.2 – Vertical displacement for varying radii.*

### 14.4 References

Poulos, H. G. and Davis, E. H. (1974), *Elastic Solutions for Soil and Rock Mechanics*, New York: John Wiley and Sons.

# 15 Rotation of a Rigid Circular Footing

## 15.1 Problem Description

This problem verifies the rotation of a rigid circular footing due an applied moment loading. The notation with regards to the co-ordinate system is shown in Figure 15.1.

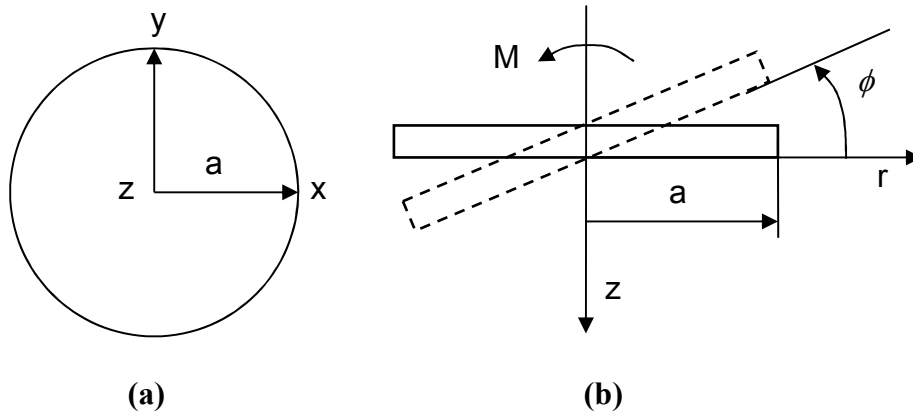


*Figure 15.1 – The notation with regard to the co-ordinate system.*

The circular footing is subjected to a moment of 10 kN m. The rotation due to the moment  $M$  is then analyzed. Different cases of varying radii  $a$ , ranging from 1 to 10 m, were considered. The soil modulus  $E$  equals 100 kPa and Poisson's ratio  $\nu$  equals 0.2.

## 15.2 Closed Form Solutions

The rotation  $\phi$  due to a moment  $M$  as depicted in Figure 15.1 is given by:

$$\phi = \frac{3M(1-\nu^2)}{4Ea^3} \quad [1]$$

## 15.3 Results and Discussion

The rotations due to the moment loading are shown in Figure 15.2. The Boussinesq method was used for stress calculation. The rotations given by equation [1] are plotted for comparison. Note that rotation is simply the vertical displacement at any point divided by the radial distance, hence it is unitless.

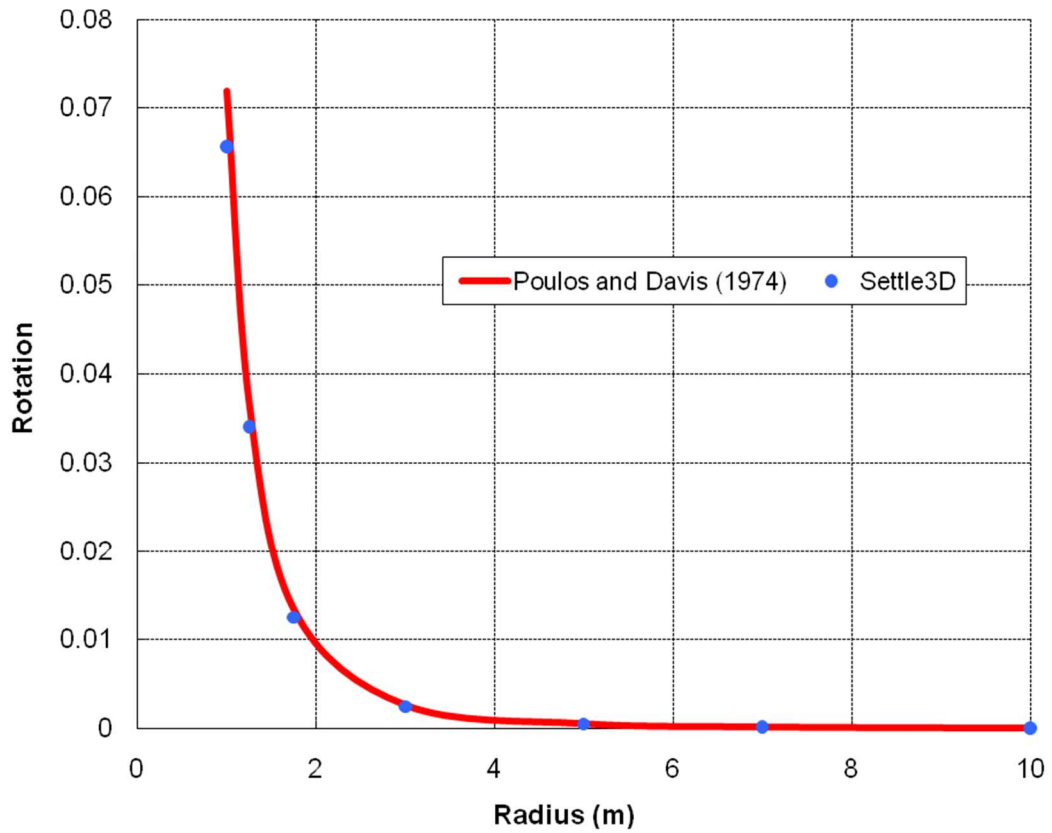


*Figure 15.2 – Rotation due to moment loading for different radii.*

## 15.4 References

Poulos, H. G. and Davis, E. H. (1974), *Elastic Solutions for Soil and Rock Mechanics*, New York: John Wiley and Sons.

# 16 Immediate Settlement beneath a Rigid Rectangular Footing

## 16.1 Problem Description

This problem verifies the immediate settlement beneath a rigid rectangular footing. The notation with regards to the co-ordinate system is shown in Figure 16.1. In the figure, the origin of the coordinate system is taken as the point of application of the total load  $P$ .

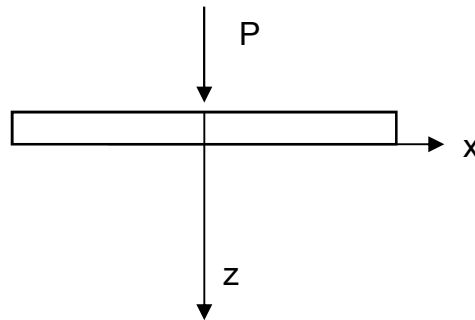


*Figure 16.1 – The notation with regard to the co-ordinate system.*

The footing is subjected to a total load of 10 kN. Let  $L$  and  $B$  designate the dimensions of a rectangular footing being considered (refer to Figure 16.2). The following ratios of  $L/B$  were considered: 1.25, 1.75, 3, 5, 7 and 9. In all cases, the soil modulus  $E$  was set at 100 kPa, the Poisson's ratio  $\nu$  was set at 0.2.

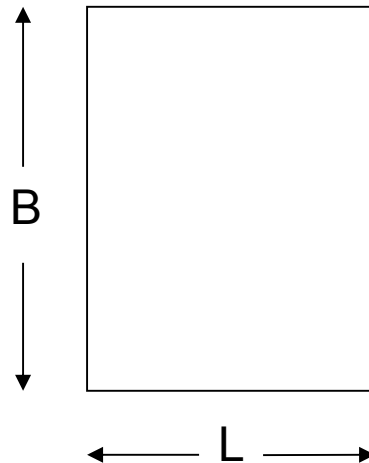


*Figure 16.2 – Model geometry for both square and rectangular rigid loading.*

## 16.2 Closed Form Solutions

The approximate vertical displacement of the rectangular footing shown in Figure 16.2 is given by:

$$\delta_z = \frac{P(1-\nu^2)}{\beta_z \sqrt{BLE}} \quad [1]$$

where:  $\beta_z$  is a factor dependent on the ratio  $L/B$  (refer to Figure 16.3)

Figure 16.3 shows the coefficient  $\beta_z$  for different values of  $L/B$ .

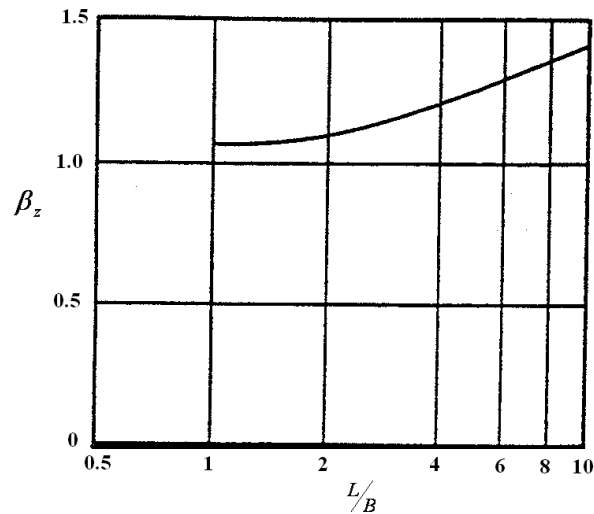


*Figure 16.3 – Coefficient  $\beta_z$  for rigid rectangle.*

## 16.3 Results and Discussion

The resulting displacements obtained from *Settle3D* are compared to the approximate solution given by equation [1]. The Boussinesq method was used for the stress calculation. Figure 16.4 shows the vertical displacement for different side lengths ( $L$ ) of a square. Note that for all cases,  $L/B = 1$ . Figure 16.5 shows the vertical displacements for different values of  $L/B$ .

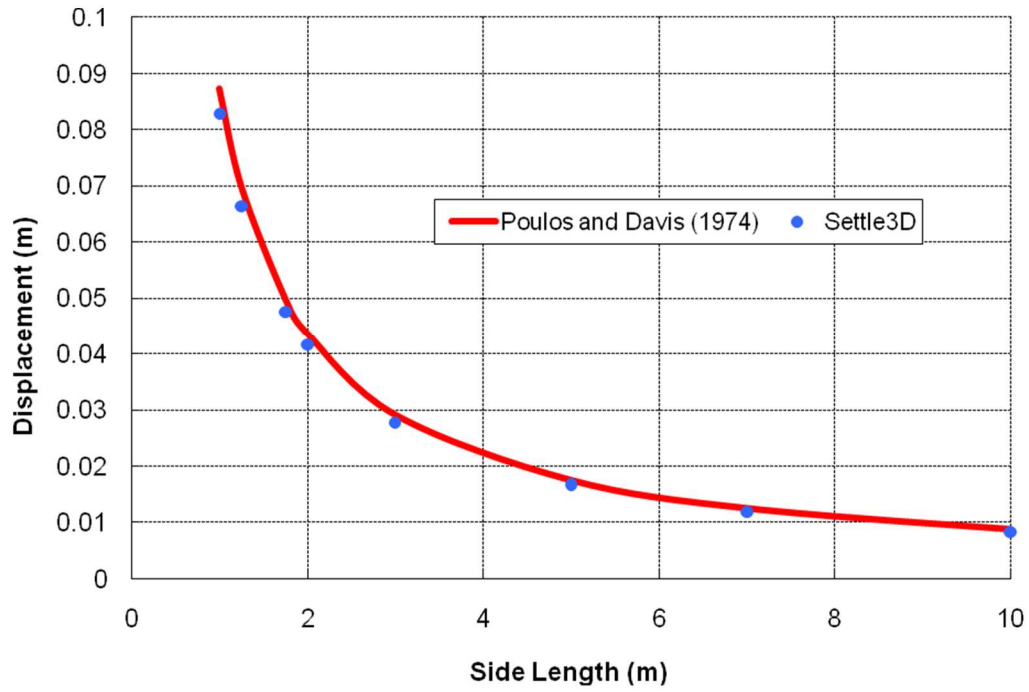


**Figure 16.4 – Vertical displacement for different side lengths of a square.**

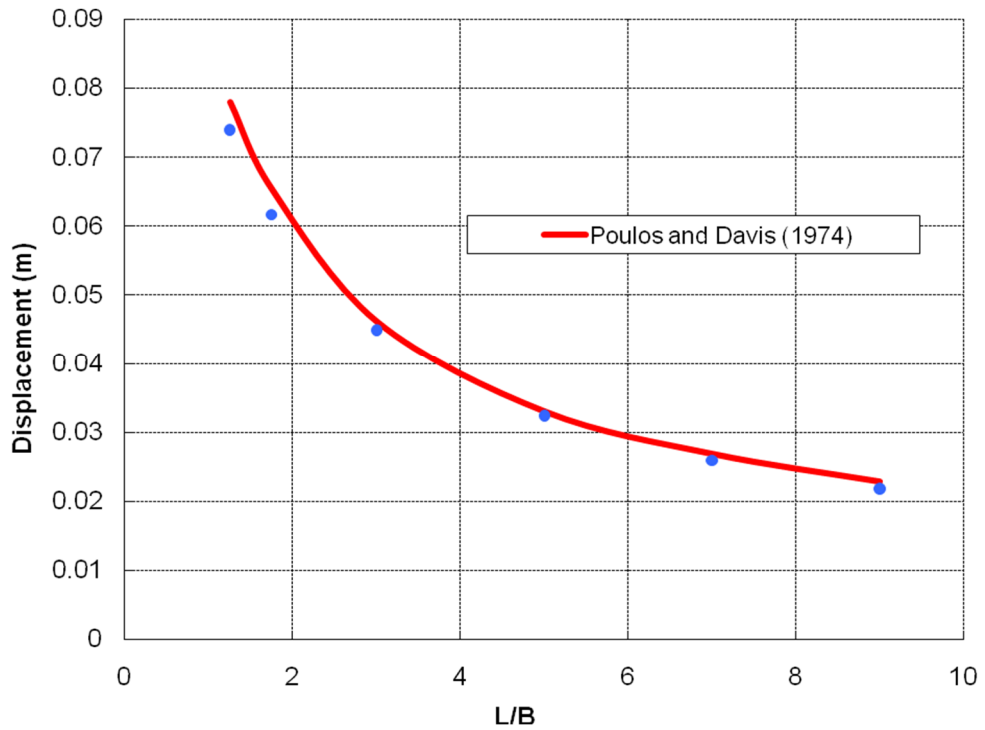


**Figure 16.5 – Rectangular load, displacements for different L/B ratios.**

## 16.4 References

Poulos, H. G. and Davis, E. H. (1974), *Elastic Solutions for Soil and Rock Mechanics*, New York: John Wiley and Sons.

# 17 Rotation of a Rigid Rectangular Footing

## 17.1 Problem Description

This problem verifies the rotation of a rigid rectangular footing due to an applied moment loading. The notation with regards to the co-ordinate system is shown in Figure 17.1. Figure 17.2 shows the model geometry. The moment is applied along the direction of  $B$  and the axis of rotation is about the origin.

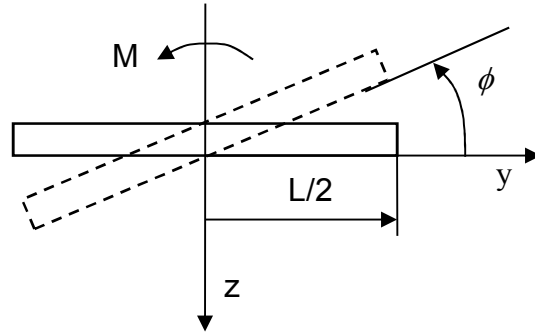


*Figure 17.1 – The notation with regard to the co-ordinate system.*

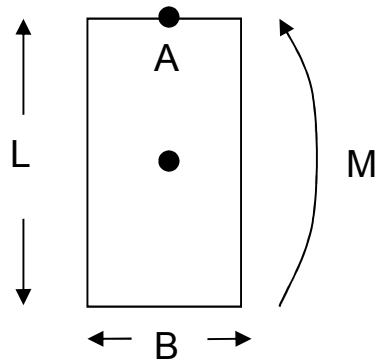


*Figure 17.2 – Model geometry for moment loading of a rectangle.*

The footing is subjected to a total moment of 10 kN m. Let  $L$  and  $B$  designate the dimensions of a rectangular footing being considered (refer to Figure 17.2). Certain ratios of  $L/B$  were considered: 0.1, 0.2, 0.5, 1, 1.5 and 2. The soil modulus  $E$  equals 100 kPa and Poisson's ratio  $\nu$  equals 0.2. In all cases,  $B$  was kept constant at 1 m only  $L$  was varied.

## 17.2 Closed Form Solutions

The approximate rotation of the rectangular footing shown in Figure 17.2 is given by:

$$\phi = \frac{M(1-\nu^2)}{B^2 LE} I_\theta \quad [1]$$

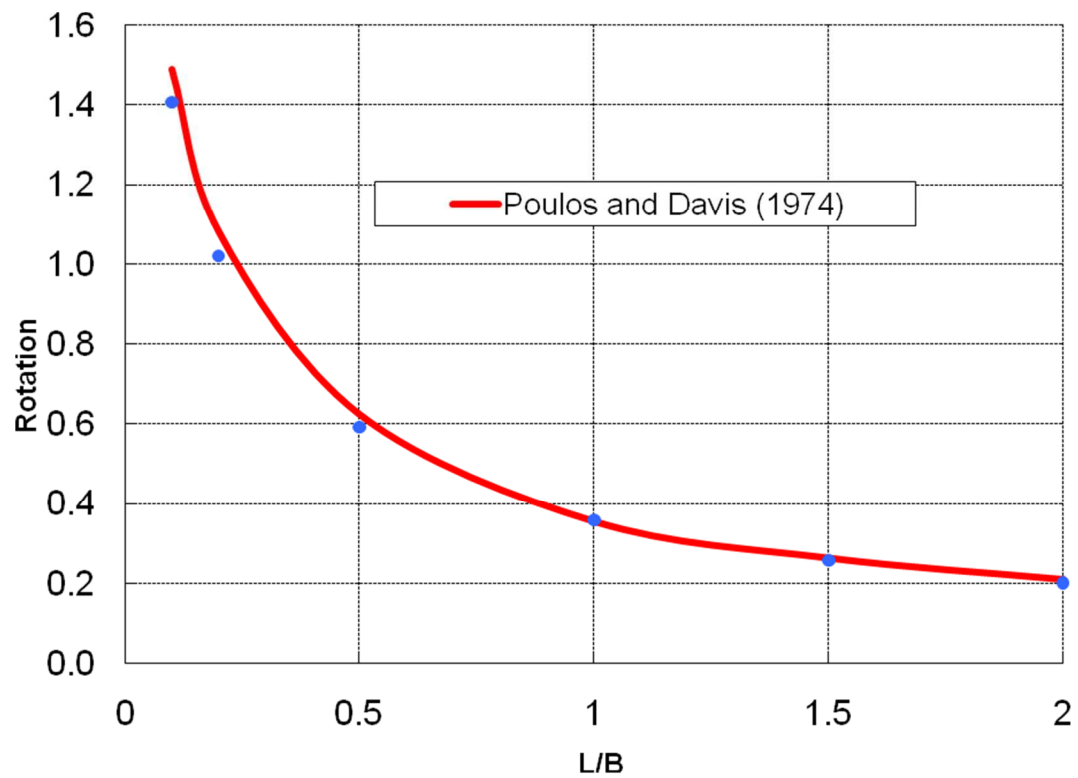
where:  $I_\theta$  is a factor dependent on the ratio  $L/B$  (refer to Table 17.1)

Table 17.1.  $I_\theta$  values for different  $L/B$  ratios.

|            |      |      |      |     |      |      |
|------------|------|------|------|-----|------|------|
| $L/B$      | 0.1  | 0.2  | 0.5  | 1   | 1.5  | 2    |
| $I_\theta$ | 1.59 | 2.29 | 3.33 | 3.7 | 4.12 | 4.38 |

## 17.3 Results and Discussion

The resulting rotations obtained from *Settle3D* are compared to the approximate solution given by equation [1]. The Boussinesq method was used for the stress calculation. Figure 17.3 shows the calculated rotations for different values of  $L/B$ .



*Figure 17.3 – Rotation of rectangle for different L/B ratios.*

## 17.4 References

Poulos, H. G. and Davis, E. H. (1974), *Elastic Solutions for Soil and Rock Mechanics*, New York: John Wiley and Sons.

# 18 Immediate Settlement beneath a Rigid Circular Footing on a Finite Layer

## 18.1 Problem Description

This problem verifies the immediate settlement beneath a rigid circular footing on a finite layer. Figure 18.1 shows the notation with regards to the co-ordinate system. In the figure, the origin of the coordinate system is taken as the point of application of the total load  $P$ .

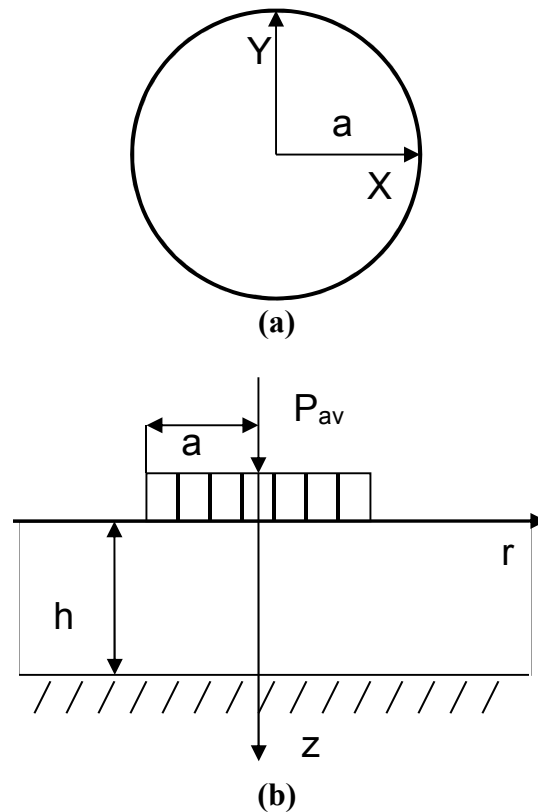


*Figure 18.1 – The notation with regard to the co-ordinate system.*

For the circular footing, the radius  $a$  is taken to be 2 m. The footing is subjected to a total load  $P$  of 1 kN. The vertical displacement due to symmetric loading is then analyzed. Different layer thicknesses  $h$  were considered, ranging from 1.25 m to 20m.

In order to model a finite layer correctly, two separate layers are used. Figure 18.2 shows an example of the two layers. For the top layer, the soil modulus  $E_1$  is set at 100 kPa and Poisson's ratio  $\nu$  is set at 0.2. The bottom layer has similar parameters except that its modulus  $E_2$  is set to 10000 kPa and its thickness is kept constant at 1 m. Note that the top layer's thickness is varied with each case and that Figure 18.2 only depicts an arbitrary thickness of 10 m.

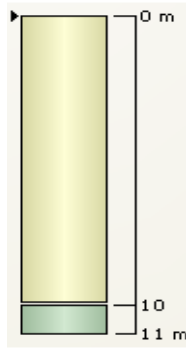


Figure 18.2 – Schematic of the Settle3D model used for the finite layer.

## 18.2 Closed Form Solutions

The vertical surface displacement of the circle shown in Figure 18.1 is given by:

$$\delta_z = \frac{P_{av} a}{E} I_p \quad [1]$$

where:  $P_{av} = \frac{P}{\pi a^2}$  which is the average pressure across the surface  
and  $I_p$  is the influence factor for a particular  $\nu$  and ratio  $a/h$ .

Figure 18.3 plots the corresponding  $I_p$  values for different values of  $a$ ,  $h$  and  $\nu$ .

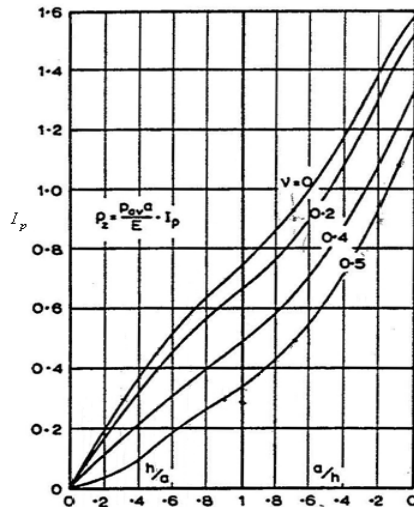
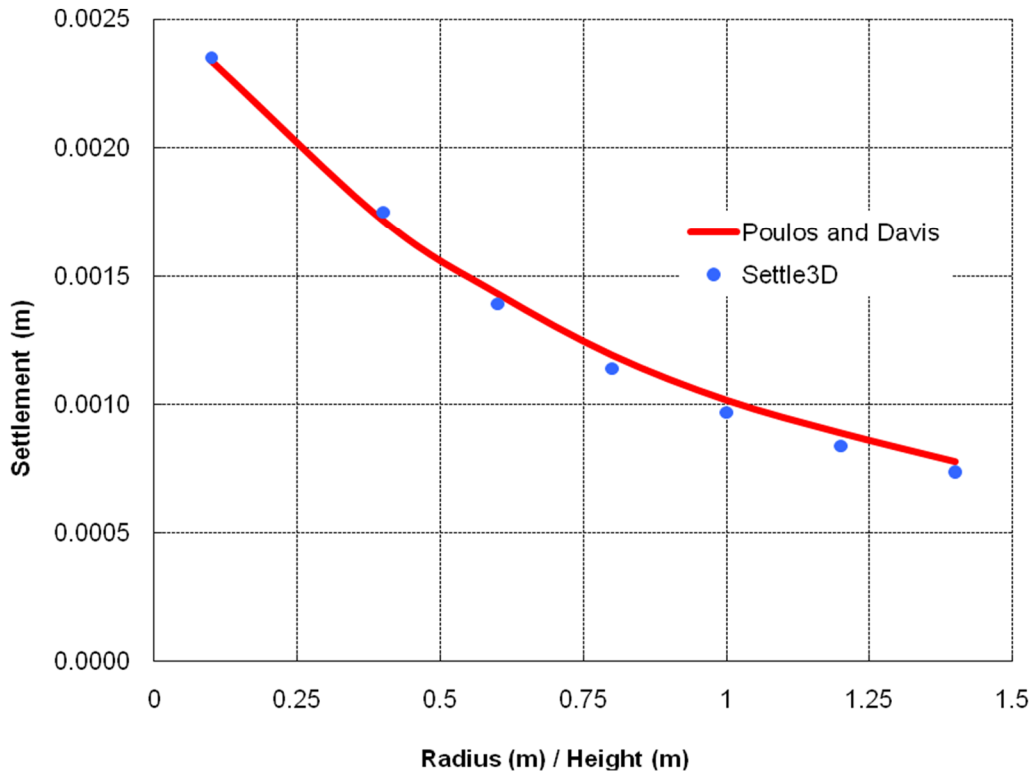


Figure 18.3 – Values of  $I_p$  for different values of  $a$ ,  $h$  and  $\nu$ .

### 18.3 Results and Discussion

The resulting displacements obtained from *Settle3D* are compared to the approximate solution given by equation [1]. The Multiple Layer method was used for the stress calculation in *Settle3D*. Figure 18.4 shows the vertical displacement of the origin as a function of the ratio  $a/h$ .



**Figure 18.4 – Vertical displacement of a rigid circle with constant radius and varying layer thickness.**

Figure 18.5 shows the vertical displacement of the origin as a function of the ratio  $a/h$  for varying Poisson's ratios.

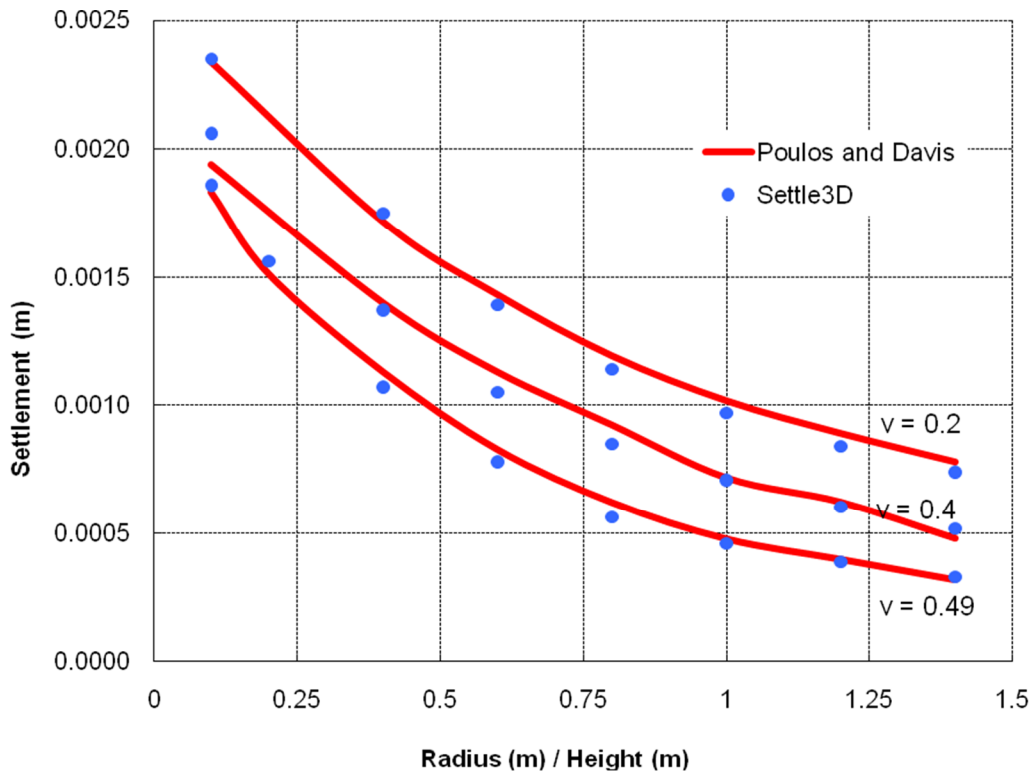


**Figure 18.5 – Vertical displacement of a rigid circle with constant radius and varying layer thickness for varying Poisson's ratios.**

## 18.4 References

Poulos, H. G. and Davis, E. H. (1974), *Elastic Solutions for Soil and Rock Mechanics*, New York: John Wiley and Sons.

# 19 Rotation of a Rigid Circular Footing on a Finite Layer

## 19.1 Problem Description

This problem verifies the rotation of a rigid circular footing due to an applied moment on a finite layer. Figure 19.1 shows the notation with regards to the co-ordinate system.

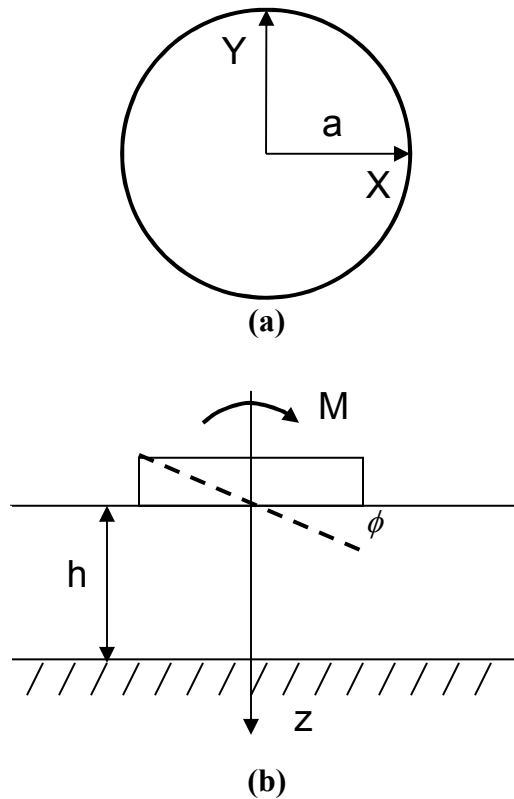


*Figure 19.1 – The notation with regard to the co-ordinate system.*

The circular footing is subjected to a total moment of 10 kN m. The rotation of a circle due to the applied moment was then analyzed. Six cases of varying radii  $a$  were considered: 3, 5, 7.5, 10, 15 and 30 m.

In order to model a finite layer correctly, two separate layers are used. Figure 19.2 shows an example of the two layers. For the top layer, the soil modulus  $E_1$  is set at 100 kPa and Poisson's ratio  $\nu$  is set at 0.2. The bottom layer has similar parameters except that its modulus  $E_2$  is set to 10000 kPa and its thickness is set to 1 m.

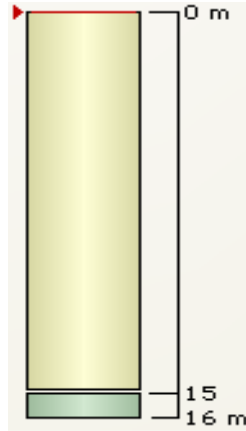


*Figure 19.2 – Schematic of the Settle3D model used for the finite layer.*

## 19.2 Closed Form Solutions

The rotation of the circle shown in Figure 19.1 (b) is given by:

$$\phi = \frac{(1 - \nu^2)M}{4a^3 BE} \quad [1]$$

where:  $B = \frac{1}{3}a_1 + \frac{1}{5}a_3$

and  $a_1$  and  $a_3$  are factors that depend on the ratio  $h/a$ .

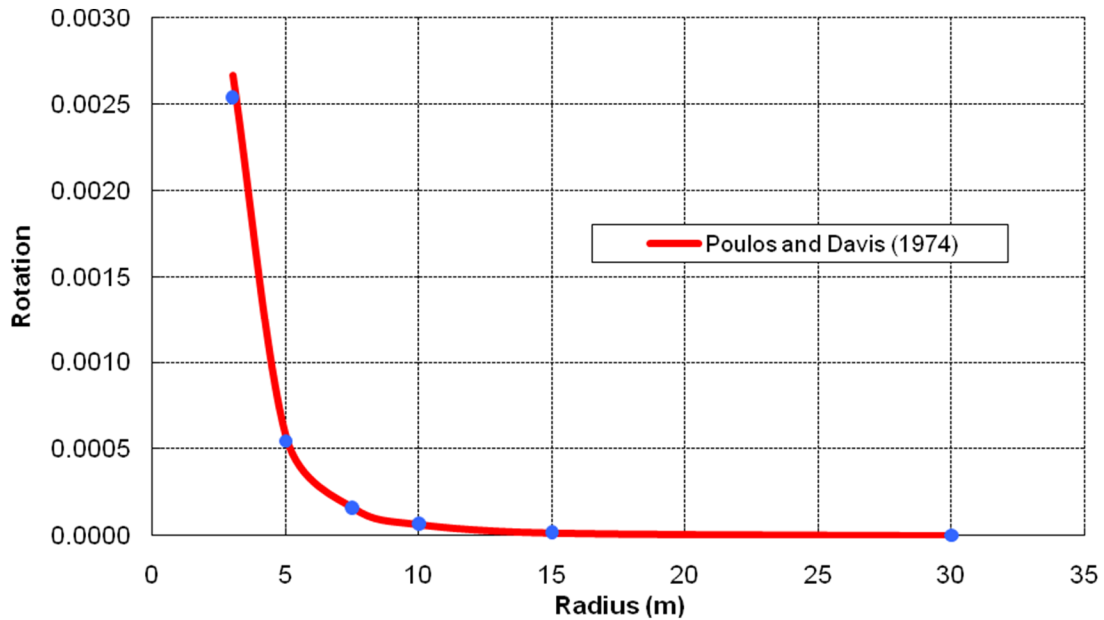
The factors  $a_1$  and  $a_3$  are tabulated in Table 19.1.

Table 19.1. Values of  $a_1$  and  $a_3$  for different ratios of  $h/a$ .

| $h/a$      | $a_1$ | $a_3$ |
|------------|-------|-------|
| 0.3        | 4.23  | -2.33 |
| 0.5        | 2.14  | -0.70 |
| 1.0        | 1.25  | -0.10 |
| 1.5        | 1.10  | -0.03 |
| 2.0        | 1.04  | 0.00  |
| 3.0        | 1.01  | 0.00  |
| $\geq 5.0$ | 1.00  | 0.00  |

### 19.3 Results and Discussion

The resulting rotations obtained from *Settle3D* are compared to the approximate solution given by equation [1]. The Multiple Layer method was used for the stress calculation in *Settle3D*. Figure 19.3 shows the rotations of a circle due to a rigid load on a finite layer.



*Figure 19.3 – Rotations of a circle for varying radii on a finite layer.*

### 19.4 References

Poulos, H. G. and Davis, E. H. (1974), *Elastic Solutions for Soil and Rock Mechanics*, New York: John Wiley and Sons.

## 20 Vertical Stress beneath Uniform Circular load based on Westergaard's Theory

### 20.1 Problem Description

This problem verifies the vertical stresses beneath a uniform circular load, using the Westergaard stress computation method. The notation with regards to the co-ordinate system is shown in Figure 20.1. In the figure, the origin of the coordinate system is taken as the point of application of load  $Q$ .

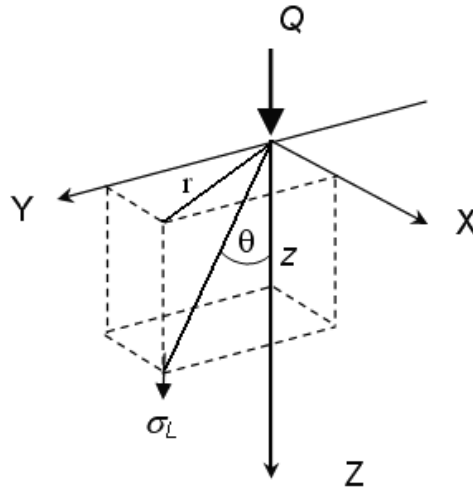


*Figure 20.1 – The notation with regard to the coordinate system and the stress component.*

Figure 20.2 shows the model geometry for the problem at hand. The circular footing is subjected to a uniform loading ( $q$ ) of 10 kPa.

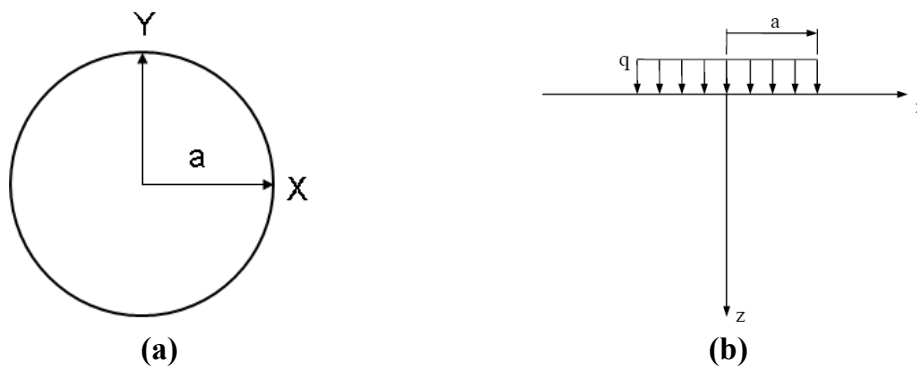


*Figure 20.2 – Model geometry for a circular load.*

## 20.2 Closed Form Solution

For a soil medium with Poisson's ratio  $\nu$ , the vertical stress  $\sigma_z$  due to a point load  $Q$  as obtained by Westergaard is given by [1]:

$$\sigma_z = \frac{Q}{z^2} \frac{\frac{1}{2\pi} \sqrt{\frac{1-2\nu}{2-2\nu}}}{\left[ \left( \frac{1-2\nu}{2-2\nu} \right) + \left( \frac{r}{z} \right)^2 \right]^{\frac{3}{2}}} \quad [1]$$

For large lateral restraint,  $\nu$  may be taken as zero. The vertical stress below the center of a circular footing can be obtained analytically by integrating [1]. The solution of which is given by:

$$\sigma_z = q \left[ 1 - \frac{1}{\sqrt{1 + \left( \frac{a}{\eta z} \right)^2}} \right] \quad [2]$$

where:

$$\eta = \sqrt{\frac{1-2\nu}{2-2\nu}} \text{ and}$$

$q$  is a uniform load.

## 20.3 Results and Discussion

The resulting vertical stresses are compared to the Westergaard analytical solution. Figure 20.3 shows the vertical stress profiles underneath the center of a circle, given by *Settle3D* for  $\nu = 0.2$  with  $a = 1$  m. The analytical solution from Westergaard is also plotted for comparison.

Figure 20.4 plots the Westergaard stress profile of a uniformly loaded circular footing with  $a = 1$  m and varying Poisson's ratios ( $\nu = 0.01, 0.2, 0.4$  and  $0.49$ ). The Boussinesq solution is plotted for comparison.

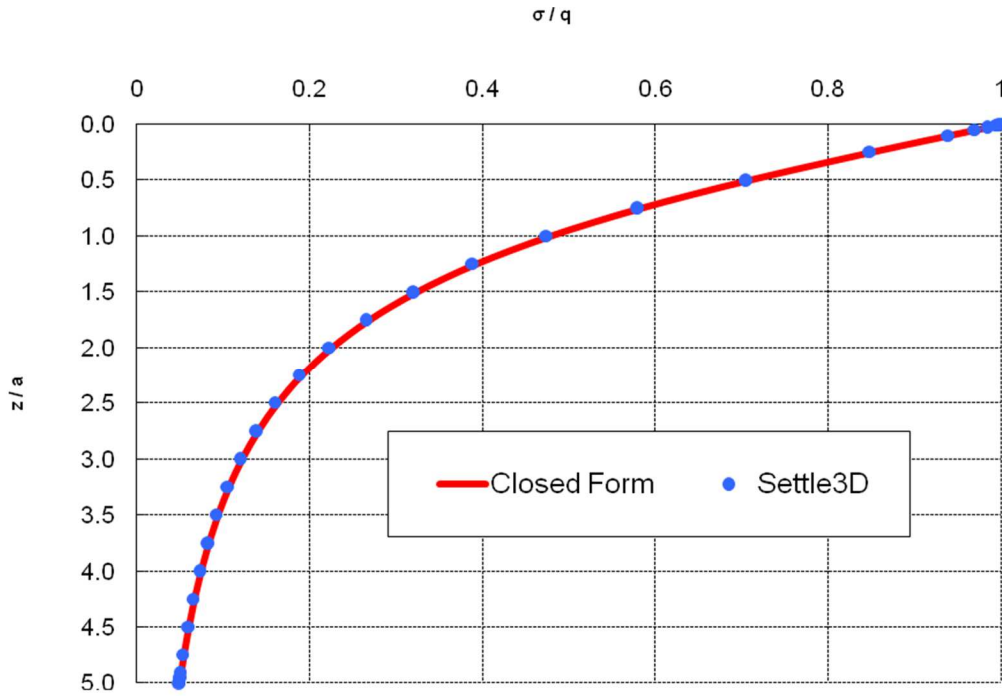


**Figure 20.3 – Vertical stress under the center of uniform circular load**

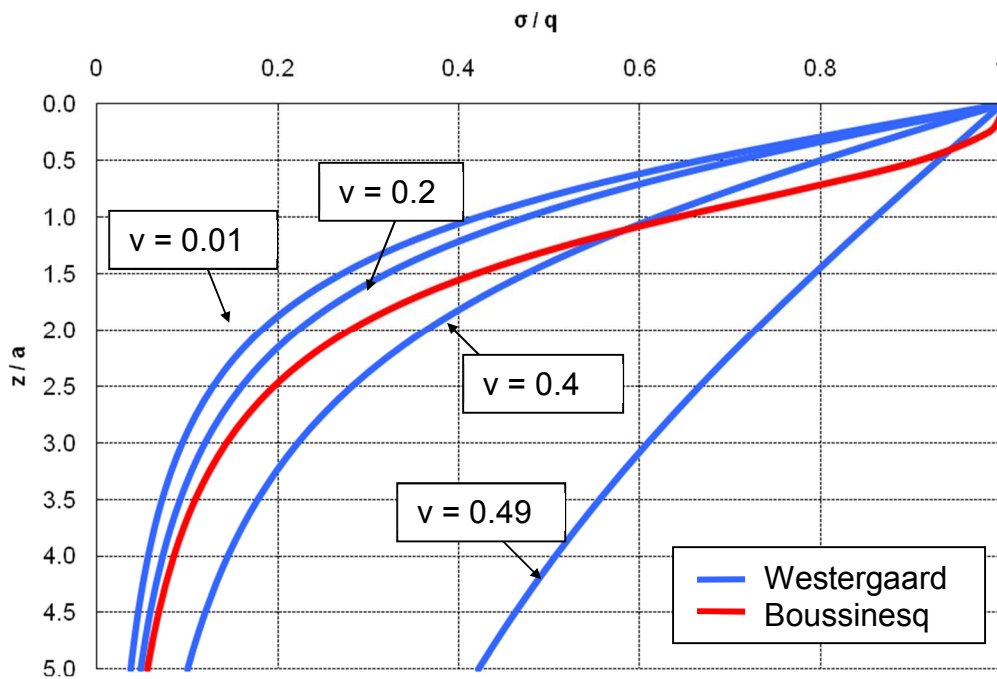


**Figure 20.4 – Westergaard stress profiles with varying Poisson's ratios compared to a Boussinesq stress profile**

## 20.4 References

Venkatramaiah, C. (2006). *Geotechnical Engineering, Revised 3<sup>rd</sup> Edition*, New Age International.

## 21 Vertical Stress beneath Uniform Square load based on Westergaard's Theory

### 21.1 Problem Description

This problem verifies the vertical stresses beneath a uniform square load, using the Westergaard stress computation method. The notation with regards to the co-ordinate system is shown in Figure 21.1. In the same figure, the origin of the coordinate system is taken as the point of application of load  $Q$ .

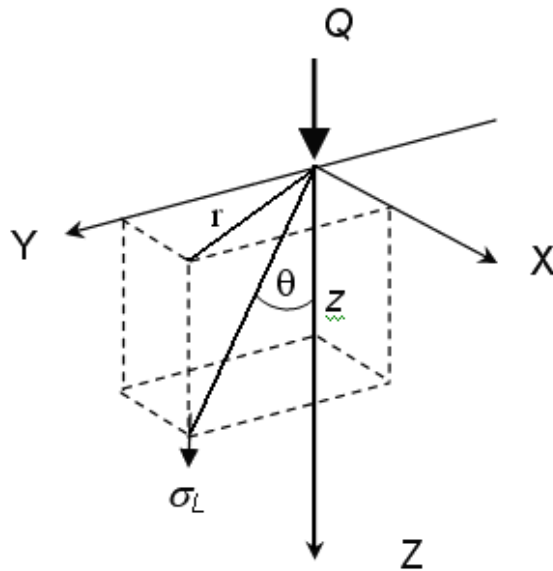


*Figure 21.1 – The notation with regard to the coordinate system and the stress component.*

Figure 21.2 shows the model geometry for the problem at hand. The square footing is subjected to a uniform loading ( $q$ ) of 10 kPa.

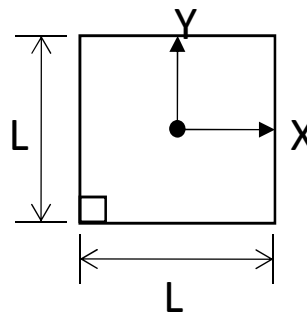


*Figure 21.2 – Model geometry for a square load.*

## 21.2 Closed Form Solution

For a soil medium with Poisson's ratio  $\nu$ , the vertical stress  $\sigma_z$  due to a point load  $Q$  as obtained by Westergaard is given by [1]:

$$\sigma_z = \frac{Q}{z^2} \frac{\frac{1}{2\pi} \sqrt{\frac{1-2\nu}{2-2\nu}}}{\left[ \left( \frac{1-2\nu}{2-2\nu} \right) + \left( \frac{r}{z} \right)^2 \right]^{3/2}} \quad [1]$$

For large lateral restraint,  $\nu$  may be taken as zero. The vertical stress below the corner of a rectangular footing can be obtained analytically by integrating [1]. The solution of which is given by:

$$\sigma_z = \frac{q}{2\pi} \cot^{-1} \sqrt{\left( \frac{1-2\nu}{2-2\nu} \right) \left( \frac{1}{m^2} + \frac{1}{n^2} \right) + \left( \frac{1-2\nu}{2-2\nu} \right)^2 \left( \frac{1}{m^2 n^2} \right)} \quad [2]$$

where:  $m = L / z$                        $n = W / z$   
L and W are the respective lengths and widths of the rectangle  
z is the depth  
and q is a uniform load.

For the case of a square,  $L = B$ . Hence,  $m = n$ .

To obtain the stress at the center of a rectangular or square footing, the quadrilateral may be divided into four equal pieces. The intersecting corner of these pieces then will coincide with the center of the quadrilateral. Figure 21.3 shows this situation. Using the principle of superposition, the contributions of each of the four pieces (using [2] to calculate the stress for each piece's corner) sum up to the total stress experienced at the center. Note that the side lengths (L and B) used for equation [2] for the new smaller quadrilateral must be that of the new smaller piece (i.e.  $L/2$ ). More details are contained in reference [1] (Venkatramaiah, 2006).

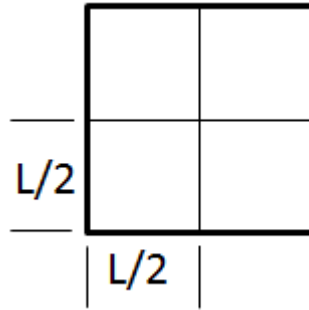


Figure 21.3 – Calculation of the stress at the center of a square.

### 21.3 Results and Discussion

The resulting vertical stresses are compared to the Westergaard analytical solution. Figure 21.4 shows the vertical stress underneath the center of a square given by *Settle3D* for  $\nu = 0.2$  with  $S = 1$  m. The analytical solution from Westergaard is also plotted for comparison.

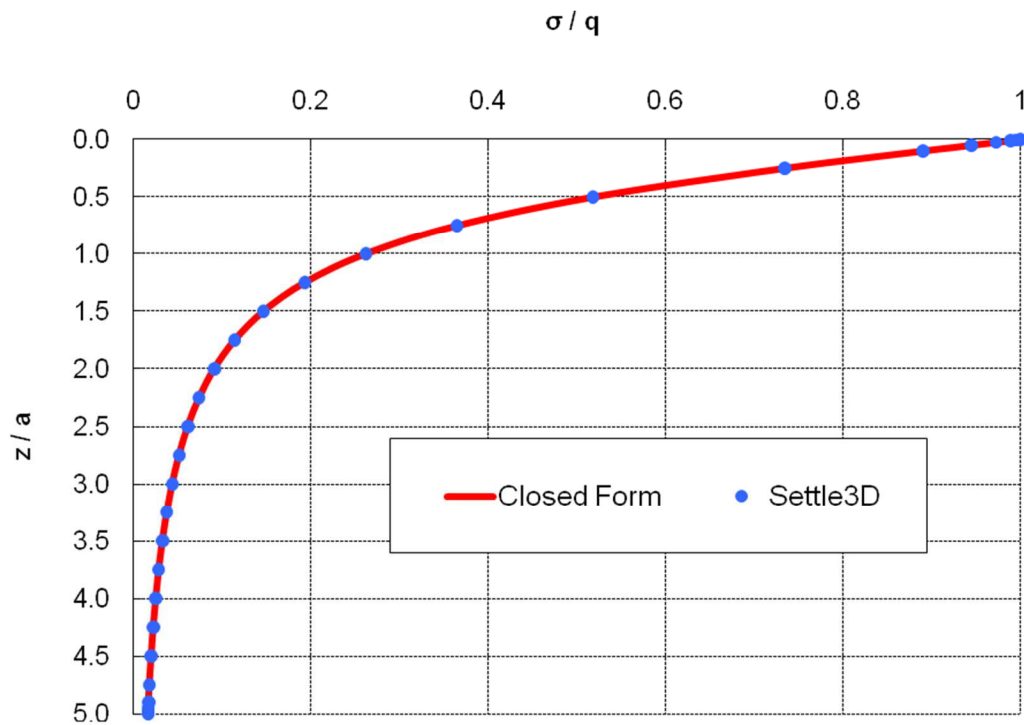
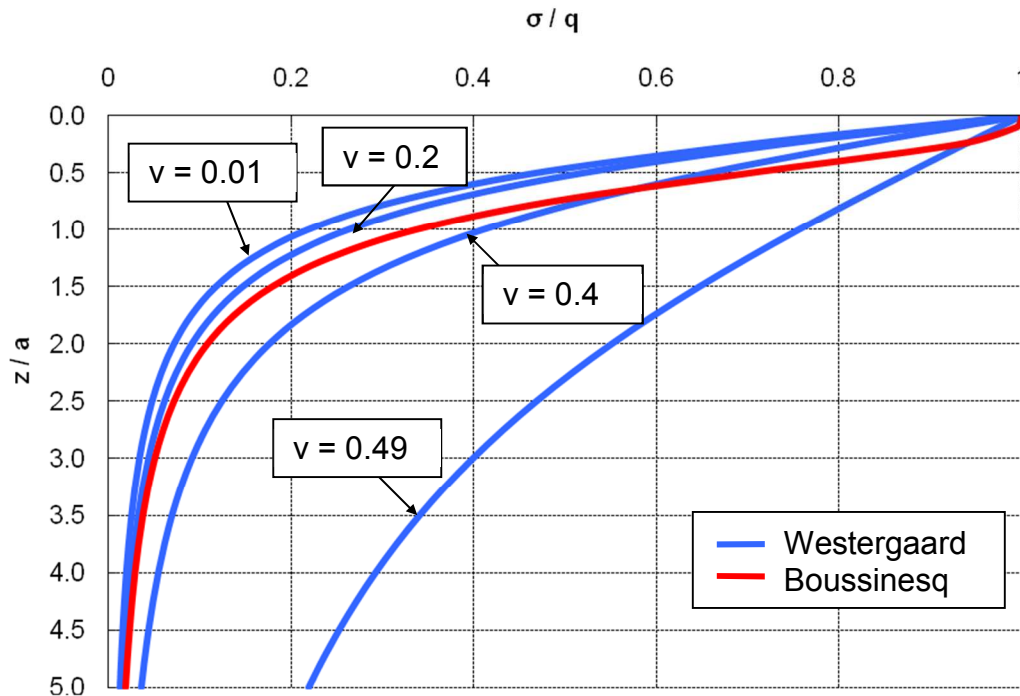


Figure 21.4 – Vertical stress under the center of uniformly loaded square

Figure 21.5 plots the Westergaard stress profile of a uniformly loaded square footing with  $S = 1$  m with varying Poisson's ratios ( $\nu = 0.01, 0.2, 0.4$  and  $0.49$ ) as compared to the stress profile obtained from the Boussinesq solution.



*Figure 21.5 – Westergaard stress profiles with varying Poisson's ratios compared to a Boussinesq stress profile.*

## 21.4 References

Venkatramaiah, C. (2006). *Geotechnical Engineering, Revised 3<sup>rd</sup> Edition*, New Age International.

## 22 Vertical Stress due to Uniform Loading on an Irregular Shaped Footing using Westergaard's Theory

### 22.1 Problem Description

This problem verifies the vertical stresses underneath one of the corners of an irregularly shaped footing, using the Westergaard stress computation method. The notation with regards to the co-ordinate system is shown in Figure 22.1. In the same figure, the origin of the coordinate system is taken as the point of application of load  $Q$ .

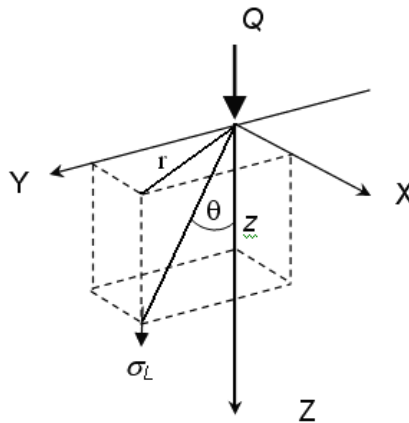


*Figure 22.1 – The notation with regard to the coordinate system and the stress component.*

Figure 22.2 shows the model geometry for the problem at hand. The footing is “L-shaped” and subjected to a uniform loading ( $q$ ) of 10 kPa. The point A is the current point of interest for the analysis.

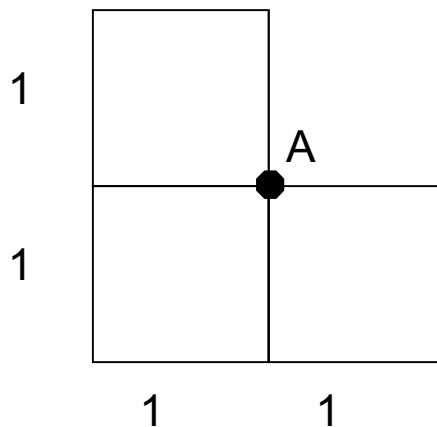


*Figure 22.2 – Model geometry for an L-shaped load.*

## 22.2 Closed Form Solution

For a soil medium with Poisson's ratio  $\nu$ , the vertical stress  $\sigma_z$  due to a point load  $Q$  as obtained by Westergaard is given by [1]:

$$\sigma_z = \frac{Q}{z^2} \frac{\frac{1}{2\pi} \sqrt{\frac{1-2\nu}{2-2\nu}}}{\left[ \left( \frac{1-2\nu}{2-2\nu} \right) + \left( \frac{r}{z} \right)^2 \right]^{3/2}} \quad [1]$$

For large lateral restraint,  $\nu$  may be taken as zero. The vertical stress below the corner of a rectangular footing can be obtained analytically by integrating [1]. The solution of which is given by:

$$\sigma_z = \frac{q}{2\pi} \cot^{-1} \sqrt{\left( \frac{1-2\nu}{2-2\nu} \right) \left( \frac{1}{m^2} + \frac{1}{n^2} \right) + \left( \frac{1-2\nu}{2-2\nu} \right)^2 \left( \frac{1}{m^2 n^2} \right)} \quad [2]$$

where:  $m = L / z$                        $n = W / z$   
L and W are the respective lengths and widths of the rectangle  
z is the depth  
and q is a uniform load.

To obtain the stress at point A for the current problem, the figure may be divided into three equal pieces. Figure 22.2 already demarcates the three squares of side length 1 m. As shown in Figure 22.2, the intersecting corner of these three squares is point A. Using the principle of superposition, the contributions of each of the three squares sum up to the total stress experienced at point A. For this particular example, equation [2] can be used to calculate the stress at the corner of one of the squares with  $L = 1$ . The overall stress at A is then the calculated stress for a square multiplied by three (3).

This approach uses the influence factors of the smaller squares to determine the overall stress at point A. More details on influence factors are contained in reference [1] (Venkatramaiah, 2006).

## 22.3 Results and Discussion

The resulting vertical stresses are compared to the Westergaard analytical solution. Figure 22.3 shows the vertical stress underneath point A given by *Settle3D* for  $\nu = 0.2$ . The analytical solution from Westergaard is also plotted for comparison.

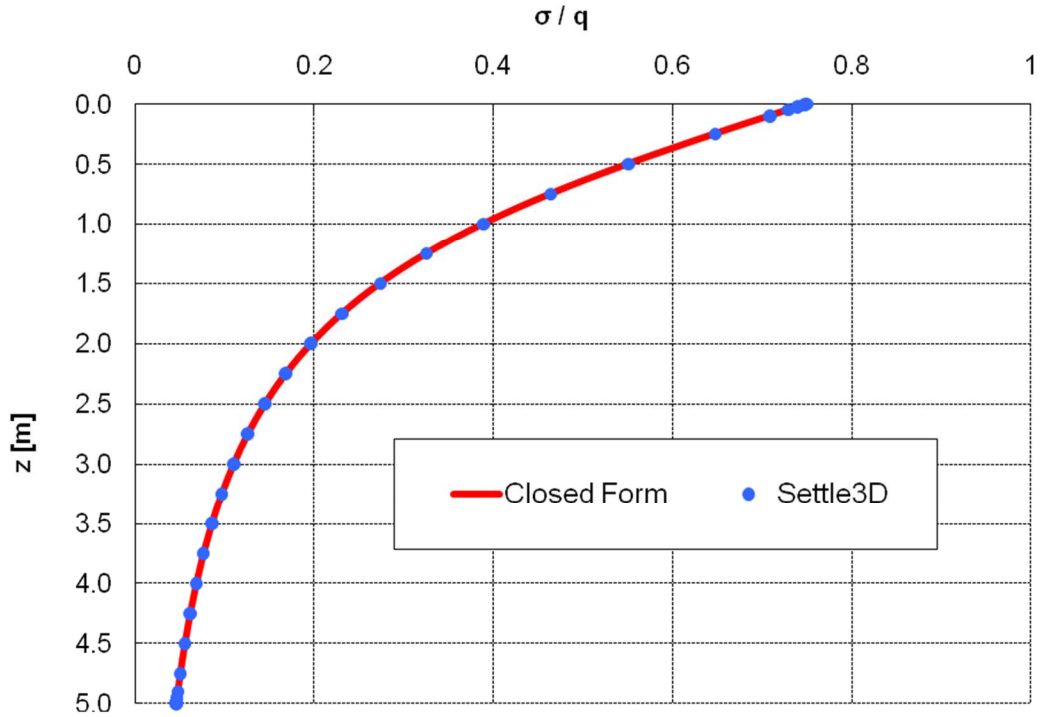


**Figure 22.3 – Stress profile at point A of irregularly shaped load.**

In addition, comparisons are made to the Boussinesq solution for different Poisson's ratios. Figure 22.4 plots the Westergaard stress profile with varying Poisson's ratios ( $\nu = 0.01, 0.2, 0.4$  and  $0.49$ ) compared to the stress profile obtained from the Boussinesq solution.

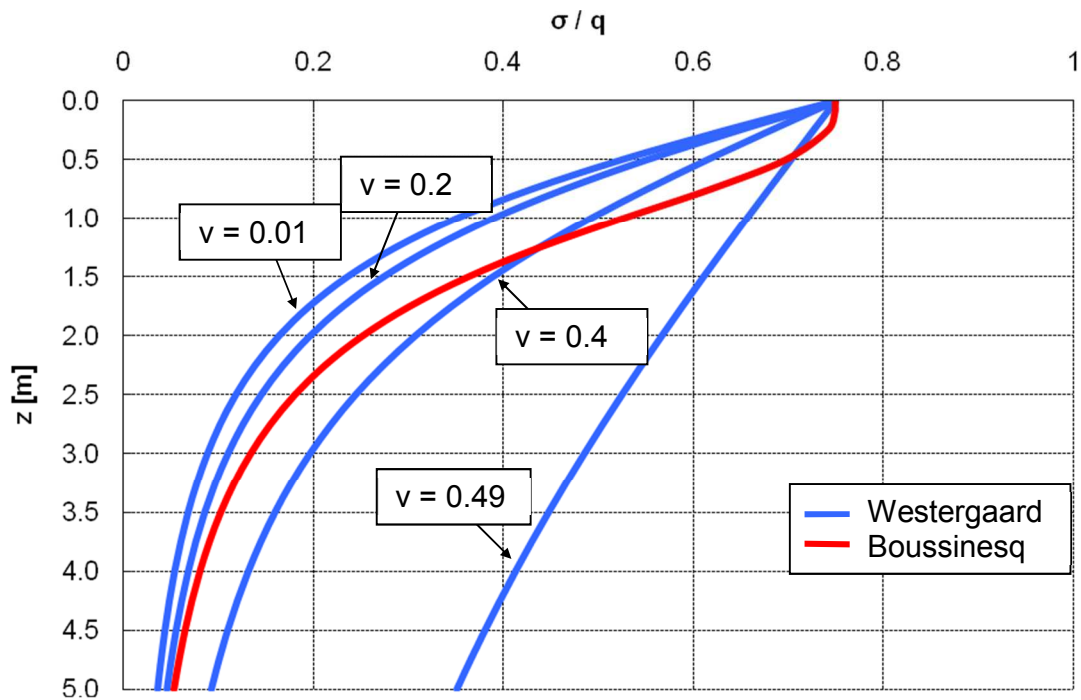


*Figure 22.4 – Westergaard stress profiles with varying Poisson's ratios compared to a Boussinesq stress profile*

## 22.4 References

Venkatramaiah, C. (2006). *Geotechnical Engineering, Revised 3<sup>rd</sup> Edition*, New Age International.

## 23 Horizontal Stresses due to Uniform Loading on a Square Footing using Boussinesq Theory

### 23.1 Problem Description

This problem verifies the horizontal stresses beneath a rectangular footing of length  $L$  and width  $B$ . The model geometry and the location of points of interest are shown in Figure 23.1. The footing is subjected to a uniform loading ( $q$ ) of 1kPa. Three footings were considered in this verification with the different  $L/B$  ratios of:

- Case 1:  $L/B = 1$
- Case 2:  $L/B = 2$
- Case 3:  $L/B = 4$

where  $B = 1\text{m}$ .

The horizontal stress results are compared to the analytical solution for each case.

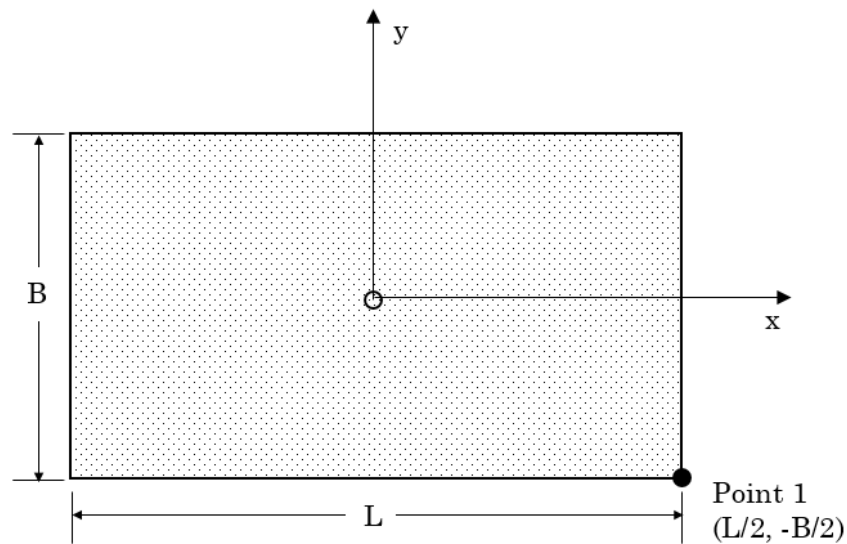


*Figure 23.1 – Model Geometry & Point of Interest Location*

### 23.2 Closed Form Solution

For a  $\nu = 0.5$  the horizontal stresses beneath the corner of a rectangle are calculated as (Poulos and Davis, 1974):

$$\sigma_x = \frac{p}{2} \left[ \tan^{-1} \frac{lb}{zR_3} - \frac{lbz}{R_1^2 R_3} \right]$$

$$\sigma_y = \frac{p}{2} \left[ \tan^{-1} \frac{lb}{zR_3} - \frac{lbz}{R_2^2 R_3} \right]$$

where

$$R_1 = (l^2 + z^2)^{\frac{1}{2}}$$

$$R_2 = (b^2 + z^2)^{\frac{1}{2}}$$

$$R_3 = (l^2 + b^2 + z^2)^{\frac{1}{2}}$$

### 23.3 Results and Discussion

Figures 23.2 and 23.4 show the x- and y- horizontal stress profiles, respectively, given by *Settle3D* compared to the analytical solutions.

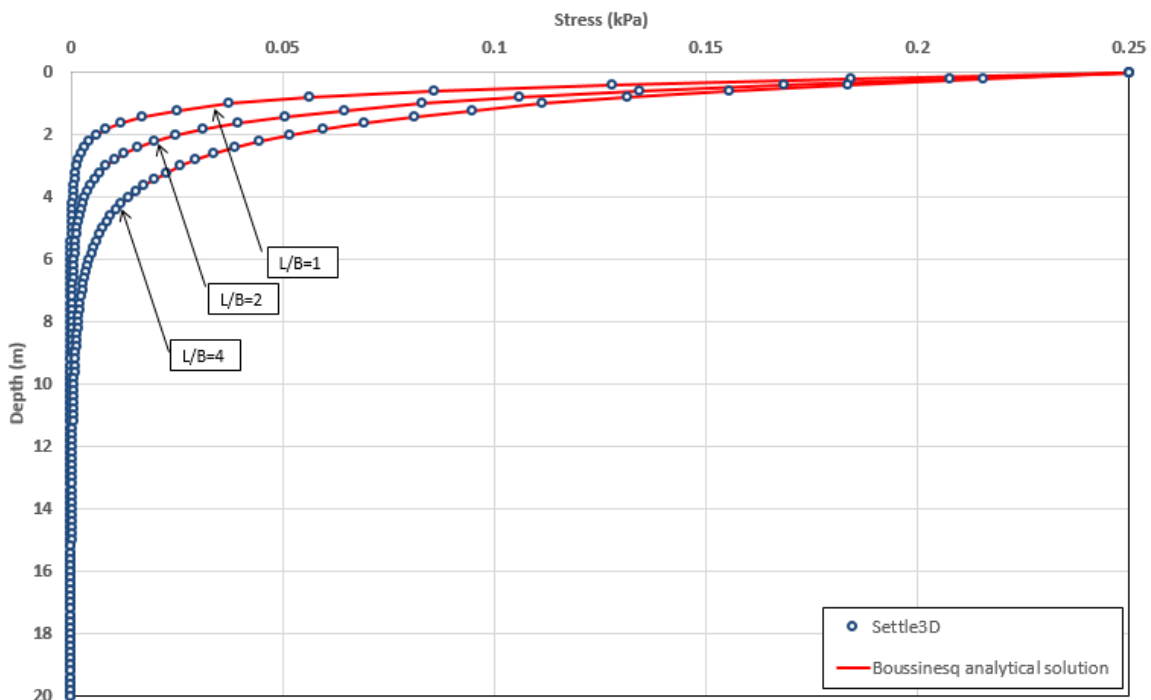


**Figure 23.2 – Horizontal (x-direction) Stress Profile at Point 1**

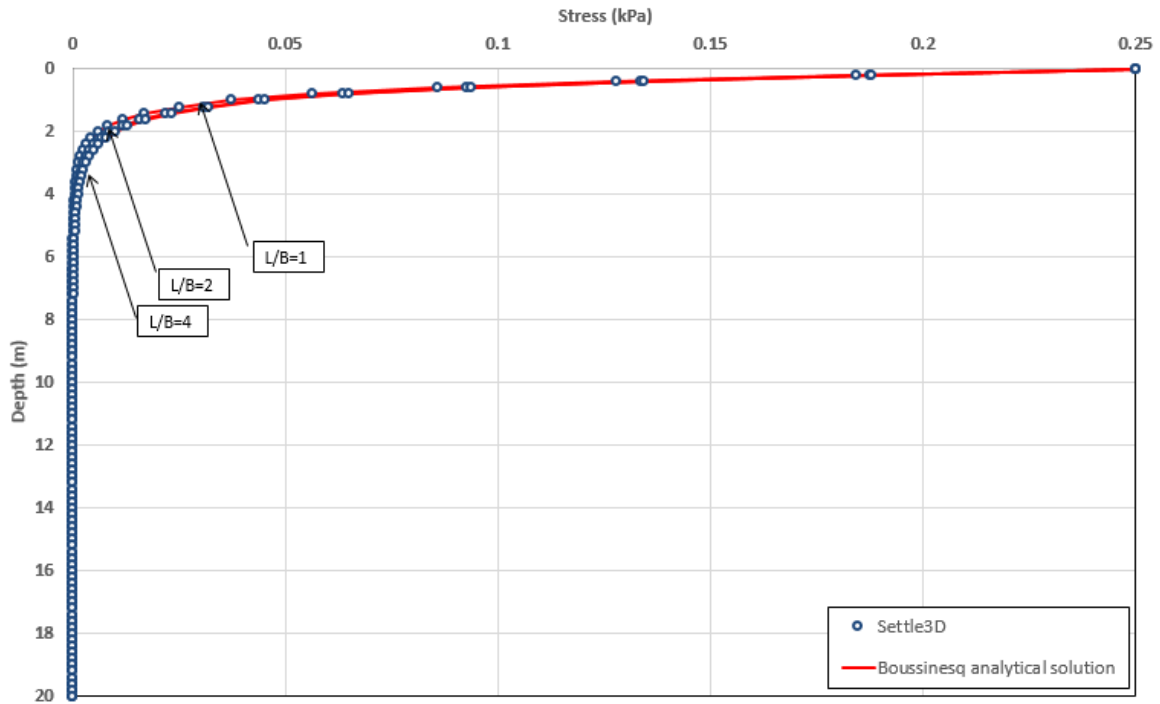


**Figure 23.2 – Horizontal (y-direction) Stress Profile at Point 1**